Title
The Physiological Ecology of Californian Blue Oak (Quercus douglasii) and Valley Oak (Quercus lobata) Woodlands in Response to Extreme Drought

Author
Weitz, Andrew

Publication Date
2018

Peer reviewed|Thesis/dissertation

The Physiological Ecology of Californian Blue Oak (*Quercus douglasii*) and Valley Oak (*Quercus lobata*) Woodlands in Response to Extreme Drought

By

Andrew P. Weitz

A dissertation submitted in partial satisfaction of the

requirements for the degree of

Doctor of Philosophy

in

Integrative Biology

in the

Graduate Division

of the

University of California, Berkeley

Committee in charge:

Professor David D. Ackerly, Co-Chair
Professor Todd E. Dawson, Co-Chair
Professor Sally E. Thompson

Fall 2018

Abstract

The Physiological Ecology of Californian Blue Oak (*Quercus douglasii*) and Valley Oak (*Quercus lobata*) Woodlands in Response to Extreme Drought

by

Andrew P. Weitz

Doctor of Philosophy in Integrative Biology

University of California, Berkeley

Professor David D. Ackerly, Co-Chair

Professor Todd E. Dawson, Co-Chair

Anthropogenic climate change is expected to increase the frequency, intensity, and duration of extreme drought events around the world, with one of the consequences being widespread episodes of tree mortality. Drought-induced tree mortality is now widely documented across diverse ecosystems. Consequently, understanding the physiological causes and ecological consequences of drought-induced tree mortality is critically important to effectively predict and manage the consequences of future drought events around the world. However, accurately predicting drought-induced mortality risk for different species across broad climatic, topographic, and environmental conditions is challenging, because drought exposure can vary substantially both within and across species' geographic ranges. For plant communities facing increased likelihoods of exposure to extreme drought, acclimation and survival of individual trees will require morphological and physiological modifications that offset the negative impacts of drought. Therefore, investigating such responses when historic, multi-year drought conditions arise is essential to advance our understanding of the physiological capacities of different plant species, and will improve modelling efforts geared towards predicting vulnerability to future extreme drought events. This work examines how variation in climate, topography, and drought exposure affected the *in-situ* responses of two coexisting tree species to a historic five-year drought event at several sites spanning a climatic gradient.

This work focuses on two long-lived, drought-adapted tree species in California: blue oak (*Quercus douglasii*, Hook. & Arn., Fagaceae) and valley oak (*Quercus lobata*, Née, Fagaceae). These oaks are iconic endemic tree species that coexist with each other in deciduous woodlands in the Mediterranean-climate region of California. In response to the onset of California's historic 2012 - 2016 drought (the region's most severe drought in over 160 years of meteorological records and 1200 years of dendro-climatological reconstructions), I established three study sites across a climate gradient that captured a wide range of variation in historical climate and overall drought exposure. Within these sites, I quantified the differential extent of seasonal water stress and water status recovery until the drought subsided in spring 2016. I found that water stress though each growing season was associated with the restriction of roots to

seasonal precipitation in shallow soil zones compared to deeper soil moisture reserves. Seasonal water status recovery was driven by the extent of water stress experienced during the previous growing season, likely due to promotion of xylem embolism. This lack of recovery was most pronounced in the blue oaks at the most xeric and drought exposed study site, where the greatest extent of canopy damage and mortality was also documented.

To place these results involving water status, canopy damage, and mortality into more of an ecophysiological context, I quantified seasonal changes in the stable isotope composition of leaves and xylem water, and how these changes reflect differential photosynthetic performance of the two species as a function of their capacity to uptake water through the drought. I found that these species had different water acquisition strategies within and across my study sites, likely reflecting differences in root architecture or placement in relation to soil water profiles spread throughout the landscape. These differences translated into differing degrees of carbon fixation through the drought, such that seasonal gas exchange was most inhibited in blue oaks at the most xeric and drought exposed site. Across sites, seasonal reductions in transpiration and water potential in both species were all directly associated with a lack of root access to stable groundwater resources in deeper soils.

To investigate how morphological modifications of the canopy architectures and of the leaves of each species may have allowed for acclimation to the high evaporative demands imposed by the drought, I quantified seasonal changes in leaf size, leaf mass per area, and leaf area-to-sapwood area ratios. I found that large reductions in the number and size of leaves were exhibited by blue oaks at the most xeric and drought exposed site that had roots which were restricted to shallow rooting zones. These reductions consequently reduced the effective leaf area per unit of sapwood area throughout their canopies, which acts to reduce vulnerability to hydraulic failure and drought-induced mortality. Conversely, valley oaks maintained larger leaves and larger leaf area-to-sapwood area ratios through the drought in response to more stable access to deeper groundwater resources. Seasonal changes in leaf mass per area were not observed in either species.

Taken together, these results indicate that the maintenance of physiological water-carbon balance for these species under multiple years of extreme drought is driven by variation in functional rooting depth and its effects on the seasonal trajectories of plant water status, seasonal water status recovery, and canopy architecture modifications, which control the efficiency of gas exchange through growing seasons. Despite the resilience of these oak species to such extreme drought conditions demonstrated in this work under natural, *in-situ* field conditions, their inability to sufficiently acclimate and maintain water-carbon balance can still lead to significant degrees of canopy damage and mortality. With the greatest drought impacts observed in individuals of both species that had more restricted capacities for water acquisition through this historic drought event, this work demonstrates the ecophysiological conditions under which these species are most vulnerable to damage and mortality.

TABLE OF CONTENTS

For my parents, Sharon and Paul,
for their unconditional and boundless love and support.

"I mean, if you've looked at a hundred thousand acres or so of trees – you know, a tree is a tree, how many more do you need to look at?"

– Ronald Reagan, Western Wood Products Association, San Francisco, March 12th, 1966

ACKNOWLEDGEMENTS

One of the most important discoveries that I was fortunate to have made through this work was that scientific progress is best achieved in collaborative academic environments rather than isolationist ones, where mutual aid and the free exchange of diverse intellectual perspectives is celebrated and take precedence over more antiquated, individualistic paths of scientific inquiry. I am incredibly grateful for my advisor David Ackerly for fostering such an inclusive, supportive, and intellectually stimulating academic environment within the lab, for always challenging me as my mentor to become a better and more critical scientist, and for giving me the opportunity both financially and scientifically to perform this research. Completing this dissertation would simply not have been possible without the support of my family as well as many other different people, from extensive amounts of help in the field to many hours working in the lab, as well as with emotional and intellectual support outside of the lab. With that, I would specifically like to thank Blair McLaughlin, Isabel Schroeter, Rob Skelton, Xue Feng, Chris Wong, Jay Scherf, Ken Schwab, and Cameron Williams, who together helped make this research actually happen. I would also like to thank Todd Dawson and Sally Thompson for their intellectual support and for their professional advice as my committee members and academic mentors alike, as well as for their financial support of the years of research that went into this dissertation. I would also of course like to thank everyone in the Ackerly Lab for their help over the past five years with honing down the statistical, graphical, and rhetorical details of my work, as well as simply for being interesting and thoughtful people to work with. I would also like to thank all of my friends both inside and outside of the Department of Integrative Biology for keeping me grounded through this whole process. And of course, all of my love, admiration, and appreciation for my wife Tesla, who was always there for me from the start of this work to its completion.

INTRODUCTION

Drought-induced tree mortality has become one of the most pervasive and ecologically transformative impacts associated with anthropogenic climate change (IPCC 2014, National Climate Assessment 2018), with worldwide events of tree and forest mortality increasingly documented in the scientific literature across diverse ecosystems (Breshears et al. 2005, Adams et al. 2009, Allen et al. 2010, Park Williams et al. 2013, Bennett et al. 2015). Consequently, understanding the physiological causes and ecological consequences of drought-induced tree mortality is critically important to predict and manage the consequences of future drought events around the world (Allen et al. 2015).

Although anthropogenic climate change is expected to increase the frequency, intensity, and duration of climatic droughts around the world (Dai 2013, Cook et al. 2014), predicting the vulnerability of different tree species to drought-induced mortality across the broad climatic, topographic, and environmental conditions that they inhabit is complicated. For example, the physiological impacts of drought can be mediated by spatial heterogeneity in climate and the velocity of climate change across species' ranges (Loarie et al. 2009, Ackerly et al. 2010), as well as variability in climatic microrefugia (Petit et al. 2008, McLaughlin and Zavaleta 2012) and hydrologic refugia (McLaughlin et al. 2017) across the landscape. Consequently, these factors are rarely equally accounted for in drought response modelling efforts that are geared towards predicting mortality risks for different species (Feng et al. 2017), which predominantly focus on the importance of plant hydraulic traits for predicting drought-induced mortality (Choat et al. 2012, Delzon and Cochard 2014, Anderegg et al. 2015a and 2016). Although physiological damage from drought is likely to be associated with hydraulic traits involving embolism formation (Anderegg et al. 2015b, Hartmann et al. 2018), predicting drought-induced water stress and its effect on inducing mortality from such traits alone is not straightforward, because the trajectory of plant water potentials during a drought arises from the interaction of a suite of different interacting plant traits with climate and a complex environment (Feng et al. 2017 and 2018). One of the most complex of these environmental conditions that challenges drought impact predictions is spatial and temporal heterogeneity in subsurface hydrologic dynamics that affect plant available moisture under drought as a function of differing plant functional root architectures (West et al. 2008, Grossiord et al. 2017a, Feng et al. *in press*). Thus, *in-situ* observations of physiological responses of different species to drought paired with characterizations of their subsurface water uptake strategies are essential to link climatic, landscape, and plant-level characteristics to estimates of mortality risk. Moreover, investigating such responses when historic, multi-year drought conditions arise is essential for progressing our understanding of the overall physiological capacities of different plant species to acclimate and survive through them.

Recent advances in stable isotope mass spectrometry have allowed for the quantification of fluxes and stores of water and carbon by plants undergoing drought in variable environments (Herrero et al. 2013, Barbeta et al. 2015, Grossiord et al. 2017a), because stable isotopes can act as excellent indicators and integrators of a variety of different plant physiological processes in response to a range of differing environmental conditions (Dawson et al. 2002). For example, seasonal changes in the stable isotope composition of xylem water in comparison with the isotopic composition of the local meteoric water sources that a given tree is exposed to can

indicate the degree to which it relies on seasonal precipitation stored in shallow soils versus groundwater stored at greater depth from the soil surface (Simonin et al. 2014, Oshun et al. 2016, Benettin et al. 2018). Likewise, seasonal changes in the stable carbon isotope composition of leaves and the carbohydrates they assimilate during photosynthesis can indicate the degree of physiological drought stress a given tree experiences through entire growing seasons, because these carbon isotope ratios are sensitive to temporal changes in stomatal conductance and the biochemical photosynthetic demands for CO_2 as a function of water availability (Farquhar et al. 1982, Brugnoli et al. 1988, and reviewed in Gessler et al. 2014). Nonetheless, field studies investigating *in-situ* drought impacts via seasonally-measured stable isotopes of xylem water and leaf organic matter and are fairly limited, despite the utility of stable isotopes for understanding the mechanistic ecophysiological impacts of extreme drought on plant performance.

In addition to these stable isotope approaches, seasonal measurements of plant traits that reflect different capacities for plasticity in investment, allocation, and acclimation in response to changes in water availability also allow for powerful insights into how different plant species maintain homeostatic water-carbon balance under drought (Grossiord et al. 2017b). Central to these trait modifications are those that reduce canopy-level evaporative demands, which predominantly involve morphological changes in leaf size and leaf mass per area (Quero et al. 2006, Lopez-Iglesias et al. 2014, Enrique et al. 2016), leaf count (Carter and White 2009), and leaf area-to-sapwood area ratios (Mencuccini and Grace 1995, Mencuccini 2002, Bhaskar et al. 2007, McBranch et al. 2018). However, drought response models also tend to fail to incorporate seasonal changes in plant traits under projected warming and drought scenarios, despite the fact that plant physiologists have long demonstrated the ability of plants to seasonally modify such traits in response to rapid changes in water availability. It has therefore become equally important to quantify the *in-situ* morphological responses of different plant species to extreme drought events in order to more accurately assess their vulnerability to drought-induced mortality in the future.

Motivated by these research frontiers, my work in this dissertation utilizes the 2012 - 2016 drought in California, the region's most severe drought in over 160 years of meteorological records and 1200 years of dendro-climatological reconstructions (Griffin and Anchukaitis 2014, Swain 2015), as a natural experiment in which to investigate the *in-situ* physiological responses and water uptake dynamics of two coexisting tree species to exceptionally severe water deficits in the field. My focal study species include blue oak (*Quercus douglasii*, Hook. & Arn., Fagaceae) and valley oak (*Quercus lobata*, Née, Fagaceae), two iconic endemic tree species that coexist with each other in deciduous woodlands in the Mediterranean-climate region of California. These woodlands form among the most diverse and geographically extensive ecosystems within the entire state (Stahle et al. 2013). In this research, I utilize three study sites from Northern to Southern California that captured a wide range of variation in historical climate and overall drought exposure. Across these sites, I measured a suite of morphological and ecophysiological changes in over 80 adult tree individuals from the peak of the drought in the summer of 2014 through its cessation in the spring of 2016. By integrating high resolution seasonal precipitation and climate water deficit estimates throughout the drought (Flint et al. 2013), this work examines how spatial variation in climate, topography, and drought exposure translated into differing physiological impacts between these two species, with the aim of

understanding the specific environmental conditions and mechanistic physiological responses that give rise to tree damage and mortality.

In Chapter 1, I tested the effects of growing season water stress, its effect on exceeding water potential thresholds of xylem embolism formation, and variation in root water uptake dynamics on the extent of seasonal water potential recovery, canopy damage, and mortality between each species. To accomplish this, I measured predawn and midday shoot water potentials and collected canopy shoot samples for stable isotope analysis of xylem water. I also quantified tree mortality and canopy damage through the drought period. These data were then paired with optical measurements of shoot xylem embolism formation thresholds of each species, and isotopic signatures of xylem water that reflect utilization of different soil water zones.

In Chapter 2, I tested the effects of differing soil water acquisition strategies in these two species on their relative ability to assimilate carbon through the drought, and identified the physiological pathways governing differential degrees of photosynthetic performance across the climatic, topographic, and drought exposure gradients captured by my study sites. To accomplish this, I measured temporal changes in the stable isotope composition of xylem water of each species through the drought period, and paired them with seasonal measurements of predawn and midday plant water status. These water status measurements were then tested as a function of measurements of midday stomatal conductance, which were then tested as a function of the foliar c_i concentrations derived from stable isotope measurements of leaves and leaf photosynthate. In doing so, I focused on bulk leaf c_i and leaf sugar c_i as seasonally- and daily-integrated measurements of carbon fixation as a function of water limitation through the drought period.

In Chapter 3, I tested the effects of drought exposure and differential water acquisition capacities between these species on seasonal changes in the functional and structural responses of their leaves and sapwood area (a proxy for water delivery to leaves). To accomplish this, I measured seasonal changes in leaf size, leaf mass per area, and shoot-level leaf area-to-sapwood area ratios from summer 2014 - fall 2015, and tested them as a function of the changes in drought exposure that my study sites capture.

Though this work, I demonstrate that although both species can exhibit extensive degrees of morphological and physiological acclimation to years of extreme drought and are incredibly resilient in the face of such conditions, both species are still prone to damage and mortality under certain circumstances. Identifying the ecophysiological context underlying these circumstances is precisely what is required for successfully predicting and managing the consequences of future drought events across the wide ranges of climatic, topographic, and environmental conditions that they inhabit throughout the state.

REFERENCES

Ackerly, D.D., Loarie, S.R., Cornwell, W.K., Weiss, S.B., Hamilton, H., Branciforte, R. and Kraft, N.J.B., 2010. The geography of climate change: implications for conservation biogeography. *Diversity and Distributions*, 16(3), pp.476-487.

Adams, H.D., Guardiola-Claramonte, M., Barron-Gafford, G.A., Villegas, J.C., Breshears, D.D., Zou, C.B., Troch, P.A. and Huxman, T.E., 2009. Temperature sensitivity of drought-induced tree mortality portends increased regional die-off under global-change-type drought. *Proceedings of the National Academy of Sciences*, 106(17), pp.7063-7066.

Allen, C.D., Macalady, A.K., Chenchouni, H., Bachelet, D., McDowell, N., Vennetier, M., Kitzberger, T., Rigling, A., Breshears, D.D., Hogg, E.T. and Gonzalez, P., 2010. A global overview of drought and heat-induced tree mortality reveals emerging climate change risks for forests. *Forest Ecology and Management*, 259(4), pp.660-684.

Allen, C.D., Breshears, D.D. and McDowell, N.G., 2015. On underestimation of global vulnerability to tree mortality and forest die-off from hotter drought in the Anthropocene. *Ecosphere*, 6(8), pp.1-55.

Anderegg, W.R., Hicke, J.A., Fisher, R.A., Allen, C.D., Aukema, J., Bentz, B., Hood, S., Lichstein, J.W., Macalady, A.K., McDowell, N. and Pan, Y., 2015a. Tree mortality from drought, insects, and their interactions in a changing climate. *New Phytologist*, 208(3), pp.674-683.

Anderegg, W.R., Flint, A., Huang, C.Y., Flint, L., Berry, J.A., Davis, F.W., Sperry, J.S. and Field, C.B., 2015b. Tree mortality predicted from drought-induced vascular damage. *Nature Geoscience*, 8(5), p.367.

Anderegg, W.R., Klein, T., Bartlett, M., Sack, L., Pellegrini, A.F., Choat, B. and Jansen, S., 2016. Meta-analysis reveals that hydraulic traits explain cross-species patterns of drought-induced tree mortality across the globe. *Proceedings of the National Academy of Sciences*, 113(18), pp.5024-5029.

Barbeta, A., Mejía-Chang, M., Ogaya, R., Voltas, J., Dawson, T.E. and Peñuelas, J., 2015. The combined effects of a long-term experimental drought and an extreme drought on the use of plant-water sources in a Mediterranean forest. *Global Change Biology*, 21(3), pp.1213-1225.

Benettin, P., Volkmann, T.H., Freyberg, J.V., Frentress, J., Penna, D., Dawson, T.E. and Kirchner, J.W., 2018. Effects of climatic seasonality on the isotopic composition of evaporating soil waters. *Hydrology and Earth System Sciences*, 22(5), pp.2881-2890.

Bennett, A.C., McDowell, N.G., Allen, C.D. and Anderson-Teixeira, K.J., 2015. Larger trees suffer most during drought in forests worldwide. *Nature Plants*, 1(10), p.15139.

Bhaskar, R., Valiente-Banuet, A. and Ackerly, D.D., 2007. Evolution of hydraulic traits in closely related species pairs from mediterranean and nonmediterranean environments of North America. *New Phytologist*, 176(3), pp.718-726.

Breshears, D.D., Cobb, N.S., Rich, P.M., Price, K.P., Allen, C.D., Balice, R.G., Romme, W.H., Kastens, J.H., Floyd, M.L., Belnap, J. and Anderson, J.J., 2005. Regional vegetation die-off in response to global-change-type drought. *Proceedings of the National Academy of Sciences*, 102(42), pp.15144-15148.

Brugnoli, E., Hubick, K.T., von Caemmerer, S., Wong, S.C. and Farquhar, G.D., 1988. Correlation between the carbon isotope discrimination in leaf starch and sugars of C3 plants and the ratio of intercellular and atmospheric partial pressures of carbon dioxide. *Plant Physiology*, 88(4), pp.1418-1424.

Carter, J.L. and White, D.A., 2009. Plasticity in the Huber value contributes to homeostasis in leaf water relations of a mallee Eucalypt with variation to groundwater depth. *Tree Physiology*, 29(11), pp.1407-1418.

Choat, B., Jansen, S., Brodribb, T.J., Cochard, H., Delzon, S., Bhaskar, R., Bucci, S.J., Feild, T.S., Gleason, S.M., Hacke, U.G. and Jacobsen, A.L., 2012. Global convergence in the vulnerability of forests to drought. *Nature*, 491(7426), p.752.

Cook, B.I., Smerdon, J.E., Seager, R. and Coats, S., 2014. Global warming and 21st century drying. *Climate Dynamics*, 43(9-10), pp.2607-2627.

Dai, A., 2013. Increasing drought under global warming in observations and models. *Nature Climate Change*, 3(1), p.52.

Dawson, T.E., Mambelli, S., Plamboeck, A.H., Templer, P.H. and Tu, K.P., 2002. Stable isotopes in plant ecology. *Annual Review of Ecology and Systematics*, 33(1), pp.507-559.

Delzon, S. and Cochard, H., 2014. Recent advances in tree hydraulics highlight the ecological significance of the hydraulic safety margin. *New Phytologist*, 203(2), pp.355-358.

Enrique, G., Olmo, M., Poorter, H., Ubera, J.L. and Villar, R., 2016. Leaf mass per area (LMA) and its relationship with leaf structure and anatomy in 34 Mediterranean woody species along a water availability gradient. *PloS one*, 11(2), p.e0148788.

Farquhar, G.D., O'Leary, M.H. and Berry, J.A., 1982. On the relationship between carbon isotope discrimination and the intercellular carbon dioxide concentration in leaves. *Functional Plant Biology*, 9(2), pp.121-137.

Feng, X., Dawson, T.E., Ackerly, D.D., Santiago, L.S. and Thompson, S.E., 2017. Reconciling seasonal hydraulic risk and plant water use through probabilistic soil–plant dynamics. *Global Change Biology*, 23(9), pp.3758-3769.

Feng, X., Ackerly, D.D., Dawson, T.E., Manzoni, S., Skelton, R.P., Vico, G. and Thompson, S.E., 2018. The ecohydrological context of drought and classification of plant responses. *Ecology Letters*, 21(11), pp.1723-1736.

Feng, X., Ackerly, D.D., Dawson, T.E., Manzoni, S., McLaughlin, B.C., Skelton, R.P., Vico, G., Weitz, A.P., Thompson, S.E., 2018. Beyond isohydricity: the role of environmental variability in determining plant drought responses. *Plant, Cell & Environment*, *in press*.

Flint, L.E., Flint, A.L., Thorne, J.H., Boynton, R., 2013. Fine-scale hydrologic modeling for regional landscape applications: the California Basin Characterization Model development and performance. *Ecological Processes*, 2(5), pp.1-21.

Gessler, A., Ferrio, J.P., Hommel, R., Treydte, K., Werner, R.A. and Monson, R.K., 2014. Stable isotopes in tree rings: towards a mechanistic understanding of isotope fractionation and mixing processes from the leaves to the wood. *Tree Physiology*, 34(8), pp.796-818.

Griffin, D. and Anchukaitis, K.J., 2014. How unusual is the 2012–2014 California drought? *Geophysical Research Letters*, 41(24), pp.9017-9023.

Grossiord, C., Sevanto, S., Dawson, T.E., Adams, H.D., Collins, A.D., Dickman, L.T., Newman, B.D., Stockton, E.A. and McDowell, N.G., 2017a. Warming combined with more extreme precipitation regimes modifies the water sources used by trees. *New Phytologist*, 213(2), pp.584-596.

Grossiord, C., Sevanto, S., Adams, H.D., Collins, A.D., Dickman, L.T., McBranch, N., Michaletz, S.T., Stockton, E.A., Vigil, M. and McDowell, N.G., 2017b. Precipitation, not air temperature, drives functional responses of trees in semi-arid ecosystems. *Journal of Ecology*, 105(1), pp.163-175.

Hartmann, H., Moura, C.F., Anderegg, W.R., Ruehr, N.K., Salmon, Y., Allen, C.D., Arndt, S.K., Breshears, D.D., Davi, H., Galbraith, D. and Ruthrof, K.X., 2018. Research frontiers for improving our understanding of drought-induced tree and forest mortality. *New Phytologist*, 218(1), pp.15-28.

Herrero, A., Castro, J., Zamora, R., Delgado-Huertas, A. and Querejeta, J.I., 2013. Growth and stable isotope signals associated with drought-related mortality in saplings of two coexisting pine species. *Oecologia*, 173(4), pp.1613-1624.

IPCC, 2014: Climate Change 2014: Synthesis Report. Contribution of Working Groups I, II and III to the Fifth Assessment Report of the Intergovernmental Panel on Climate Change [Core Writing Team, R.K. Pachauri and L.A. Meyer (eds.)]. IPCC, Geneva, Switzerland, 151 pp.

Loarie, S.R., Duffy, P.B., Hamilton, H., Asner, G.P., Field, C.B. and Ackerly, D.D., 2009. The velocity of climate change. *Nature*, 462(7276), p.1052.

Lopez-Iglesias, B., Villar, R. and Poorter, L., 2014. Functional traits predict drought performance and distribution of Mediterranean woody species. *Acta Oecologica*, 56, pp.10-18.

McBranch, N.A., Grossiord, C., Adams, H., Borrego, I., Collins, A.D., Dickman, T., Ryan, M., Sevanto, S., McDowell, N.G. and Maurizio, M., 2018. Lack of acclimation of leaf area: sapwood area ratios in piñon pine and juniper in response to precipitation reduction and warming. *Tree Physiology*, *in press*.

Mencuccini, M. and Grace, J., 1995. Climate influences the leaf area/sapwood area ratio in Scots pine. *Tree Physiology*, 15(1), pp.1-10.

Mencuccini, M., 2002. Hydraulic constraints in the functional scaling of trees. *Tree Physiology*, 22(8), pp.553-565.

National Climate Assessment, 2018. Volume II: Impacts, Risks, and Adaptation in the United States. US Global Change Research Program.

Oshun, J., Dietrich, W.E., Dawson, T.E. and Fung, I., 2016. Dynamic, structured heterogeneity of water isotopes inside hillslopes. *Water Resources Research*, 52(1), pp.164-189.

Park Williams, A., Allen, C.D., Macalady, A.K., Griffin, D., Woodhouse, C.A., Meko, D.M., Swetnam, T.W., Rauscher, S.A., Seager, R., Grissino-Mayer, H.D. and Dean, J.S., 2013. Temperature as a potent driver of regional forest drought stress and tree mortality. *Nature Climate Change*, 3(3), p.292.

Petit, R.J., Hu, F.S. and Dick, C.W., 2008. Forests of the past: a window to future changes. *Science*, 320(5882), pp.1450-1452.

Quero, J.L., Villar, R., Marañón, T. and Zamora, R., 2006. Interactions of drought and shade effects on seedlings of four Quercus species: physiological and structural leaf responses. *New Phytologist*, 170(4), pp.819-834.

Simonin, K.A., Link, P., Rempe, D., Miller, S., Oshun, J., Bode, C., Dietrich, W.E., Fung, I. and Dawson, T.E., 2014. Vegetation induced changes in the stable isotope composition of near surface humidity. *Ecohydrology*, 7(3), pp.936-949.

Stahle, D.W., Griffin, R.D., Meko, D.M., Therrell, M.D., Edmondson, J.R., Cleaveland, M.K., Stahle, L.N., Burnette, D.J., Abatzoglou, J.T., Redmond, K.T. and Dettinger, M.D., 2013. The ancient blue oak woodlands of California: Longevity and hydroclimatic history. *Earth Interactions*, 17(12), pp.1-23.

Swain, D.L., 2015. A tale of two California droughts: Lessons amidst record warmth and dryness in a region of complex physical and human geography. *Geophysical Research Letters*, 42(22), pp.9999-10.

West, A.G., Hultine, K.R., Sperry, J.S., Bush, S.E. and Ehleringer, J.R., 2008. Transpiration and hydraulic strategies in a piñon–juniper woodland. *Ecological Applications*, 18(4), pp.911-927.

CHAPTER 1

Failure to recover water status through years of extreme drought due to variation in minimum water potential, functional root distributions, and xylem embolism accumulation in Californian blue oak and valley oak

ABSTRACT

The historic 2012-2016 Californian drought provided an unprecedented opportunity to investigate the *in-situ* responses of different plant species to severe water deficit, including inferred hydraulic failure and drought-induced damage and mortality. From summer 2014 – spring 2016, I monitored a suite of physiological indicators in adult blue oaks (*Quercus douglasii*, Fagaceae) and valley oaks (*Q. lobata*) across three sites. These sites spanned a gradient of climate and drought severity as measured by seasonal precipitation and climatic water deficit through the drought period, with 44 % - 56 % reductions in precipitation and 14% - 18% increases in climatic water deficit relative to 30-year site means. During the late spring and late summer at each site, I measured predawn and midday shoot water potentials (Ψ) and collected canopy shoot samples for stable isotope analysis of xylem water. I also quantified tree mortality and canopy damage through the drought period. These data were paired with optical measurements of shoot xylem embolism formation thresholds of these oak species, and isotopic signatures of xylem water that reflect utilization of different soil water zones.

Both oak species experienced shoot water potentials below their stem air-entry embolism thresholds (P_e). Following winter rains, trees at the northern and central Californian sites were able to recover their shoot water potentials to a relatively consistent spring value. At the more xeric southern Californian site, which had the greatest climatic water deficits and least precipitation, this spring-recovery only occurred for a subset of the monitored trees. At this site, failure to recover spring water potentials was associated with the magnitude of isotopic departure of xylem water from its local meteoric water line, as well as the extent to which minimum water potentials exceeded xylem P_e thresholds. Additionally, trees at this site exhibited the greatest canopy damage and mortality. I infer that the trees that did not recover spring water potentials repeatedly accumulated xylem emboli in their stems through the growing season of each subsequent drought year, predisposing them to higher mortality risk. These results exhibit how under natural field conditions, a reliance on seasonal precipitation in shallow soil zones during extreme drought conditions combined with repeated xylem embolism accumulation reduces the capacity for these tree species to recover and maintain functional water status, thus compromising their ability to survive the recurrent impacts of canopy damage.

INTRODUCTION

Anthropogenic climate change is expected to increase the frequency, intensity, and duration of climatic droughts around the world (Dai 2013, Cook et al. 2014), with one of the consequences expected to be widespread episodes of tree and forest mortality (Allen et al. 2010). Indeed, tree mortality in response to drought is now widely documented across diverse ecosystems (Adams et al. 2009, Allen et al. 2010, Park Williams et al. 2013). Consequently, understanding the physiological causes and ecological consequences of drought-induced tree mortality is critically important to predict and manage the consequences of future drought events around the world (Allen et al. 2015).

A thorough understanding of the physiological mechanisms underlying drought-induced tree mortality remains contested due to the difficulty in resolving the relative roles of carbon starvation, hydraulic failure, biotic attack by pests and pathogens, and their interactions in causing tree damage and mortality (McDowell et al. 2008, Sala et al. 2010, Delzon and Cochard 2014, Anderegg et al. 2015a). Nonetheless, plant hydraulic traits that convey resistance to embolism formation in xylem tissues have emerged as important predictors of species' ability to tolerate, survive, and recover from drought events (Choat et al. 2012, Delzon and Cochard 2014, Anderegg et al. 2016). Xylem emboli impose physical inhibitions on plant hydraulic conductance. Thus, if drought causes plant water potential thresholds to drop below the air-entry water potential at which xylem begin to embolize (P_e), hydraulic recovery after post-drought soil rehydration may be impaired (Skelton et al. 2017). Instances of plants experiencing more extreme degrees of xylem embolism formation, e.g., at or above P_{88} (i.e. water potentials coinciding with 88 % cavitation of the hydraulic architecture), are associated with irreversible physiological damage and mortality (Choat 2013, Urli et al. 2013).

Although drought damage is likely to be associated with xylem embolism traits (Anderegg et al. 2015b, Hartmann et al. 2018), predicting drought-induced water stress from such traits alone is not straightforward, because the trajectory of leaf and shoot water potentials during a drought arises from the interaction of a suite of plant traits with climate and a complex environment (Feng et al. 2017, Feng et al. 2018 and *in press*). Predicting population-level drivers of seasonal water potential recovery from drought stress across broad climatic, topographic, and environmental conditions is equally complicated. For example, thermal and hydrological micro-refugia may ameliorate the negative effects of climatic drought on plant water status and health, and the degree of drought severity can vary across and within species' geographic ranges (McLaughlin and Zavaleta 2012, McLaughlin et al. 2017). In California, climate change is not only expected to increase drought intensity and duration, but also the variability of climate across the landscape (Diffenbaugh et al. 2015, Swain et al. 2016). Moreover, this climatic variability propagates into spatial and temporal variations in subsurface water availability, directly affecting the distribution of species' functional roots and their ability to uptake water during periods of drought (West et al. 2008, Grossiord et al. 2017). Thus, *in-situ* observations of physiological responses to drought paired with characterizations of subsurface water uptake strategies are essential to link climatic, landscape, and plant-level characteristics to estimates of mortality risk.

With this motivation, I used the 2012 – 2016 California drought, the region's most severe drought in over 160 years of meteorological records and 1200 years of dendro-climatological

reconstructions (Griffin and Anchukaitis 2014, Swain 2015), as a natural experiment in which to investigate the physiological responses and water uptake dynamics of two long-lived oak species to exceptionally severe precipitation deficits in the field. In California's Mediterranean-type climate, plant water availability fluctuates seasonally, even during the course of a multi-year drought, with water availability generally being greatest following winter rains and lowest at the end of the dry summer growing season. One indicator of physiological stress is thus the degree to which plant water potentials fail to increase to more positive water potential values following winter rains. I refer to the magnitude of this increase as the *recovery of spring water potentials*, and hypothesize that:

H1: The degree of spring water potential recovery is reduced in trees that experience more negative minimum water potentials during the previous growing season.
H2: The degree of spring water potential recovery is reduced in trees with functional roots that are more reliant on seasonal precipitation via shallow soils rather than groundwater via deeper soils.
H3: The degree of spring water potential recovery is reduced in trees that experience minimum water potentials that exceed their air-entry xylem embolism thresholds (P_e).

To test these hypotheses, I monitored a suite of physiological characteristics in adult blue oaks (*Quercus douglasii*, Fagaceae) and valley oaks (*Q. lobata*) from the peak of the drought in 2014 to its cessation in spring 2016. These oaks are drought-adapted, long-lived species with geographic ranges spanning the core of the Mediterranean-climate region of California. They coexist with each other in woodlands and savannas, making them ideal candidates for investigating species- and site-specific drought impacts. Physiological measurements were made at three study sites that spanned a range of climate and drought severity conditions, and which covered a substantial extent of the oak species' geographic ranges. Drought conditions associated with each plant's location within and across the study sites were estimated by integrating high resolution seasonal precipitation and climate water deficit estimates throughout the drought (Flint et al. 2013). I measured predawn and midday water potentials in multiple individuals ($6 \leq n \leq 19$ of each species per site) during late spring and late summer, and quantified tree mortality and canopy damage. My analysis incorporated recently-derived shoot xylem embolism thresholds for both species (Skelton et al. 2018), which were generated using an optically-based method (Brodribb et al. 2017). Lastly, I analyzed the stable isotope ratios of shoot xylem water each season and quantified their degree of isotopic departure from each site's local meteoric water line to characterize the variation in water uptake dynamics through the drought period (Benettin et al. 2018).

MATERIALS AND METHODS

Study species, site selection, and study design

Blue oak (*Quercus douglasii*, Hook. & Arn., Fagaceae) and valley oak (*Quercus lobata*, Née, Fagaceae) are iconic California endemic tree species that coexist in woodlands and savannas throughout the foothills of the Sierra Nevada and Coast Range Mountains (Griffin and Critchfield 1972). Both species are winter deciduous. Leaves senesce at the end of the growing

season in the fall and flush in the following spring. Both species are well adapted to seasonal drought (Griffin 1971, 1973) and have been routinely documented to live from 200 to more than 500 years old (Griffin 1976, Stahle et al. 2013). Thus, they are excellent candidates in which to investigate extreme drought effects on plant physiological response.

To capture the variation in drought exposure across the geographic range of these two species, three study sites were selected: Pepperwood Preserve in Sonoma County (PW), the Blue Oak Ranch Reserve in Santa Clara County (BORR), and a private ranch in San Luis Obispo County referred to here as "the Cattle Ranch" (CR) (Figure 1). Within each site, three subsites were selected along a topographic gradient from hilltop to valley-bottom, with the aim of capturing within-site variations in drought severity and water availability. At each subsite, at least three coexisting adult trees per species were identified for study. Due to differences in the abundance of coexisting trees per species at the subsites, the total sample sizes of *Q. lobata* are smaller at two sites (Table 1).

To capture seasonal variation in plant water status and thus get partial insight into environmental water availability, field campaigns of water potential measurements were conducted in spring (early growing season), summer (peak growing season), and fall (end of growing season). Measurement campaigns began in summer of 2014 at the peak of the drought. Measurements concluded in spring of 2016. Dates for all campaigns at each site are reported in Table 2.

Climate and spatial water deficit

Climate was characterized at 10 m scales for each study site using an unpublished downscaling of the California Basin Characterization Model (CA-BCM) (Flint et al. 2013). CA-BCM is a fine-scale regional water balance hydrological model that integrates historical and contemporary climate data to estimate climatic water deficit (a measurement of cumulative energy load in excess of water supply) on daily timescales. Macroclimate variables from the model are downscaled from PRISM (Daly et al. 2008). The 10 m resolution incorporates fine-scale influences of topography on potential evapotranspiration (PET), and the role of soil water storage during the dry season. Data were obtained from the 1981 water year (beginning October 1st, 1980) through the end of the water year of 2016 (ending September 30th, 2016). The primary climate variables obtained from CA-BCM include precipitation (PPT, mm) and climatic water deficit (CWD, mm), the quantity of water when PET is in excess of actual evapotranspiration (AET) (Stephenson 1998). Average conditions were computed per water-year month over the water year period of 1981 – 2010. The weather conditions and the monthly trajectory of climatic water deficit for each site during each water year of the drought (2012 – 2016) were then calculated by averaging the monthly climate values for each tree location. Average annual PPT and CWD values for each site and accumulated annual values during the drought period are reported in Table 3. Accumulating monthly PPT and CWD values through the drought period at each site are plotted in Figure 2.

Plant water status in response to water deficit

To quantify seasonal changes in plant water status as a function of changes in plant available moisture through the drought, measurements of xylem water potential were made on terminal

canopy shoots both before the onset of dawn (predawn Ψ [MPa], interpreted as a measure of plant water availability) and in the middle of the day (midday Ψ [MPa], interpreted as the peak water stress) on all trees during each field campaign. Samples of terminal, sun-exposed canopy shoots were excised with razor blades, immediately air-sealed in plastic bags, and transported in light-proof coolers prior to measurement to minimize water loss and changes in water potential after collection. All samples were measured $\leq$ 5 min after collection using cross-calibrated Scholander pressure chambers (PMS Instrument Company, Corvallis, OR, USA). Two shoot samples were measured for each tree and averaged. Specific water potential measurement dates for all five seasonal campaigns at each site are reported in Table 2, and the seasonal trajectories of predawn and midday water potential values for blue oak and valley oak are plotted in Figures 3 and 4, respectively. These data were then used to test my first hypothesis (**H1**) that spring water potential values will be reduced in trees that experience more negative minimum water potentials at the end of the prior dry season.

Xylem water isotopes and local meteoric water lines

To determine the seasonal dynamics of root water uptake through the drought, I analyzed the isotopic composition of xylem water of all study trees during each measurement campaign following Dawson and Ehleringer (1993). I accomplished this by collecting approximately 30 cm long pieces of stem tissue during the day from terminal, sun-exposed regions of each tree's canopy. Immediately upon their collection, these stem samples were sealed in air-tight cryogenic vials using Parafilm prevent evaporative water loss from samples. The vials were stored in dry ice to further impede the effects of evaporative isotopic enrichment on xylem waters. All samples were stored in freezers prior to extraction of xylem waters using cryogenic vacuum distillation following (West et al. 2006) at the Center for Stable Isotope Biogeochemistry (CSIB) at UC Berkeley. Subsequent stable isotope analysis of extracted xylem water was also performed at the CSIB. For determining xylem water $\delta^{18}O$ values, a GasBench II (Thermo Fisher Scientific, Waltham, MA, USA) was linked to a Delta Plus XL isotope ratio mass spectrometer (Thermo Fisher Scientific) via continuous flow. For determining xylem water $\delta^{2}H$ values, an H/Device (Finnigan MAT GmbH, Bremen, Germany) was used for hot chromium hydrogen reduction, which was connected via dual inlet to a Delta Plus XL isotope ratio mass spectrometer (Thermo Fisher Scientific). All stable isotope ratios are herein expressed in 'per-mil' or ‰ notation as:

$$\delta^{18}O \text{ or } \delta^{2}H \text{ (in ‰)} = (R_{sample} / R_{standard} - 1)1000, \qquad (1)$$

where R_{sample} and $R_{standard}$ are the respective isotope ratios for each sample type and its IAEA approved standard. The $^{18}O/^{16}O$ and $^{2}H/^{1}H$ ratios of samples is referenced to the $^{18}O/^{16}O$ and $^{2}H/^{1}H$ ratios of the 'Vienna-SMOW' or VSMOW standard, respectively (Coplen 1995). Specific stem collection dates for all five seasonal campaigns at each site are reported in Table 2.

To characterize the variation in the stable isotope composition of precipitation at my sites, I constructed or derived a local meteoric water line (LMWL) for each (Craig 1961, Dansgaard 1964). As I was not able to sample rainwater at each site under drought conditions and build my own LMWL's, I obtained modeled precipitation isotope values using the Online Isotopes in Precipitation Calculator (OIPC) (Welker 2000, Bowen et al. 2005, Bowen 2018). I derived each site's LMWL equation using linear regression on monthly isotope outputs from the OIPC. To

ensure their accuracy, I compared my derived LMWL equation for BORR to an LMWL equation previously derived for this site using actual monthly precipitation samples (T.E. Dawson, unpublished) and found that they were almost identical, with slopes and *d*-excess differing by only 3 % (Appendix Table S1). Therefore, I am confident in the utility of these derived LMWL's in characterizing the isotopic composition of precipitation at each of my three sites.

To quantify the degree of evaporative enrichment processes on the water obtained by each tree during each spring recovery comparison, I calculated the minimum Euclidean distance of these spring growing season xylem water isotope values normal to each site's LMWL (Figure 5). The Euclidean distance of these values in dual-isotope space (δ^2H as a function of $\delta^{18}O$, ‰ VSMOW) away from the LMWL reflects the magnitude of each tree's uptake of soil water that has undergone fractionation effects in response to evaporation. It can therefore be used to understand the degree to which trees rely on seasonal precipitation stored in shallow soils versus groundwater stored at greater depth from the soil surface (Simonin et al. 2014, Oshun et al. 2016, Benettin et al. 2018). LMWL distances were calculated using:

$$\text{LMWL distance} = (ax_0 + by_0 + c) / \text{sqrt}(a^2 + b^2), \qquad (2)$$

where (x_0, y_0) are dual-isotope coordinates normal to an LMWL equation $ax + by + c = 0$. I refer to these distances here as LWML departure, and use them to test my second hypothesis (**H2**) that utilization of precipitation via shallow, evaporatively enriched soil water during spring growing seasons of the drought is correlated with a reduction in the recovery of spring water potentials.

Xylem vulnerability to embolism formation

To relate the extent of xylem embolism accumulation to the *in-situ* shoot water potential measurements conducted through the study, I use the recently published shoot air-entry water potential thresholds (P_e) for the two study species (Skelton et al. 2018). I specifically focus on shoot P_e rather than leaf P_e because I conducted my water potential measurements on branch shoots rather than on individual leaves. Nonetheless, for context I include the optical vulnerability curves for both leaves and stems of each oak species in Figure 6 as well as all relevant derived embolism thresholds (P_{12}, P_{50}, and P_{88}) in Table 4.

Although exceedance of the P_e thresholds of plant leaves and stems is not necessarily lethal, exceeding these values suggests that tissues have experienced embolism (Delzon and Cochard 2014). Because embolism has been routinely observed to be a non-recoverable process that directly reduces xylem hydraulic conductance, particularly in long-vesseled tree genera such as *Quercus* (Choat et al. 2018), I hypothesize that the extent to which the most negative minimum seasonal water potential of trees surpasses the air-entry embolism threshold P_e negatively affects the ability of these trees to recover their water potential the following spring. I test this hypothesis (**H3**) by quantifying the numerical extent (in MPa) that each tree exceeded this threshold in the field, where trees that did not surpass this threshold are scored as 0 MPa and any cumulative degree of numerical excess from stem P_e in MPa is enumerated via:

$$P_e \text{ excess} = \Psi_{\text{minimum}} - P_{e\ \text{stem}} \qquad (3)$$

Tree mortality and canopy damage

Every study tree was surveyed during each field campaign for physical and physiological indicators of canopy dieback and mortality. These indicators included presence/absence of swollen buds throughout terminal canopy branches during spring campaigns, the presence and persistence of live versus senesced leaves, and whether a field water potential measurement could be obtained. Terminal canopy branches without swollen buds indicated canopy dieback during the previous growing season; leaf senescence indicated within-season drought-induced damage, and the inability to obtain field water potential measurements indicated that stems were dehydrated and presumably dead. When these criteria indicated that a tree had died, the tree was re-surveyed in all subsequent campaigns for confirmation.

By the end of the 2016 water year, field measurements were complete and the drought had abated. In spring 2017, historically average rainfall had occurred again at each site and trees had sufficient time to flush new leaves. At this time, an additional survey of canopy damage was conducted to quantify the extent of overall drought-induced canopy dieback at each site. All previously documented instances of mortality were confirmed during this survey. Additionally, the presence or absence of epicormic resprouting events was recorded. I interpret new epicormic growth occurring in trees where the canopy is devoid of new terminal growth as a direct reflection that embolism-induced canopy dieback occurred. Together, these data were used to determine whether or not drought-induced canopy damage and/or mortality was greater among trees in sites where they exceeded their air-entry xylem embolism thresholds and failed to recover their seasonal water potentials.

Statistical analyses

To test my three hypotheses involving the relative effects of minimum water potential (**H1**), LMWL departure (**H2**), and P_e excess (**H3**) on the extent of spring water potential recovery, I took a multiple generalized linear regression approach for each of these three predictor variables. Because my study encompassed two distinct spring growing seasons (spring 2015 and spring 2016) preceded by two fall growing seasons (fall 2014 and fall 2015), I statistically treated each spring water potential recovery period separately from its previous fall campaign. Thus, these two spring recovery campaigns test each of these three hypotheses in distinct generalized linear regression models (n = 6 models total). The spring predawn water potential values for each recovery season were treated as the response variables in all models (i.e. the ability to recover seasonal water status), each accounting for three-way interactions between sites, species, and each of my three predictor variables. Significance tests for each coefficient factor in each model was performed using Type III ANOVA to account for all three-way model interactions.

To infer the effects of exceeding P_e during the growing season and failing to recover water status on experiencing canopy damage and tree mortality across my sites, I report the cumulative results of my canopy damage and mortality rate surveys through the entirety of the study period. These data are presented as proportions of study trees in each site that exhibited signs of canopy damage and epicormic resprouting, and proportions of study trees in each site that ended up dying within the course of the study, respectively.

All statistical analyses and figures were produced using the R statistical platform (R Core Team 2017) and the following packages: *raster* (Hijmans 2016), *maptools* (Bivand and Lewin-Koh 2017), *sp* (Pebesma and Bivand 2005, Bivand et al. 2013), *rgdal* (Bivand et al. 2017), *car* (Fox and Weisberg 2011), *dplyr* (Wickham et al. 2017), and *ggplot2* (Wickham 2009).

RESULTS AND DISCUSSION

Spatial variation in historical climate and drought intensity

My three study sites exhibited a strong spatial gradient in historical climate with respect to mean annual precipitation and mean accumulated climatic water deficit (Table 3). By the 2012 water year, these sites began to repeatedly experience historically low levels of accumulated water year precipitation and historically high levels of climatic water deficit each subsequent year (Figure 2). There was a north-to-south gradient in the comparative mean historical precipitation and climatic water deficit across all three sites, with PW being the most mesic of the three, BORR at intermediate levels of precipitation and climatic water deficit, and CR being the most xeric. Total average rainfall at PW was approximately twice that at BORR, which was approximately twice that of CR, and this pattern remained consistent throughout the drought (Table 3). At the start of the study in the summer of 2014, all sites had been experiencing what would be the most extreme individual year of the five-year drought period, with low levels of precipitation and very high levels of climatic water deficit. During this year, rainfall was 44% - 56% reduced across sites, and CWD had increased 14% - 18% relative to 30-year site means. With the exception of the 2016 water year at BORR, all seasons sampled were well below average rainfall and above average CWD. Water years 2012, 2013, and 2015 were also consistently below average across all sites with respect to accumulated precipitation, and by extension, were also consistently above average with respect to climatic water deficit. In all years, winter precipitation ended in late April, supporting the timing of my spring measurement campaigns (Figure 2). These conditions collectively reflect just how severe this drought was, and the three study sites were able to capture different degrees of this severity.

The effect of minimum water potential on spring recovery (H1)

My first pair of models testing **H1** yielded contrasting results for the effects of minimum water potential on water potential recovery in 2015 and 2016. For spring water potential recovery in 2015, I found a significant two-way interaction between site and 2014 minimum water potential (Table 5, LR chisquare 26.453, $P < 0.001$). Comparing these slopes shows just how dramatic the lack of recovery of trees at CR was compared to PW and BORR in response to the absolute minimum water potential reached during the previous fall (Figure 7a). Although the minimum water potential values that trees experienced at PW and BORR were just as negative as those experienced at CR in fall 2014, they all recovered to much more positive water potentials compared to trees at CR, which exhibited significantly reduced recovery (Figures 3 and 4). However, for spring water potential recovery in 2016, there were neither significant main effects nor interactions of any coefficients (Figure 8a, Table 6). Just like in the previous year, all trees at PW and BORR recovered from very low water potentials again despite how negative their water potentials declined at the end of the 2015 growing season. Though trees at CR trend towards

reduced recovery in response to minimum water potential (Figure 9a), I interpret this lack of significance as a potential sign of a physiological decoupling of water potential in these trees from declining soil water potentials. Though this behavior has previously been described to be 'isohydric' (McDowell et al. 2008), I assert that other hydrological characteristics discussed below in my test of **H2** involving soil water resources can further explain why trees at CR failed to recover while those at PW and BORR did not.

The effect of LMWL departure on spring recovery (H2)

My second pair of models testing **H2** revealed the importance of functional root distributions and access to stable soil water resources on the recovery of spring water potentials. For spring water potential recovery in 2015, I found that water potential recovery was significantly associated with a three-way interaction between site, species, and the magnitude of departure plants showed from the LMWL (Table 5, LR chisquare 7.276, $P = 0.0263$). Blue oaks at CR were most significantly affected and showed that they were drawing their water from a shallow, evaporatively enriched soil water zone (i.e. the stable isotope values of plant waters showed the greatest departure from the CR LMWL). Reliance on shallow moisture during the severe drought lead to an inability to recover their water status (Figure 7b). This result is further supported in the recovery comparison of spring 2016, where I again found that water potential recovery was significantly driven by a two-way interaction between site and how far the plant's water isotope values departed from the LMWL (Table 6, LR chisquare 27.199, $P < 0.0001$). Once again, the extent to which trees at CR recovered their water potentials was significantly reduced with increasing dependence on shallow water resources rather than the deeper, more stable water resources being utilized by trees at PW and BORR (i.e. water isotope signatures falling closer to PW and BORR LMWL's) (Figure 8b). These results highlight the importance of needing to understand the dynamic groundwater acquisition strategies plants may possess under extreme drought conditions. For my investigation, trees that are restricted to using shallow soil water resources (such as those at CR) rather than multiple, and more stable water sources (such as those at PW and BORR) appear to have been pushed past their tolerance limit and therefore suffered dramatic losses as seen in other studies (Dawson and Pate 1996, Grossiord et al. 2017).

Combined effects of minimum water potential and water source use

To further test the combined effects of minimum growing season water potential and the zone of water extraction as assessed with the magnitude of departure from the LMWL (see above) on water potential recovery rather than their effects apart from one another, I performed two additional multiple generalized linear regression analyses that include both of these predictor coefficients together for each recovery comparison. Combining them in these additional analyses further supports the interpretation that minimum water potential and the magnitude of departure from the LMWL are different and distinct causal factors that significantly influence water potential recovery (Appendix Tables S2 and S3). As in my main reported models (Tables 5 and 6), these additional models reiterate that minimum water potential and the magnitude of departure from the LMWL *interact* to influence the extent of water potential recovery, because trees with more negative growing season water potentials that were utilizing only shallow water sources (e.g., evaporatively enriched soil waters) had significantly more negative spring water potentials, and thus failed to recover compared to trees with more stable (deeper) soil water

sources that roots could access. These results are consistent with recent calls for accounting for environmental context in the pursuit of characterizing drought responses and understanding overall vulnerability to drought-induced mortality (Feng et al. 2018 and *in press*), because I found that incorporating analyses of subsurface water availability with traditional measurements of seasonal water potential allowed for a more nuanced understanding of water status maintenance in response to extreme drought. Without jointly accounting for the environmental context of this drought event, understanding the important drivers of water potential recovery of these tree species would have been insufficient.

The effect of P_e excess on spring recovery (H3)

My final pair of models testing **H3** revealed additional yet contrasting results on the effects of exceeding air-entry xylem embolism thresholds (P_e) during fall growing seasons on the ability of trees to recover their water potentials in the following spring. Spring water potential recovery in 2015 was significantly associated with a three-way interaction between site, species, and fall 2014 P_e excess (Table 5, LR chisquare 6.077, P = 0.0137). Once again, the blue oaks at CR were most significantly affected, where spring recovery was most drastically reduced in trees that exceeding these embolism thresholds in the previous fall (Figure 7c). Moreover, blue oaks and valley oaks at PW and BORR also managed to exceed these thresholds and yet still recovered in the spring, which in my view further reiterates the importance of water source on recovery dynamics rather than minimum water potential or P_e excess alone. Nonetheless, for spring water potential recovery in 2016 there were neither significant main effects nor interactions of any coefficients (Figure 8c, Table 6). Like in the degree of P_e excess seen in 2014, trees at PW and BORR far exceeded these embolism thresholds and still were completely able to recover. And for trees at CR, this similar degree of recovery could potentially be attributed to the increases in water year precipitation and reductions in climatic water deficit seen in the 2016 water year compared to that of previous drought years (Figure 2), where recovery could have been ameliorated or even facilitated by reduced climatic severity.

Patterns of canopy damage and tree mortality

Surveys of tree mortality during the progression of the drought along with canopy damage surveys conducted after the drought concluded provide support for the damaging effects of extreme water deficit, xylem embolism formation, and failure to recover seasonal water potential (Appendix Tables S4). Of the blue oaks that survived at the most xeric site, CR, 88.3 % showed signs of extensive canopy damage and epicormic resprouting, and 88.9 % of the valley oaks at CR exhibited these signs of damage as well. Trees at this site also failed to recover their seasonal water status to a significantly poorer degree than all other study trees (Figures 7 and 8), and had the highest mortality rate (Figures 3 and 4). At BORR, where water potentials were most impaired, 94.4 % of the blue oaks and 93.8 % of the valley oaks that survived showed these same signs of canopy damage. And at PW, where water potentials were comparatively the least impaired and trees had the highest recovery rates, only 55.6 % of the blue oaks and 66.7 % of the valley oaks showed these signs of canopy damage. Ultimately, instances of tree mortality and canopy damage tended to occur in trees that failed to recover their water potential through the drought, and by extension, in trees that were repeatedly accumulating xylem emboli in their stems through the growing season of each subsequent drought year. Therefore, these rates of

canopy damage and mortality are consistent with studies that assert embolism formation is a damaging process that can lead to mortality rather than a benign, seasonally-recoverable or repairable one (Choat 2013, Urli et al. 2013, Choat et al. 2018).

This study took advantage of a unique historical drought that occurred throughout the state of California from 2012 to 2016. This drought event allowed us to take advantage of a "natural experiment" of extreme water deficit to test the importance of drought intensity, subsurface water availability, as well as xylem embolism resistance traits for two long-lived, drought-adapted tree species to maintain their capacity to recover from and survive through multiple years of historically severe drought. By integrating two and a half years of field water potential measurements with measurements of xylem water isotopes and different thresholds of hydraulic vulnerability to embolism, this work provides support for the hypotheses that stress from excessively low minimum water potentials, poor access to stable soil water resources, and xylem embolism formation all interact to inhibit the overall water relations of these tree species in response to extreme drought conditions. By impairing their water status over time and inhibiting the ability of these species to recover their growing season water status under historic hydric deficits, I infer that this drought pushed these trees beyond their physiological tolerances of resisting sustained xylem embolism formation within their stems. Consequently, I infer that trees with the most limited soil water acquisition sources (i.e. those with functional roots that could only access precipitation in shallow soils rather than deeper soil water sources) continuously experienced the damaging effects of xylem embolism formation, which translated into substantial degrees of canopy damage in both species throughout all study sites to the extent that multiple study trees ended up dying. Nonetheless, trees in sites with comparatively stable, deeper water access sources were still able to recover their water potentials even in response to below-average rainfall inputs and despite surpassing their air-entry water potential thresholds during the growing season, highlighting the joint importance of subsurface hydrology dynamics, functional root architectures, and xylem hydraulic traits in causing physiological damage and drought-induced mortality.

The results underscore the importance of seasonal precipitation, climatic water deficit, water uptake dynamics, and xylem embolism resistance thresholds for these tree species to survive and maintain functional water status during such extreme climatic events, which are only expected to become more common and severe in California's future due to climate change. Understanding the physiological limits of these species to this degree of water deficit (hydric deficit) is key to understanding their capacity of ecophysiological resilience to such climatic disturbances into the future. In Chapter 2, I further explore the changes in hydrological conditions throughout these sites that were responsible for inducing the variation in physiological changes in water status that were observed here in this study. By further drawing on the power of stable isotopes of leaf tissues, this chapter dives deeper into the ecophysiology and ecohydrology of these oak woodlands in response to this historic drought event.

REFERENCES

Adams, H.D., Guardiola-Claramonte, M., Barron-Gafford, G.A., Villegas, J.C., Breshears, D.D., Zou, C.B., Troch, P.A. and Huxman, T.E., 2009. Temperature sensitivity of drought-induced tree mortality portends increased regional die-off under global-change-type drought. *Proceedings of the National Academy of Sciences*, 106(17), pp.7063-7066.

Allen, C.D., Macalady, A.K., Chenchouni, H., Bachelet, D., McDowell, N., Vennetier, M., Kitzberger, T., Rigling, A., Breshears, D.D., Hogg, E.T. and Gonzalez, P., 2010. A global overview of drought and heat-induced tree mortality reveals emerging climate change risks for forests. *Forest Ecology and Management*, 259(4), pp.660-684.

Allen, C.D., Breshears, D.D. and McDowell, N.G., 2015. On underestimation of global vulnerability to tree mortality and forest die-off from hotter drought in the Anthropocene. *Ecosphere*, 6(8), pp.1-55.

Anderegg, W.R., Hicke, J.A., Fisher, R.A., Allen, C.D., Aukema, J., Bentz, B., Hood, S., Lichstein, J.W., Macalady, A.K., McDowell, N. and Pan, Y., 2015a. Tree mortality from drought, insects, and their interactions in a changing climate. *New Phytologist*, 208(3), pp.674-683.

Anderegg, W.R., Flint, A., Huang, C.Y., Flint, L., Berry, J.A., Davis, F.W., Sperry, J.S. and Field, C.B., 2015b. Tree mortality predicted from drought-induced vascular damage. *Nature Geoscience*, 8(5), p.367.

Anderegg, W.R., Klein, T., Bartlett, M., Sack, L., Pellegrini, A.F., Choat, B. and Jansen, S., 2016. Meta-analysis reveals that hydraulic traits explain cross-species patterns of drought-induced tree mortality across the globe. *Proceedings of the National Academy of Sciences*, 113(18), pp.5024-5029.

Benettin, P., Volkmann, T.H., Freyberg, J.V., Frentress, J., Penna, D., Dawson, T.E. and Kirchner, J.W., 2018. Effects of climatic seasonality on the isotopic composition of evaporating soil waters. *Hydrology and Earth System Sciences*, 22(5), pp.2881-2890.

Bivand, R.S., Pebesma, E. and Gomez-Rubio, V., 2013. Applied spatial data analysis with R, Second edition. Springer, NY. http://www.asdar-book.org/.

Bivand, R. and Lewin-Koh, N., 2017. maptools: Tools for Reading and Handling Spatial Objects. R package version 0.9-2. https://CRAN.R-project.org/package=maptools.

Bivand, R., Keitt, T. and Rowlingson, B., 2017. rgdal: Bindings for the 'Geospatial' Data Abstraction Library. R package version 1.2-15. https://CRAN.R-project.org/package=rgdal.

Bowen, G.J., Wassenaar, L.I. and Hobson, K.A., 2005. Global application of stable hydrogen and oxygen isotopes to wildlife forensics. *Oecologia*, 143(3), pp.337-348.

Bowen, G.J., 2018. The Online Isotopes in Precipitation Calculator, version 3.1. http://www.waterisotopes.org.

Brodribb, T.J., Carriqui, M., Delzon, S. and Lucani, C., 2017. Optical measurement of stem xylem vulnerability. *Plant Physiology*, pp.pp-00552.2017.

Choat, B., Jansen, S., Brodribb, T.J., Cochard, H., Delzon, S., Bhaskar, R., Bucci, S.J., Feild, T.S., Gleason, S.M., Hacke, U.G. and Jacobsen, A.L., 2012. Global convergence in the vulnerability of forests to drought. *Nature*, 491(7426), p.752.

Choat, B., 2013. Predicting thresholds of drought-induced mortality in woody plant species. *Tree Physiology*, 33(7), pp.669-671.

Choat, B., Nolf, M., Lopez, R., Peters, J.M., Carins-Murphy, M.R., Creek, D. and Brodribb, T.J., 2018. Non-invasive imaging shows no evidence of embolism repair after drought in tree species of two genera. *Tree Physiology*, *in press.*

Cook, B.I., Smerdon, J.E., Seager, R. and Coats, S., 2014. Global warming and 21st century drying. *Climate Dynamics*, 43(9-10), pp.2607-2627.

Coplen, T.B., 1995. Discontinuance of SMOW and PDB. *Nature*, 375(6529), p.285.

Craig, H., 1961. Isotopic variations in meteoric waters. *Science*, 133(3465), pp.1702-1703.

Dai, A., 2013. Increasing drought under global warming in observations and models. *Nature Climate Change*, 3(1), p.52.

Daly, C., Halbleib, M., Smith, J.I., Gibson, W.P., Doggett, M.K., Taylor, G.H., Curtis, J. and Pasteris, P.P., 2008. Physiographically sensitive mapping of climatological temperature and precipitation across the conterminous United States. *International Journal of Climatology: a Journal of the Royal Meteorological Society*, 28(15), pp.2031-2064.

Dansgaard, W., 1964. Stable isotopes in precipitation. *Tellus*, 16(4), pp.436-468.

Dawson, T.E. and Ehleringer, J.R., 1993. Isotopic enrichment of water in the" woody" tissues of plants: Implications for plant water source, water uptake, and other studies which use stable isotopic composition of cellulose. *Geochimica et Cosmochimica Acta*, 57, pp.3487-3487.

Dawson, T.E. and Pate, J.S., 1996. Seasonal water uptake and movement in root systems of Australian phraeatophytic plants of dimorphic root morphology: a stable isotope investigation. *Oecologia*, 107(1), pp.13-20.

Delzon, S. and Cochard, H., 2014. Recent advances in tree hydraulics highlight the ecological significance of the hydraulic safety margin. *New Phytologist*, 203(2), pp.355-358.

Diffenbaugh, N.S., Swain, D.L. and Touma, D., 2015. Anthropogenic warming has increased drought risk in California. *Proceedings of the National Academy of Sciences*, p.201422385.

Feng, X., Dawson, T.E., Ackerly, D.D., Santiago, L.S. and Thompson, S.E., 2017. Reconciling seasonal hydraulic risk and plant water use through probabilistic soil–plant dynamics. *Global Change Biology*, 23(9), pp.3758-3769.

Feng, X., Ackerly, D.D., Dawson, T.E., Manzoni, S., Skelton, R.P., Vico, G. and Thompson, S.E., 2018. The ecohydrological context of drought and classification of plant responses. *Ecology Letters*, 21(11), pp.1723-1736.

Feng, X., Ackerly, D.D., Dawson, T.E., Manzoni, S., McLaughlin, B.C., Skelton, R.P., Vico, G., Weitz, A.P., Thompson, S.E., 2018. Beyond isohydricity: the role of environmental variability in determining plant drought responses. *Plant, Cell & Environment*, *in press*.

Flint, L.E., Flint, A.L., Thorne, J.H., Boynton, R., 2013. Fine-scale hydrologic modeling for regional landscape applications: the California Basin Characterization Model development and performance. *Ecological Processes*, 2(5), pp.1-21.

Fox, J. and Weisberg, S., 2011. An R Companion to Applied Regression, Second Edition. Thousand Oaks, CA. http://socserv.socsci.mcmaster.ca/jfox/Books/Companion

Griffin, J.R., 1971. Oak regeneration in the upper Carmel Valley, California. *Ecology*, 52(5), pp.862-868.

Griffin, J.R. and Critchfield, W.B., 1972. The distribution of forest trees in California. U.S. Forest Service, Research Paper PSW-82. Pacific Southwest Forest and Range Experiment Station, Berkeley, CA.

Griffin, J.R., 1973. Xylem sap tension in three woodland oaks of central California. *Ecology*, 54(1), pp.152-159.

Griffin, J.R., 1976. Regeneration in *Quercus lobata* savannas, Santa Lucia Mountains, California. *American Midland Naturalist*, pp.422-435.

Griffin, D. and Anchukaitis, K.J., 2014. How unusual is the 2012–2014 California drought? *Geophysical Research Letters*, 41(24), pp.9017-9023.

Grossiord, C., Sevanto, S., Dawson, T.E., Adams, H.D., Collins, A.D., Dickman, L.T., Newman, B.D., Stockton, E.A. and McDowell, N.G., 2017. Warming combined with more extreme precipitation regimes modifies the water sources used by trees. *New Phytologist*, 213(2), pp.584-596.

Hartmann, H., Moura, C.F., Anderegg, W.R., Ruehr, N.K., Salmon, Y., Allen, C.D., Arndt, S.K., Breshears, D.D., Davi, H., Galbraith, D. and Ruthrof, K.X., 2018. Research frontiers for

improving our understanding of drought-induced tree and forest mortality. *New Phytologist*, 218(1), pp.15-28.

Hijmans, R.J., 2016. raster: Geographic Data Analysis and Modeling. R package version 2.5-8. https://CRAN.R-project.org/package=raster.

McDowell, N., Pockman, W.T., Allen, C.D., Breshears, D.D., Cobb, N., Kolb, T., Plaut, J., Sperry, J., West, A., Williams, D.G. and Yepez, E.A., 2008. Mechanisms of plant survival and mortality during drought: why do some plants survive while others succumb to drought? *New Phytologist*, 178(4), pp.719-739.

McLaughlin, B.C. and Zavaleta, E.S., 2012. Predicting species responses to climate change: demography and climate microrefugia in California valley oak (Quercus lobata). *Global Change Biology*, 18(7), pp.2301-2312.

McLaughlin, B.C., Ackerly, D.D., Klos, P.Z., Natali, J., Dawson, T.E. and Thompson, S.E., 2017. Hydrologic refugia, plants, and climate change. *Global Change Biology*, 23(8), pp.2941-2961.

Oshun, J., Dietrich, W.E., Dawson, T.E. and Fung, I., 2016. Dynamic, structured heterogeneity of water isotopes inside hillslopes. *Water Resources Research*, 52(1), pp.164-189.

Park Williams, A., Allen, C.D., Macalady, A.K., Griffin, D., Woodhouse, C.A., Meko, D.M., Swetnam, T.W., Rauscher, S.A., Seager, R., Grissino-Mayer, H.D. and Dean, J.S., 2013. Temperature as a potent driver of regional forest drought stress and tree mortality. *Nature Climate Change*, 3(3), p.292.

Pebesma, E.J. and Bivand, R.S., 2005. Classes and methods for spatial data in R. R News 5(2), https://cran.r-project.org/doc/Rnews/.

R Core Team, 2017. R: A language and environment for statistical computing. R Foundation for Statistical Computing, Vienna, Austria.

Sala, A., Piper, F. and Hoch, G., 2010. Physiological mechanisms of drought-induced tree mortality are far from being resolved. *New Phytologist*, 186(2), pp.274-281.

Simonin, K.A., Link, P., Rempe, D., Miller, S., Oshun, J., Bode, C., Dietrich, W.E., Fung, I. and Dawson, T.E., 2014. Vegetation induced changes in the stable isotope composition of near surface humidity. *Ecohydrology*, 7(3), pp.936-949.

Skelton, R.P., Brodribb, T.J., McAdam, S.A. and Mitchell, P.J., 2017. Gas exchange recovery following natural drought is rapid unless limited by loss of leaf hydraulic conductance: evidence from an evergreen woodland. *New Phytologist*, 215(4), pp.1399-1412.

Skelton, R.P., Dawson, T.E., Thompson, S.E., Shen, Y., Weitz, A.P. and Ackerly, D.D., 2018. Low vulnerability to xylem embolism in leaves and stems of North American oaks. *Plant Physiology*, pp-00103.2018.

Stahle, D.W., Griffin, R.D., Meko, D.M., Therrell, M.D., Edmondson, J.R., Cleaveland, M.K., Stahle, L.N., Burnette, D.J., Abatzoglou, J.T., Redmond, K.T. and Dettinger, M.D., 2013. The ancient blue oak woodlands of California: Longevity and hydroclimatic history. *Earth Interactions*, 17(12), pp.1-23.

Stephenson, N., 1998. Actual evapotranspiration and deficit: biologically meaningful correlates of vegetation distribution across spatial scales. *Journal of Biogeography*, 25(5), pp.855-870.

Swain, D.L., 2015. A tale of two California droughts: Lessons amidst record warmth and dryness in a region of complex physical and human geography. *Geophysical Research Letters*, 42(22), pp.9999-10.

Swain, D.L., Horton, D.E., Singh, D. and Diffenbaugh, N.S., 2016. Trends in atmospheric patterns conducive to seasonal precipitation and temperature extremes in California. *Science Advances*, 2(4), p.e1501344.

Urli, M., Porté, A.J., Cochard, H., Guengant, Y., Burlett, R. and Delzon, S., 2013. Xylem embolism threshold for catastrophic hydraulic failure in angiosperm trees. *Tree Physiology*, 33(7), pp.672-683.

Welker, J.M., 2000. Isotopic (δ18O) characteristics of weekly precipitation collected across the USA: an initial analysis with application to water source studies. *Hydrological Processes*, 14(8), pp.1449-1464.

West, A.G., Patrickson, S.J. and Ehleringer, J.R., 2006. Water extraction times for plant and soil materials used in stable isotope analysis. *Rapid Communications in Mass Spectrometry: An International Journal Devoted to the Rapid Dissemination of Up-to-the-Minute Research in Mass Spectrometry*, 20(8), pp.1317-1321.

West, A.G., Hultine, K.R., Sperry, J.S., Bush, S.E. and Ehleringer, J.R., 2008. Transpiration and hydraulic strategies in a piñon–juniper woodland. *Ecological Applications*, 18(4), pp.911-927.

Wickham, H., 2009. ggplot2: Elegant Graphics for Data Analysis. Springer-Verlag New York.

Wickham, H., Francois, R., Henry, L. and Müller, K., 2017. dplyr: A Grammar of Data Manipulation. R package version 0.7.4. https://CRAN.R-project.org/package=dplyr.

Figure 1. Study site locations as a function of statewide climatic gradients of **a.** precipitation (PPT) and **b.** climatic water deficit (CWD). Climate averages were derived as 30-year means of annual variable totals across the 1981 - 2010 water years from the CA-BCM at 270 m spatial resolution (Flint et al. 2013).

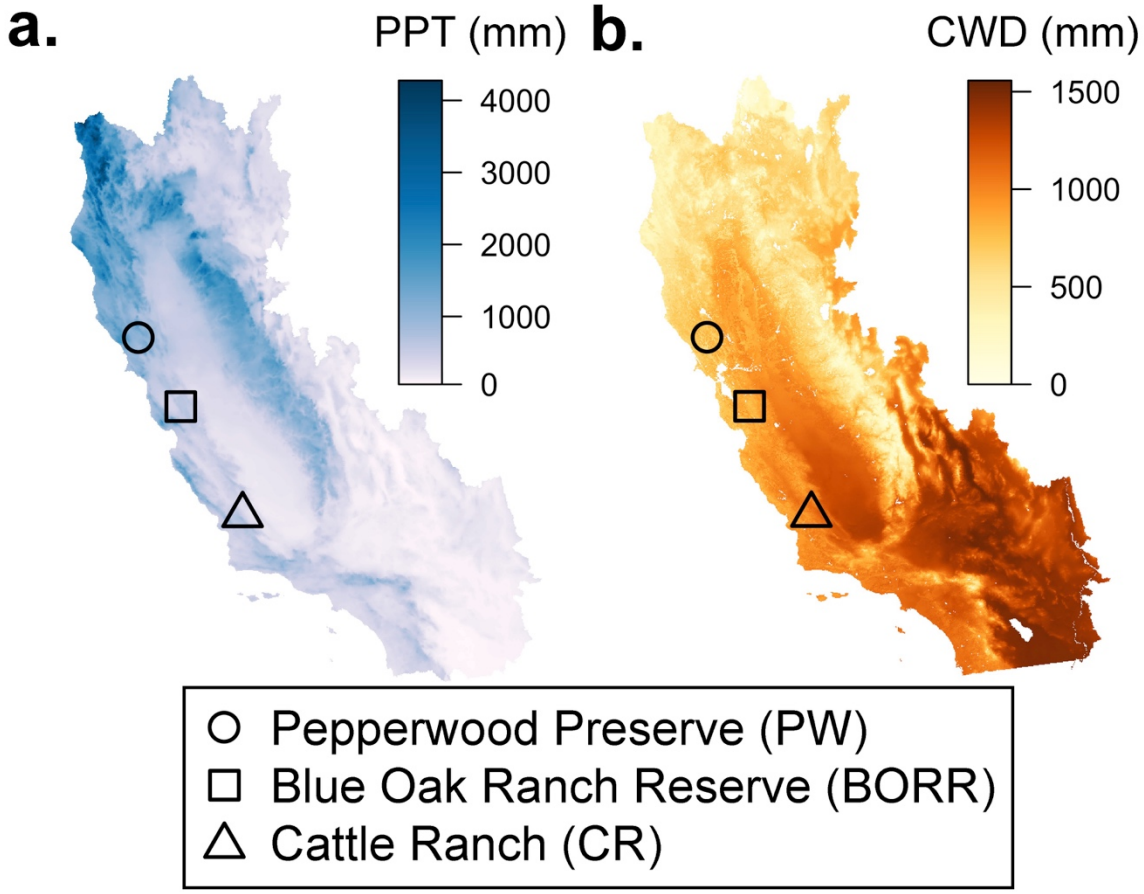

Figure 2. Accumulated monthly values of precipitation and climatic water deficit across each study site through water years 2012 - 2016 compared with each site's historical climatic average. Climate averages were derived as 30-year means across monthly variable totals from water years 1981 - 2010 via 10 m spatial resolution outputs of the CA-BCM at each site (Flint and Flint, unpublished).

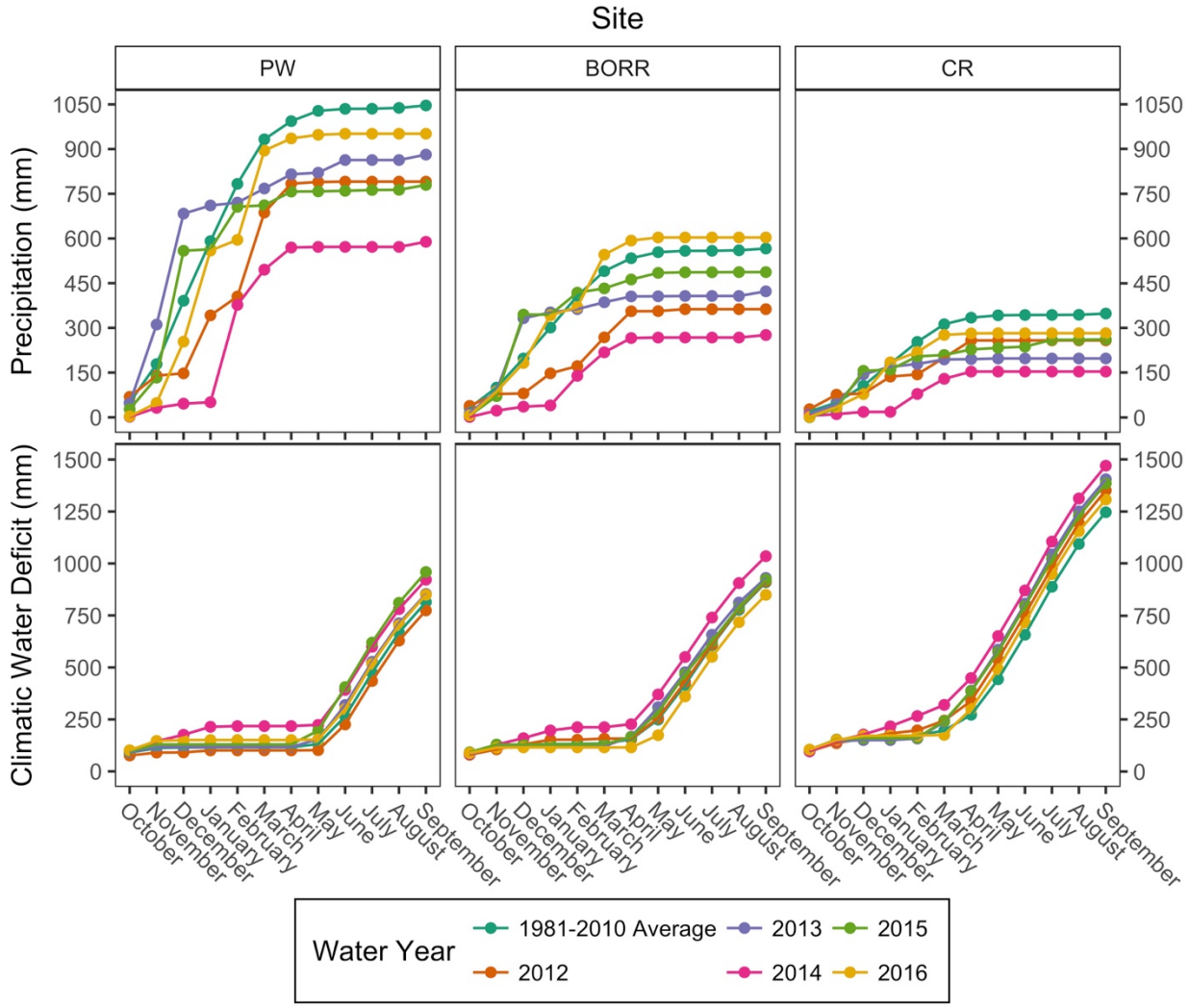

Figure 3. Seasonal predawn and midday water potential trajectories of all blue oak (*Q. douglasii*) study trees in each study site as a function of their stem air-entry thresholds (P_e, black dashed lines). Water status trajectories of individual trees that died are highlighted in black dashed lines, where X's indicate the last measurement made before the tree was found dead in the following season's measurement campaign.

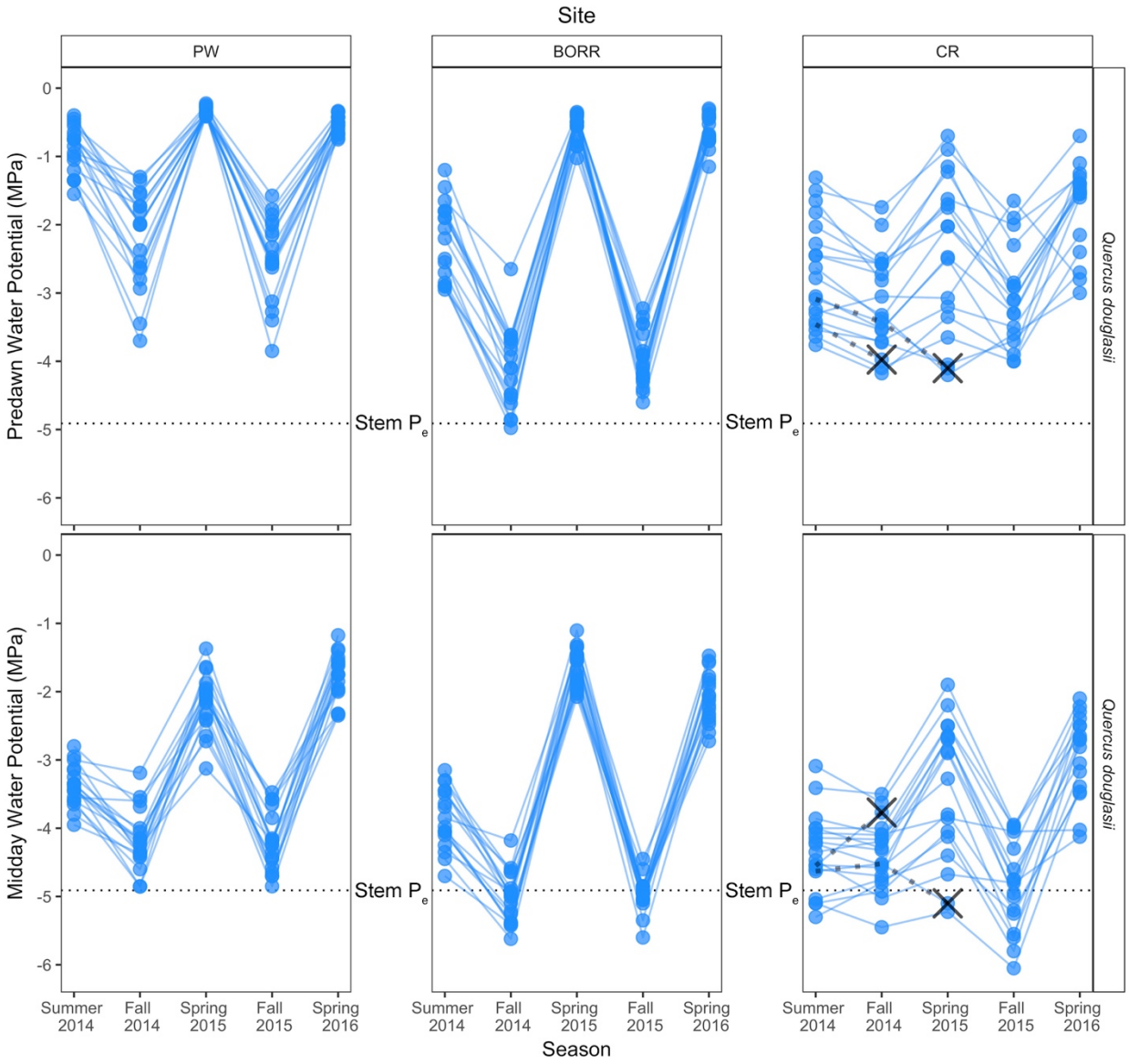

Figure 4. Seasonal predawn and midday water potential trajectories of all valley oak (*Q. lobata*) study trees in each study site as a function of their stem air-entry thresholds (P_e, black dashed lines). Water status trajectories of the individual tree that died is highlighted in black dashed lines, where X's indicate the last measurement made before the tree was found dead in the following season's measurement campaign.

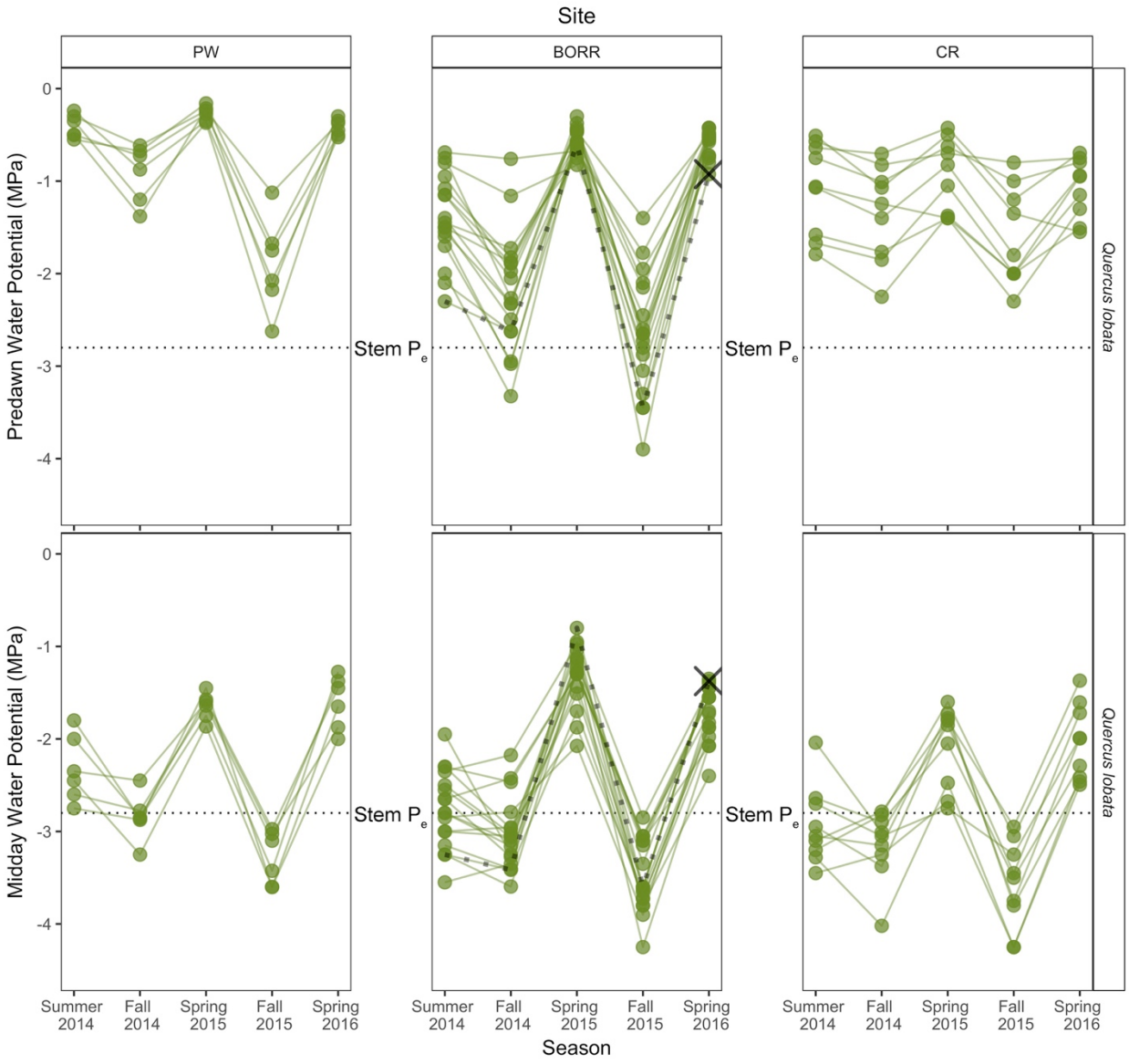

Figure 5. Dual-isotope bivariate plots of xylem water δ^2H and $\delta^{18}O$ extracted from *Q. douglasii* and *Q. lobata* stems across each field site during the 2015 and 2016 spring water potential recovery campaigns. Points represent the values of stable isotope ratios from individual study trees during each field campaign and are plotted as a function of the local meteoric water line (LMWL) of each site. LWML regression equations for each site are $\delta^2H = 7.82\ \delta^{18}O + 9.42$ ‰ for PW, $\delta^2H = 7.93\ \delta^{18}O + 9.21$ ‰ for BORR, and $\delta^2H = 7.45\ \delta^{18}O - 0.95$ ‰ for CR.

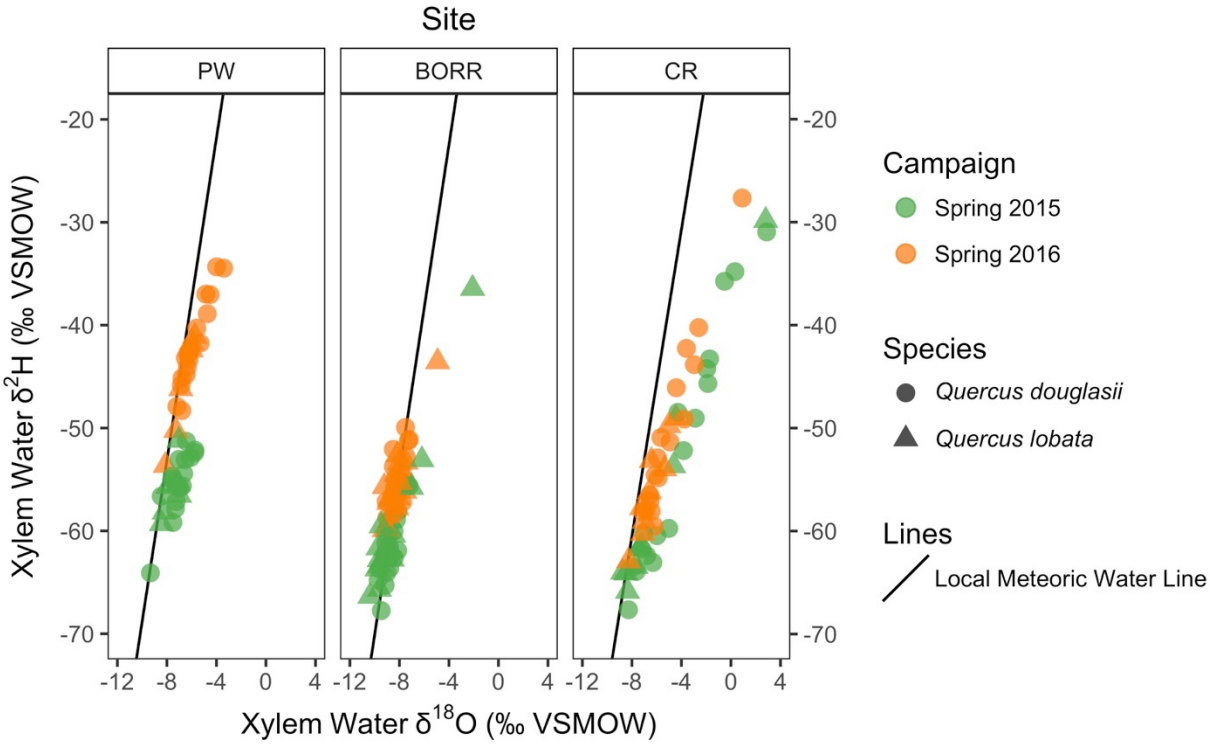

Figure 6. Optical vulnerability to embolism curves between *Q. douglasii* and *Q. lobata* leaves and stems. Raw values of embolism formation for each tissue type are plotted with transparent lines. Sigmoidal fits of tissue means are plotted as solid lines with ± 1 standard error in transparent shading. Replotted from (Skelton et al. 2018).

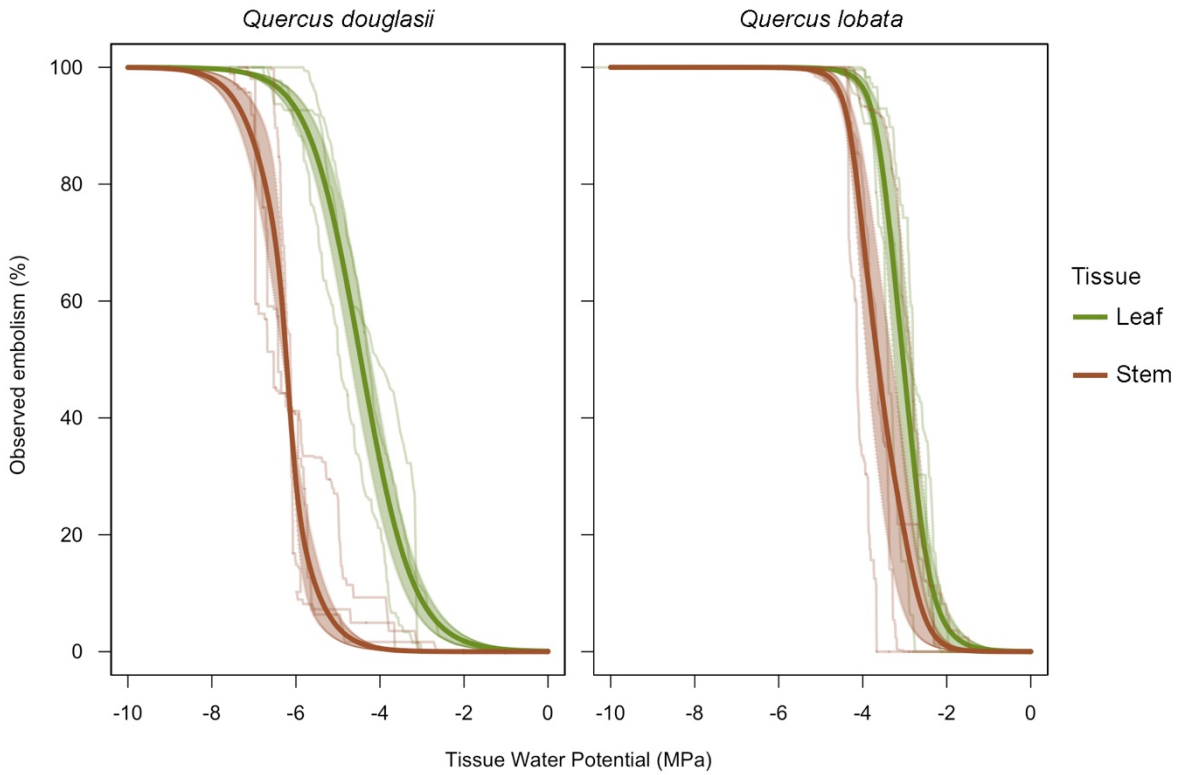

Figure 7. Model fits from Type III ANOVA for the first water potential recovery comparison (spring 2015): **a.** the effect of fall 2014 minimum water potential on water potential recovery during spring 2015 (**H1**); **b.** the effect of LMWL departure on water potential recovery during spring 2015 (**H2**); **c.** the effect of exceeding stem P_e during fall 2014 on water potential recovery during spring 2015 (**H3**). Fitted slopes represent significant coefficients (including their interactions) from each model. See Table 5 for analysis of deviance tables.

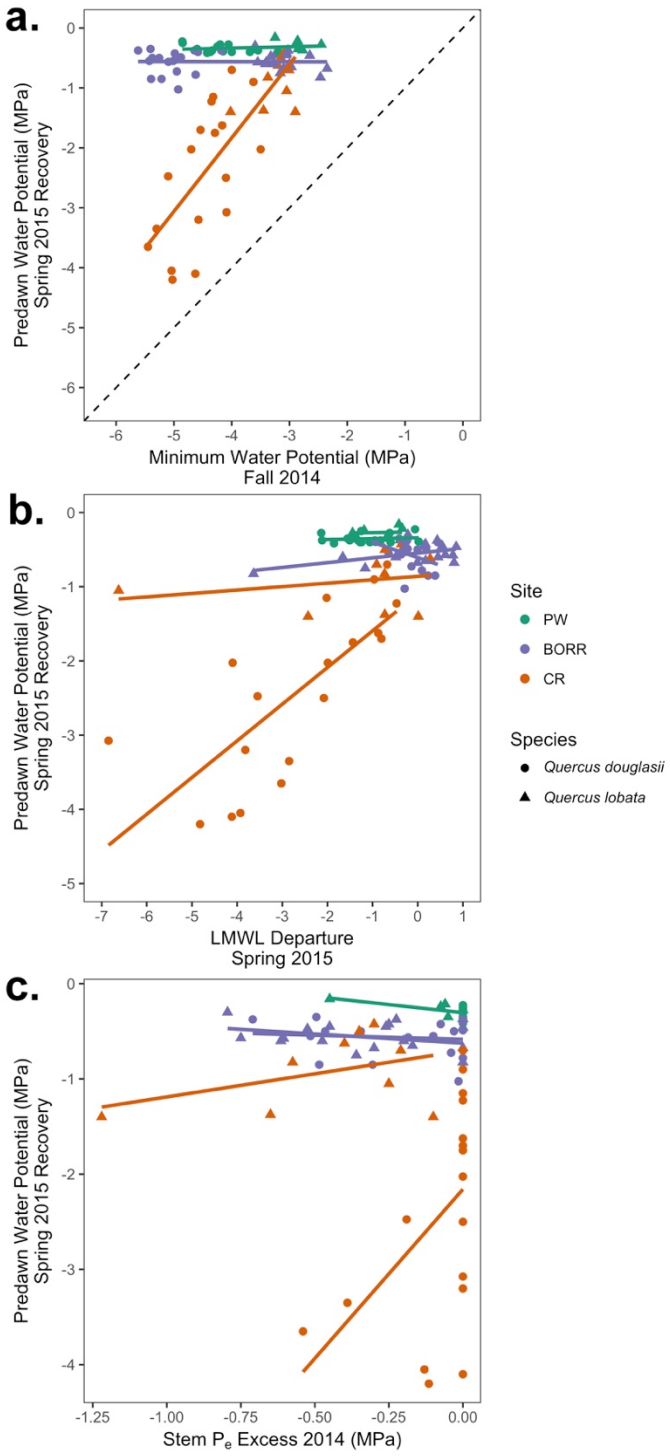

Figure 8. Model fits from Type III ANOVA for the second water potential recovery comparison (spring 2016): **a.** the effect of fall 2015 minimum water potential on water potential recovery during spring 2016 (**H1**); **b.** the effect of LMWL departure on water potential recovery during spring 2016 (**H2**); **c.** the effect of exceeding stem P_e during fall 2015 on water potential recovery during spring 2016 (**H3**). Fitted slopes represent significant coefficients (including their interactions) from each model. See Table 6 for analysis of deviance tables.

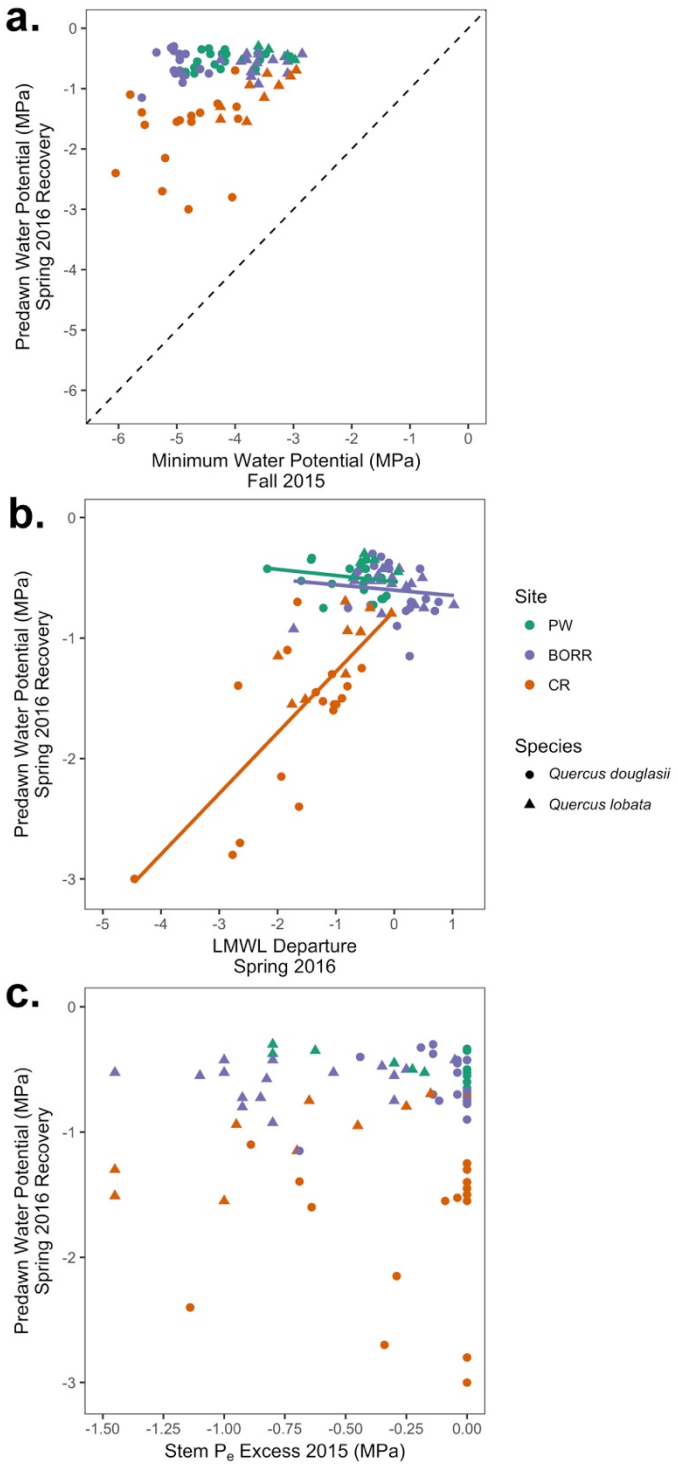

Table 1. Sample sizes of study trees across field sites.

	Total Site Sample Size	
Site	*Q. douglasii*	*Q. lobata*
Pepperwood Preserve (PW)	$n = 18$	$n = 6$
Blue Oak Ranch Reserve (BORR)	$n = 18$	$n = 17$
Cattle Ranch (CR)	$n = 19$	$n = 9$

Table 2. Seasonal water status measurement and stem collection dates across all field campaigns.

	Field Campaign[1]				
Site	Summer 2014	Fall 2014	Spring 2015	Fall 2015	Spring 2016
PW	2014-06-26	2014-09-16	2015-04-28	2015-09-24	2016-05-04
BORR	2014-07-03	2014-09-07	2015-04-02	2015-09-11	2016-05-11
CR	2014-06-16	2014-08-05	2015-04-15	2015-08-26	2016-04-28

[1]Dates are reported in Year-Month-Day format (YYYY-MM-DD).

Table 3. Accumulated annual values of water year precipitation and climatic water deficit across each study site through water years 2012 - 2016 compared with each site's historical climatic average. Climate averages were derived as 30-year means across annual variable totals from water years 1981 - 2010 via 10 m spatial resolution outputs of the CA-BCM at each site (Flint and Flint, unpublished).

	Precipitation (mm)					
	Water Year					
Site	1981 - 2010 Average	2012	2013	2014	2015	2016
PW	1046	790.8	881.4	588.8	779.7	951.5
BORR	566.3	362.8	422.7	276.1	487.1	603.4
CR	348.1	257.9	197.4	153.3	261.4	282.2

	Climatic Water Deficit (mm)					
	Water Year					
Site	1981 - 2010 Average	2012	2013	2014	2015	2016
PW	814.3	774.3	853.6	922.2	959	849.6
BORR	909.8	914.8	930.7	1035.1	921.9	849.1
CR	1247	1351.9	1405.1	1470.4	1385.4	1307.4

Table 4. Water potential thresholds of xylem vulnerability to embolism between *Q. douglasii* and *Q. lobata* leaves and stems, as reported in (Skelton et al. 2018).

		Xylem Vulnerability Threshold (MPa ± 1 s.e.)[1]			
Species	Tissue	P_e	P_{12}	P_{50}	P_{88}
Quercus douglasii	Leaf	-3.13 ± 0.26	-3.99 ± 0.26	-4.45 ± 0.24	-4.90 ± 0.21
	Stem	-4.91 ± 0.30	-5.95 ± 0.07	-6.27 ± 0.06	-6.59 ± 0.06
Quercus lobata	Leaf	-2.40 ± 0.24	-2.35 ± 0.22	-3.02 ± 0.18	-3.67 ± 0.14
	Stem	-2.80 ± 0.40	-3.01 ± 0.29	-3.25 ± 0.23	-4.15 + 0.21

[1]Thresholds of xylem vulnerability to embolism were calculated and reported as sample (tissue) means as a function of one standard error. See Figure 6 for the embolism accumulation curves that these values were calculated from.

Table 5. Analysis of deviance tables for the first water potential recovery campaign (spring 2015) from Type III ANOVA's on Models 1 through 3 (testing Hypotheses 1 through 3, respectively).

Analysis of Deviance Table (Type III Tests):
Spring 2015 Water Potential Recovery

GLM 1 (**H1**): Spring 2015 Predawn Water Potential Recovery ~ Site * Species * Minimum Water Potential 2014

Effect:	LR Chisq	Df	Pr(>Chisq)
Site	**12.278**	**2**	**0.0022**
Species	3.121	1	0.0773
Minimum Water Potential 2014	**49.248**	**1**	**< 0.0001**
Site : Species	1.329	2	0.5146
Site : Minimum Water Potential 2014	**26.453**	**2**	**< 0.0001**
Species : Minimum Water Potential 2014	3.128	1	0.077
Site : Species : Minimum Water Potential 2014	1.252	2	0.5347

GLM 2 (**H2**): Spring 2015 Predawn Water Potential Recovery ~ Site * Species * LMWL Departure Spring 2015

Effect:	LR Chisq	Df	Pr(>Chisq)
Site	**8.65**	**2**	**0.0132**
Species	1.005	1	0.3161
LMWL Departure Spring 2015	**78.316**	**1**	**< 0.0001**
Site : Species	0.414	2	0.8129
Site : LMWL Departure Spring 2015	**14.329**	**2**	**0.0008**
Species : LMWL Departure Spring 2015	**26.474**	**1**	**< 0.0001**
Site : Species : LMWL Departure Spring 2015	**7.276**	**2**	**0.0263**

GLM 3 (**H3**): Spring 2015 Predawn Water Potential Recovery ~ Site * Species * P_e Excess 2014

Effect:	LR Chisq	Df	Pr(>Chisq)
Site	**111.127**	**2**	**< 0.0001**
Species	**20.383**	**1**	**< 0.0001**
P_e Excess 2014	**20.014**	**1**	**< 0.0001**
Site : Species	**14.996**	**2**	**0.0006**
Site : P_e Excess 2014	**14.665**	**1**	**0.0001**
Species : P_e Excess 2014	**10.29**	**1**	**0.0013**
Site : Species : P_e Excess 2014	**6.077**	**1**	**0.0137**

Table 6. Analysis of deviance tables for the second water potential recovery campaign (spring 2016) from Type III ANOVA's on Models 4 through 6 (testing Hypotheses 1 through 3, respectively).

Analysis of Deviance Table (Type III Tests):
Spring 2016 Water Potential Recovery

GLM 4 (**H1**): Spring 2016 Predawn Water Potential Recovery ~ Site * Species * Minimum Water Potential 2015

Effect:	LR Chisq	Df	Pr(>Chisq)
Site	0.39471	2	0.8209
Species	2.55688	1	0.1098
Minimum Water Potential 2015	2.0776	1	0.1495
Site : Species	2.00995	2	0.3661
Site : Minimum Water Potential 2015	0.30849	2	0.8571
Species : Minimum Water Potential 2015	1.74804	1	0.1861
Site : Species : Minimum Water Potential 2015	1.58945	2	0.4517

GLM 5 (**H2**): Spring 2016 Predawn Water Potential Recovery ~ Site * Species * LMWL Departure Spring 2016

Effect:	LR Chisq	Df	Pr(>Chisq)
Site	**6.297**	**2**	**0.0429**
Species	1.34	1	0.2471
LMWL Departure Spring 2016	**45.038**	**1**	**< 0.0001**
Site : Species	0.992	2	0.6089
Site : LMWL Departure Spring 2016	**27.199**	**2**	**< 0.0001**
Species : LMWL Departure Spring 2016	0.318	1	0.5726
Site : Species : LMWL Departure Spring 2016	1.744	2	0.4181

GLM 6 (**H3**): Spring 2016 Predawn Water Potential Recovery ~ Site * Species * P_e Excess 2015

Effect:	LR Chisq	Df	Pr(>Chisq)
Site	**97.517**	**2**	**< 0.0001**
Species	**18.159**	**1**	**< 0.0001**
P_e Excess 2015	0.428	1	0.5131
Site : Species	**12.024**	**2**	**0.0024**
Site : P_e Excess 2015	0.054	1	0.8163
Species : P_e Excess 2015	1.426	1	0.2325
Site : Species : P_e Excess 2015	0.982	1	0.3216

APPENDIX

Table S1. LMWL equations for BORR derived using actual precipitation samples (T.E. Dawson, unpublished) versus via the OIPC (Welker 2000, Bowen et al. 2005, Bowen 2018).

BORR LMWL Source	**LMWL Equation**
T.E. Dawson	$\delta^2H = 7.69\ \delta^{18}O + 8.94$ ‰
OIPC	$\delta^2H = 7.93\ \delta^{18}O + 9.21$ ‰

Table S2. Analysis of deviance table for the first water potential recovery campaign (spring 2015) from Type III ANOVA on an additional model including both minimum water potential (H1) and LMWL departure (H2) together.

Analysis of Deviance Table (Type III Tests):
Spring 2015 Water Potential Recovery

GLM: Spring 2015 Predawn Water Potential Recovery ~ Site + Species + Minimum Water Potential 2014 + LMWL Departure Spring 2015 + Site : Species + Site : Minimum Water Potential 2014 + Species : Minimum Water Potential 2014 + Site : LMWL Departure Spring 2015 + Species : LMWL Departure Spring 2015 + Site : Species : Minimum Water Potential 2014 + Site : Species : LMWL Departure Spring 2015

Effect:	LR Chisq	Df	Pr(>Chisq)
Site	**24.57**	**2**	**< 0.0001**
Species	2.41	1	0.1206
Minimum Water Potential 2014	**64.792**	**1**	**< 0.0001**
LMWL Departure Spring 2015	**97.453**	**1**	**< 0.0001**
Site : Species	0.827	2	0.6613
Site : Minimum Water Potential 2014	**36.342**	**2**	**< 0.0001**
Species : Minimum Water Potential 2014	0.971	1	0.3243
Site : LMWL Departure Spring 2015	**19.622**	**2**	**< 0.0001**
Species : LMWL Departure Spring 2015	**22.595**	**1**	**< 0.0001**
Site : Species : Minimum Water Potential 2014	0.193	2	0.9078
Site : Species : LMWL Departure Spring 2015	**7.961**	**2**	**0.0187**

Table S3. Analysis of deviance table for the second water potential recovery campaign (spring 2016) from Type III ANOVA on an additional model including both minimum water potential (H1) and LMWL departure (H2) together.

Analysis of Deviance Table (Type III Tests):
Spring 2016 Water Potential Recovery

GLM: Spring 2016 Predawn Water Potential Recovery ~ Site + Species + Minimum Water Potential 2015 + LMWL Departure Spring 2016 + Site : Species + Site : Minimum Water Potential 2015 + Species : Minimum Water Potential 2015 + Site : LMWL Departure Spring 2016 + Species : LMWL Departure Spring 2016 + Site : Species : Minimum Water Potential 2015 + Site : Species : LMWL Departure Spring 2016

Effect:	LR Chisq	Df	Pr(>Chisq)
Site	0.108	2	0.9476
Species	2.061	1	0.1511
Minimum Water Potential 2015	0.342	1	0.5588
LMWL Departure Spring 2016	**41.128**	**1**	**< 0.0001**
Site : Species	1.727	2	0.4217
Site : Minimum Water Potential 2015	0.020	2	0.9898
Species : Minimum Water Potential 2015	1.974	1	0.16
Site : LMWL Departure Spring 2016	**24.525**	**2**	**< 0.0001**
Species : LMWL Departure Spring 2016	1.498	1	0.2209
Site : Species : Minimum Water Potential 2015	1.873	2	0.392
Site : Species : LMWL Departure Spring 2016	2.971	2	0.2264

Table S4. Canopy damage and tree mortality survey results across all trees after the the end of the study in spring 2017.

	Blue oak (*Q. douglasii*)		
Site	Number of Study Trees	Number of Trees with Epicormic Resprouts	Number of Dead Trees
PW	$n = 18$	$n = 10$	$n = 0$
BORR	$n = 18$	$n = 17$	$n = 0$
CR	$n = 19$	$n = 15$	$n = 2$
	Valley oak (*Q. lobata*)		
Site	Number of Study Trees	Number of Trees with Epicormic Resprouts	Number of Dead Trees
PW	$n = 6$	$n = 4$	$n = 0$
BORR	$n = 17$	$n = 15$	$n = 1$
CR	$n = 9$	$n = 8$	$n = 0$

CHAPTER 2

The effects of functional root distributions, plant water status, and stomatal conductance on carbon assimilation through years of extreme drought in Californian blue oak and valley oak

ABSTRACT

The physiological impacts of severe climatic water limitation on plant species, and their consequences for photosynthetic performance, are expected to differ, even for sympatric species, due to differences in drought exposure along the landscape and tolerance of poor plant water status as a function of differing functional root distributions. One strategy that can reveal such differences on seasonal timescales is to pair measurements of the stable carbon isotope ratios of leaves and leaf sugars with measurements of the stable oxygen and deuterium isotope ratios of water in plant xylem. Using the historic 2012 - 2016 Californian drought as a natural experiment, I made seasonal measurements of the $\delta^{13}C$ of leaves and leaf photosynthate and of $\delta^{18}O$ and $\delta^{2}H$ in water extracted from xylem sap in blue oak (*Quercus douglasii*) and valley oak (*Q. lobata*) across three sites from summer 2014 - spring 2016. The sites spanned a gradient of drought and climate severity as measured by climatic water deficit, which increased by 14% - 18% relative to 30-year means, and seasonal precipitation, which was reduced by 44 % - 56 % relative to 30-year means. Carbon isotope discrimination ($\Delta^{13}C$) and the intercellular foliar carbon dioxide concentrations (c_i) were derived from leaf isotope ratios as indicators of photosynthetic performance in response to drought stress. To determine how differences in access to deeper moisture reserves impacted photosynthetic performance, the departure of xylem water isotopes from local meteoric water lines (LMWL's) was regressed against seasonal water status and foliar c_i. The stepwise physiological pathway governing differential degrees of photosynthetic performance between these species was also tested for as a function of the effects of LMWL departures on declines in water status (predawn and midday water potentials, Ψ), how declining water status was linked to seasonal declines in midday transpiration, and how these reductions in transpiration translated into reduced foliar c_i.

In terms of reductions in stomatal conductance and reductions in seasonally- and daily-integrated foliar c_i concentrations, the greatest drought impacts were experienced by blue oak at the most xeric site, which also experienced the most severe climatic drought relative to 30-year means. Contrary to predictions, however, drought exposure did not directly scale with plant access to deeper soil water resources, such that both oak species at the intermediately drought exposed site had the most seasonally-stable xylem water isotope signatures. At the most xeric site, however, these species differed substantially in their soil water access such that the root architectures of blue oaks were more restricted to shallow, evaporatively enriched soil water while the valley oaks at this site maintained stable access to deeper groundwater through the drought period. Even at the most historically mesic site, both species exhibited signs of shallow water use towards the end of the drought period. Across sites, blue oaks still exhibited more signs of the use of shallow water resources compared to valley oaks with respect to their xylem water isotope signatures through the study period, suggesting that these species tend to have fundamentally different water acquisition strategies. Increased LMWL departures were directly associated with

seasonal declines in the plant water potential of both species across sites, which directly reduced midday-predawn water potential differentials. Consequently, these declines in seasonal water status were associated with declines in midday transpiration, which directly translated into declines in both seasonally-integrated and daily-integrated measurements of foliar c_i concentrations. Due to this physiological pathway between water source, water status, and transpiration, I infer that functional rooting depth and sustained access to groundwater resources through these extreme drought conditions was essential for these species to maintain seasonal water status and photosynthetic performance. Taken together, the results reiterate how landscape position and hydrological refugia may ameliorate the negative effects of drought exposure across these species' geographic distributions. The measurements provide novel physiological metrics of the limitations of carbon assimilation and overall physiological performance of these oaks under historic drought stress conditions within natural field conditions, and provide insights into the physiological thresholds that may limit the productivity of these species under future extreme drought conditions.

INTRODUCTION

Global vegetation dynamics and plant physiological performance are changing in the Anthropocene as human activities increase atmospheric CO_2 concentrations, altering climate norms and increasing the frequency and intensity of extreme events (IPCC 2014). Conducting experimental field studies to quantify such changes is essential to projecting species and ecosystem responses to them. Accomplishing this requires methods to observe and characterize changes in plant water use, water status, and productivity as they are all essential to survival and reproduction, and to attribute them to variation in a plant's environment. Historically, such methods have been based on direct measurements of plant water potential, stomatal conductance, and carbon assimilation rates via pressure chamber measurements of plant water potential and portable leaf gas exchange equipment, respectively. Increasingly, however, tracer observations are being used to quantify fluxes and stores of carbon and water by plants in variable environments. Central to these tracer methods are the techniques surrounding stable isotope mass spectrometry. Stable isotopes act as excellent indicators and integrators of a variety of plant physiological processes in response to a range of environmental conditions (Dawson et al. 2002). A suite of biophysical fractionation processes give rise to the different stable isotope signatures of plant tissues and their water sources (Farquhar et al. 1982 and 1989, Dawson and Ehleringer 1991 and 1993). Researchers have only recently applied these principles to plant communities undergoing rapid climatic and ecological changes, for example in response to drought (e.g. Herrero et al. 2013, Barbeta et al. 2015, Grossiord et al. 2017a).

The stable isotope ratios of carbon in plant organic matter (such as leaves or leaf metabolites) and of deuterium and oxygen in water extracted from xylem sap provide different kinds of information about plant function. During photosynthesis, C_3 plant species biochemically discriminate against atmospheric ^{13}C due to the carboxylating enzyme ribulose 1,5- bisphosphate (RuBP). This discrimination can be expressed as a function of the ratio of intercellular to ambient atmospheric CO_2 concentrations of leaves:

$$\Delta^{13}C \text{ (in ‰)} = a + (b - a)(c_i / c_a), \qquad (1)$$

where a is the isotopic fractionation factor that characterizes discrimination against ^{13}C as it differentially diffuses through stomata with respect to ^{12}C (–4.4 ‰), b is the isotopic fractionation factor that characterizes discrimination against ^{13}C during enzymatic carboxylation by RuBP (–27 ‰), and c_i / c_a is the ratio of intercellular to atmospheric CO_2 concentrations at the interface of foliar stomata and the ambient air environment (Farquhar et al. 1982 and 1989). The $\Delta^{13}C$ of plant organic matter is expressed with regard to atmospheric CO_2 as:

$$\Delta^{13}C = (R_a / R_p) - 1, \qquad (2)$$

where R_a is the atmospheric ratio of $^{13}C/^{12}C$ and R_p is the ratio of $^{13}C/^{12}C$ of plant organic matter. By definition, isotope ratios are expressed in delta notation (δ) as referenced to lab standards of known isotopic composition, and are expressed in 'per-mil' notation (‰), for example as:

$$\delta^{13}C, \delta^{18}O, \text{ or } \delta^{2}H \text{ (in ‰)} = (R_{sample} / R_{standard} - 1)1000, \qquad (3)$$

where R_{sample} and $R_{standard}$ are the respective isotope ratios for each sample type and its IAEA approved standard. For carbon, the $^{13}C/^{12}C$ ratios of samples are referenced to the $^{13}C/^{12}C$ ratios of the 'Vienna-PDB' or VPDB standard (Coplen 1995). To derive the ratio c_i / c_a, these carbon isotope ratios can be used via Equation 1:

$$c_i / c_a = (\delta^{13}C_{plant} - \delta^{13}C_{air} + a) / (b - a) \qquad (4)$$

Rearranging this equation allows for the calculation of c_i as:

$$c_i = c_a [(\delta^{13}C_{plant} - \delta^{13}C_{air} + a) / (b - a)] \qquad (5)$$

The c_i / c_a ratio reflects the competition between CO_2 supply through stomata and the biochemical demand for CO_2 during carbon fixation. The $\Delta^{13}C$ imposed during photosynthesis is then recorded as carbon is incorporated into plant organic matter such as leaves and leaf photosynthates. Because this $\Delta^{13}C$ is sensitive to stomatal conductance, which varies with drought stress, the carbon discrimination in plant organic matter acts as an indicator of drought stress. The $\Delta^{13}C$ of leaf bulk tissue yields a measure of c_i / c_a *integrated over the time that the carbon was captured, which subsequently was used to build the structural tissues*. Conversely, the $\Delta^{13}C$ of assimilated sugars extracted from a leaf yields a measure of c_i / c_a *integrated across the particular day on which the leaf was collected* (Farquhar et al. 1982, Brugnoli et al. 1988, and reviewed in Gessler et al. 2014).

No isotopic fractionation occurs when plant roots take up water (Dawson and Ehleringer 1991, 1993). Therefore, the oxygen and deuterium isotope ratios ($\delta^{18}O$ and $\delta^{2}H$) of water in a plant's xylem provide an integrated measure of these ratios in the soil from which the plant took up the water. Typically, these ratios vary with specific rainfall vapor sources and history, and with depth within the soil. Variations in the isotopic ratios of rainfall are summarized by the local meteoric water lines (LMWL's) of a particular site, which are the linear regression equations of a given site's seasonal precipitation isotope values in dual-isotope space ($\delta^{2}H$ as a function of $\delta^{18}O$, ‰ VSMOW) (Craig 1961, Dansgaard 1964). When xylem water isotope ratios extracted from a given tree depart away from the LMWL of the site it is growing in, they have undergone fractionation effects in response to evaporation. This can therefore indicate the degree to which trees rely on seasonal precipitation stored in shallow soils versus groundwater stored at greater depth from the soil surface (Simonin et al. 2014, Oshun et al. 2016, Benettin et al. 2018). The $^{18}O/^{16}O$ and $^{2}H/^{1}H$ ratios of water samples are referenced to the $^{18}O/^{16}O$ and $^{2}H/^{1}H$ ratios of the 'Vienna-SMOW' or VSMOW standard, respectively (Coplen 1995).

Despite the widely demonstrated utility of stable isotopes for understanding the mechanistic impacts of extreme drought on plant physiological performance, field studies investigating *in-situ* drought impacts via seasonally-measured stable isotopes of leaf organic matter and xylem water are fairly limited. After Brugnoli et al. (1988) demonstrated the strong relationships between carbon isotope discrimination and c_i / c_a from bulk leaf material and extracted leaf sugars, the majority of field studies drawing on this approach have been restricted to the tree genera *Eucalyptus* (e.g. Cernusak et al. 2003), *Pinus* (e.g. Brandes et al. 2006, Gessler et al. 2009), and *Fagus* (e.g. Gessler et al. 2004, Scartazza et al. 2015), and horticultural species such

as grapevine (Gaudillère et al. 2002), castor bean (Gessler et al. 2008), and rice (Scartazza et al. 1998). Across these studies, daily- and seasonally-integrated foliar c_i concentrations tended to be associated with changes in water availability and subsequent declines in plant water status in response to differing degrees of CO_2 supply from transpiration and biochemical demands for CO_2 during carbon fixation. Thus, with respect to drought, daily- and seasonally-integrated c_i can be expected to decrease as a function of seasonal drought exposure, and therefore can serve as informative indicators of plant drought stress and photosynthetic performance through time.

However, recent studies of coexisting plant species that differ in their life history and water acquisition strategies have demonstrated that under drought, differing root architectures can disproportionately predispose species to physiological limitations to photosynthetic performance and survival if they are incapable of acclimating to seasonal reductions in water availability (e.g. Grossiord et al. 2017a and b, McBranch et al. 2018). This suggests that differing plant root architectures and water acquisition capacities can mediate and ameliorate the impacts of drought exposure on seasonal photosynthetic performance, especially under extreme drought conditions if seasonal water access remains relatively stable. Therefore, species with shallower root architectures undergoing multi-year drought conditions should be expected to exhibit increased xylem water LMWL departures through growing seasons due to the evaporative effects of drying soils on their xylem water isotope signatures until sufficient rainfall returns. Although drought-induced reductions of photosynthetic performance are likely to be associated with plant functional root architectures, predicting such differential impacts is not always straight forward, because the seasonal trajectory of plant water status and its effect on transpiration efficiency during a drought arises from the interaction of a suite of plant physiological traits with climate and complex environmental conditions (Feng et al. 2017, Feng et al. 2018 and *in press*). Moreover, predicting population-level drivers of seasonal photosynthetic performance across broad climatic, topographic, or environmental conditions is also complicated, because thermal and hydrological micro-refugia may ameliorate the negative effects of drought on plant water status and transpiration, and the overall degree of drought severity can vary substantially across and within species' geographic ranges (McLaughlin and Zavaleta 2012, McLaughlin et al. 2017). Thus, *in-situ* measurements of physiological responses to drought paired with isotopic characterizations of subsurface water uptake capacities and photosynthetic performance are essential to link climatic, landscape, and plant-level characteristics to estimates of productivity. Moreover, investigating such responses when historic, multi-year drought conditions arise is important for progressing our understanding of the overall physiological capacities of different plant species to acclimate and survive through them.

With this motivation, I expand on my research framework in Chapter 1 to test the effects of California's historic 2012 - 2016 drought on seasonal differences and changes in root water availability between blue oak (*Quercus douglasii*) and valley oak (*Q. lobata*). In addition, I test how these differences and changes in water access translate mechanistically into changes in seasonal plant water status, how these changes in plant water status affect transpiration efficiency, and how transpiration efficiency in turn affects different degrees of carbon assimilation with respect to seasonally- and daily-integrated measurements of foliar c_i concentrations. As I outlined in this previous chapter, these oaks are iconic California endemic tree species that coexist in woodlands, which form among the most diverse and geographically extensive ecosystems within the entire state (Stahle et al. 2013). Both oaks are drought-adapted

(Griffin 1971, 1973), and can live from 200 to more than 500 years old (Griffin 1976, Stahle et al. 2013). They are also both winter-deciduous, with leaves flushing once in the spring following precipitation inputs over the winter, and senescing at the end of the growing season in the fall. More importantly, I have demonstrated that my study design captured a range of climate and drought severity conditions, and covered a substantial extent of both oak species' geographic ranges. In addition, I have demonstrated that these species differed substantially in their ability to recover their spring seasonal water status as a function of drought exposure and potential differences in embolism formation and soil water availability, and this lack of recovery was associated with higher degrees of canopy damage and mortality (Chapter 1). This suggests that these species may differ substantially in their seasonal water acquisition strategies with respect to the zones of water extraction that they can exploit along the landscape, such that blue oaks may be more vulnerable to extreme drought with respect to their capacity to maintain contact with groundwater resources through the growing season. The signatures of this lack of deep water access would thus be reflected in having greater xylem water departures from the LMWL over time, and conversely, if indeed valley oaks are deeper rooted, the magnitude of their seasonal xylem water LMWL departures would not deviate as far from their LMWL. In turn, these signatures of shallow water use in blue oak would reduce their seasonal water status and transpiration efficiency compared to valley oak, which would then be reflected in the stable isotope record of their leaves in terms of reduced foliar c_i. However, the degree to which these species may maintain access to deeper or more stable water resources after spring leaf flush and through the rest of the growing season has yet to be demonstrated, and clearly has important implications on the capacity for these species to maintain their water status and assimilate carbon under extreme drought conditions. Many studies focusing solely on bulk foliar carbon isotopes rather than alongside leaf sugar ^{13}C within the genus *Quercus* exist throughout the literature, but only the deciduous oak *Q. petraea* has been comparably studied for carbon isotopes of photosynthate (Maunoury et al. 2007). Otherwise, comparative studies of the differential physiological capacities between these two species or experimental investigations of the isotopic signatures of drought responses between them are not well represented in the literature. Taken together, these results suggest that these oaks may differ in how they photosynthetically acclimate to extreme drought as a function of their capacity to maintain stable water access. Thus, they are excellent candidates in which to investigate differences in water acquisition strategies using stable isotopes of xylem water, and how these differences translate into differential photosynthetic performance under extreme drought conditions using stable isotopes of leaves and leaf photosynthate.

The objective of this chapter is to test for the effects of differing soil water acquisition strategies in these two coexisting, drought-adapted oak species on their relative ability to assimilate carbon under extreme drought conditions across wide range of drought exposure and historical climatic conditions, and to identify the physiological pathways governing differential degrees of photosynthetic performance across these gradients. To accomplish this, I measured temporal changes in the stable isotope composition of xylem water of each species through the drought period, and paired them with seasonal measurements of predawn and midday plant water status. These water status measurements were then tested as a function of measurements of midday stomatal conductance, which were then tested as a function of the foliar c_i concentrations derived from stable isotope measurements of leaves and leaf photosynthate. In doing so, I focus on bulk

leaf c_i and leaf sugar c_i as seasonally- and daily-integrated measurements of carbon fixation as a function of water limitation through the drought period to test the following set of hypotheses:

H1: LMWL departures will be larger in drier sites and continue to increase through each growing season, with the largest departures observed in blue oaks compared to valley oaks.
H2: Greater departures from site LMWL's will be associated with more negative predawn water potentials through the drought, which will then translate into lower seasonal midday-predawn water potential differentials.
H3: Trees with lower predawn water potentials and lower midday-predawn water potential differentials in response to LMWL departures will have lower midday transpiration rates towards the end of the growing season, which will translate into lower daily-integrated leaf c_i concentrations.
H4: Seasonal foliar $\delta^{13}C$ will be more enriched in drier sites yielding lower seasonally-integrated foliar c_i concentrations, with blue oaks exhibiting lower c_i than valley oaks through the drought.

MATERIALS AND METHODS

Study species, site selection, climate, and study design

This chapter addresses the same experimental system and design outlined in Chapter 1, and information about the selection of sites, study species, the range of drought severity and precipitation spanned across the sites, and the overall study design are not repeated here. The methods section focuses on describing the sampling and analysis to obtain foliar carbon isotopes and stomatal conductance measurements.

Foliar carbon isotope ratios

I made repeated leaf collections on a subset of the study trees at each site during each field campaign. Six individuals in each hilltop and valley-bottom landscape gradient were randomly selected at each site for my sample pool. Immediately prior to sunset leaves from terminal, sun exposed canopy branches were removed from their stems and sealed in paper coin envelopes. The dusk sampling time of leaf collection was kept consistent across sites and campaigns in order to account for the isotopic signatures imprinted in the photosynthate produced through the entirety of each collection day. Sample envelopes were immediately submerged in liquid nitrogen in the field to eliminate microbial or enzymatic fractionation of the carbon contained in bulk leaf and leaf sugar material. Samples were kept frozen at -20 ºC prior to processing for stable isotope mass spectrometry at the Center for Stable Isotope Biogeochemistry (CSIB) at UC Berkeley.

To determine the $\delta^{13}C$ of bulk leaf material, leaf samples were pooled, freeze-dried, and ground into a fine powder. Individual 4 mg subsamples were weighed and packed in tin capsules, combusted, and analyzed using an Elementar EA-IsoPrime 100 (Isoprime Ltd., Cheadle, England) in continuous flow. To determine the $\delta^{13}C$ of leaf photosynthate, sugars were extracted from the same pool of ground leaf material used for bulk leaf $\delta^{13}C$ measurements following the methods described in Brugnoli et al. (1998). Briefly, polyvinylpolypyrrolidone is used to isolate

leaf organic acids and amino acids from leaf sugars using an anion exchange resin via filtration in chromatographic columns. A minimum of 2 mg of extracted sugars was weighed and packed within tin capsules, combusted, and then also analyzed using an Elementar EA-IsoPrime 100 (Isoprime Ltd., Cheadle, England) in continuous flow. Resulting stable isotope ratios were expressed in 'per-mil' or ‰ notation following Equation 3. All leaf and leaf sugar c_i concentrations were derived using Equation 5 assuming even atmospheric mixture across the study period, with $\delta^{13}C$ of CO_2 in the air taken to be -8.3 ‰ (VPDB) at a concentration c_a of 400 μmol mol^{-1}.

Stomatal conductance

To determine midday stomatal closure, I made repeated seasonal measurements of stomatal conductance across the same subset of plants used for carbon isotope analyses. Leaf porometers (Decagon Devices, Inc., Pullman, WA, USA) were used to measure foliar stomatal conductance across six different sun-exposed leaves throughout each tree's canopy to calculate an average tree-level value of stomatal conductance. Measurements were made immediately following midday xylem water potential measurements (outlined below) and prior to leaf carbon isotope sample collections (made on the same day) to allow for consistent comparisons across sites and field campaigns. Porometers were field calibrated prior to each set of measurements to maximize measurement accuracy at each site over time, and values of stomatal conductance were recorded in mmol m^{-2} s^{-1}.

Plant water status, xylem water isotopes, and local meteoric water lines

The predawn and midday water potential measurements used in the analyses in this chapter are those described in Chapter 1. Similarly, sampling of xylem, stable isotope measurements of extracted xylem waters, the construction of site LMWL's, and the calculation of LMWL departure for each tree follow the methods described in Chapter 1. The methods are not reiterated here. Note that in the present analysis water isotope data collected from all five measurement campaigns (summer 2014, fall 2014, spring 2015, fall 2015, and spring 2016) are considered (Figure 1), in contrast to only two spring campaigns used in Chapter 1.

Statistical analyses

To test my hypotheses involving seasonal changes in LMWL departure (**H1**) and their effects on water status (**H2**), transpiration and daily-integrated c_i (**H3**), and seasonally-integrated c_i (**H4**), I ran multiple linear mixed effects models for each of these predictor variables. Because this study made repeated measures on the same individual trees among sites through time, each study tree individual is statistically treated as a random effect in each linear mixed effects model to account for non-independence of measurements. Within each model, sites, species, and measurement campaigns are therefore treated as interacting fixed effects. LMWL departure, predawn water potential, midday-predawn water potential differential, stomatal conductance, and foliar c_i were treated as response variables to test each hypothesis using the following model structures:

Model 1 (**H1**): LMWL Departure ~ Site * Species * Campaign + (1 | Tree Individual)

Model 2 (**H2**): Predawn Water Potential ~ LMWL Departure * Site * Species * Campaign + (1 | Tree Individual)
Model 3 (**H2**): Midday-Predawn Water Potential Differential ~ Predawn Water Potential * Site * Species * Campaign + (1 | Tree Individual)
Model 4 (**H3**): Stomatal Conductance ~ Predawn Water Potential * Site * Species * Campaign + (1 | Tree Individual)
Model 5 (**H3**): Leaf Sugar c_i ~ Stomatal Conductance * LMWL Departure * Site * Species * Campaign + (1 | Tree Individual)
Model 6 (**H4**): Bulk Leaf c_i ~ Site * Species * Campaign + (1 | Tree Individual)

Significance tests for each coefficient factor in each model were performed using Type III ANOVA via Wald chi-square tests to account for all model coefficient interactions. All statistical pairwise contrasts between each interacting set of site, species, and campaign factors in each model were performed via least-squares means comparisons. All statistical analyses and figures were produced using the R statistical platform (R Core Team 2017) and the following packages: *lme4* (Bates et al. 2015), *car* (Fox and Weisberg 2011), *lsmeans* (Lenth 2016), *dplyr* (Wickham et al. 2017), and *ggplot2* (Wickham 2009).

RESULTS

LMWL departure (H1)

LMWL departure was significantly different between sites, species, and campaigns, with significant interactions between sites and campaigns (Table 1, *Site : Campaign* χ^2 25.1260, P = 0.0015) and between species and campaigns (Table 1, *Species : Campaign* χ^2 9.6925, P = 0.0459). The largest departures away from site LMWL's were observed in the blue oaks at the driest site (CR) (Figure 2). Across sites, the LMWL departures of valley oaks was both smaller and less seasonally variable than values observed in blue oaks. These results fully support **H1** in that the greatest degree of uptake of evaporatively enriched soil water was predominantly observed in the blue oaks at the driest study site (CR), upwards of 70% - 83% higher than the maximum values of LMWL departure of blue oaks at PW and BORR, respectively. However, contrary to **H1**, LMWL departure in both species only increased each season up to spring 2016 (when average rainfall had returned across sites) at the most mesic site (PW) and the driest site (CR) rather than across all sites. At BORR, both blue oaks and valley oaks exhibited increased LMWL departures in all summer and fall seasons that were followed by decreases in LMWL departure during all spring campaigns. Thus, unlike at PW and CR, LMWL departures at BORR did not get progressively larger through the study period.

LMWL departure and seasonal water potential trajectories (H2)

Predawn water potential was significantly associated with the magnitude of LMWL departure across sites, species, and campaigns, with significant LMWL departure interactions between sites, species, and campaigns (Table 2, *LMWL Departure : Site : Species : Campaign* χ^2 21.1631, P = 0.0067). Across all seasons, predawn water potentials were more negative in blue oaks compared to valley oaks at each site, and became the most negative at the intermediately dry site

(BORR) at the peak of the drought in fall 2014 (Figure 3). However, at the driest site (CR), seasonal declines in predawn water potential through the drought were most strongly associated with departures from site LMWL's for both oak species. Conversely, both species at BORR and PW were more weakly correlated with LMWL departure, particularly in both spring campaigns where the overall magnitude of LMWL departures were least pronounced. These results support **H2** in that trees using more evaporatively enriched soil water through the drought also had more negative predawn water potentials.

The seasonal midday-predawn water potential differential (i.e. the water potential gradient driving transpiration and carbon fixation) was also significantly associated with predawn water potential, with significant predawn water potential interactions between sites and campaigns (Table 3, *Predawn Water Potential : Site : Campaign* χ^2 20.2078, P = 0.0096). As observed in the seasonal response of predawn water potential to LMWL departure (Figure 3), the water potential differentials of both species were less strongly correlated to predawn water potential during spring campaigns compared to summer and fall campaigns. Moreover, the seasonal water potential differentials of the blue oaks at the driest site (CR) were the least responsive to progressive declines in predawn water potential, and remained low through the drought even at more positive (i.e. more relaxed) predawn water potentials (Figure 4). Conversely, at the wetter sites (BORR and PW), seasonal declines in predawn water potential corresponded with more rapid declines in midday-predawn water potential differential. Taken together, these results fully support **H2** in that the seasonal predawn water potential of both species was significantly associated with the degree of evaporatively enriched soil water use, which then translated into lower seasonal water potential differentials.

Transpiration, LMWL departure, and daily-integrated c_i (H3)

Late season midday stomatal conductance was not significantly associated with water potential differential across sites, species, or campaigns. However, it was significantly associated with the predawn water potential during these summer and fall campaigns, with significant predawn water potential interactions between sites, species, and campaigns (Table 4, *Predawn Water Potential : Site : Species : Campaign* χ^2 10.8748, P = 0.0280). Late season predawn water potentials and transpiration rates were the highest in both species at the most mesic site (PW) (Figure 5). At this site, declines in predawn water potential were most strongly associated with declines in transpiration. By comparison, transpiration rates remained lower for both species at BORR and CR, where declines in predawn water potentials were associated with more gradual reductions in transpiration. These results only partially support **H3** in that only declines in predawn water potential were found to be associated with declines in transpiration, while midday-predawn water potential differentials had no significant effect.

The daily-integrated foliar c_i concentrations during all late growing season campaigns was significantly associated with midday stomatal conductance, with significant stomatal conductance interactions between sites and species (Table 5, *Stomatal Conductance : Site : Species* χ^2 8.0546, P = 0.0178). Moreover, these c_i concentrations were also jointly found to be significantly associated with LMWL departure within the same model, also with significant interactions between sites and species (Table 5, *Stomatal Conductance : LMWL Departure : Site : Species* χ^2 6.1763, P = 0.0456). This suggests that the magnitude of foliar c_i concentrations was

positively affected by both higher stomatal conductance rates (Figure 6) and higher degrees of the use of shallow, evaporatively enriched soil water (Figure 7). The response of foliar c_i to these two factors was strongest at the driest site (CR), where blue oaks exhibited both the greatest reductions in stomatal conductance through the drought as well as the most negative LMWL departures. Comparing the magnitude of these blue oak c_i concentrations as well as their slopes in response to changes in stomatal conductance and LMWL departure shows how compromised their photosynthetic performance was at this site compared to BORR and PW, with c_i levels reaching as low as 136.7 μmol mol^{-1}. Moreover, the response of c_i to declines in LMWL departure at this site was much stronger for both species than that observed at BORR and PW. Taken together, these results are in support of **H3** in that towards the end of each growing season, trees with greater use of shallow, evaporatively enriched waters also had lower predawn water potentials. These lower predawn water potentials then translated into lower transpiration rates, which in turn were strongly associated with lower c_i concentrations.

Seasonally-integrated c_i (H4)

Seasonally-integrated c_i was significantly different between sites, species, and campaigns, with significant interactions between sites and species (Table 6, *Site : Species* χ^2 11.7209, P = 0.0029) and sites and campaigns (Table 6, *Site : Campaign* χ^2 70.6149, P < 0.0001). Concentrations of seasonally-integrated c_i were lowest in the blue oaks at the driest site (CR), and highest in the blue oaks at the most mesic site (PW) (Figure 8). These c_i concentrations also varied seasonally to different degrees across sites, with the greatest c_i reductions observed in the valley oaks at CR and in the blue oaks at BORR during the spring 2015 campaign. Otherwise values of c_i remained consistent through the drought, with an overall directional signal of low c_i to high c_i from the driest to the wettest site in both species. However, c_i tended to be much more variable at CR compared to BORR and PW, with upwards of 75 μmol mol^{-1} variation within campaigns in both species. These results fully support **H4** in that bulk leaf $\delta^{13}C$ was more enriched in the driest study site, which reflected lower seasonally-integrated concentrations of foliar c_i.

DISCUSSION

This study expanded upon a natural experiment during a historic drought event to test the effects of water limitation in functional rooting zones, seasonal water status, and transpiration efficiency on the photosynthetic performance of two long-lived, drought-adapted oak species. By integrating years of field measurements of plant water potential, stomatal conductance, and stable isotopes of leaves and xylem water, this work provides strong support for the hypothesis that poor seasonal access to stable soil water resources translates into reductions in predawn plant water potential and midday-predawn water potential differential, which then reduces transpiration efficiency through growing seasons, ultimately leading to poorer photosynthetic performance of these species under extreme drought conditions. In this study, these responses were most pronounced in the blue oaks at the most drought exposed site, as they exhibited upwards of 70% - 83% higher degrees of local meteoric water line departure compared to blue oaks and valley oaks at the less drought-exposed and historically more mesic sites. In response to such different water acquisition strategies, these blue oaks had the most reduced transpiration rates and the lowest seasonally-integrated and daily-integrated c_i concentrations, which were

directly mediated by changes in seasonal plant water status. I infer that these differences in water acquisition capacity along the landscape translate into important differences in the capacity for these two species to maintain connectivity to sufficient groundwater resources through such extreme drought conditions, which is essential for the maintenance of seasonal plant water status and sustained photosynthetic performance. Taken together, these measurements provide unprecedented suite of interacting physiological metrics of the limitations of carbon assimilation and overall physiological performance of these oaks under historic drought stress conditions within natural field conditions, and provide important insights into the physiological thresholds these species operate under in response to such conditions within their natural habitats.

The seasonal changes in LMWL departure observed in this study between these two species suggest that they utilize very different zones of water extraction both within and among sites, and therefore may have fundamentally different water acquisition strategies along the landscape and across their geographic distributions. In this study, blue oaks at the driest site showed the greatest signs of shallow water use as well as the greatest overall variation in the range of LMWL departures in each measurement campaign through the drought. This suggests that blue oak root architecture is more restricted to shallower soil water zones and is more variable than valley oak, especially at the drier edge of their geographic distributions. Indeed, the LMWL departures of valley oaks remained much more reduced across sites and campaigns even at the most xeric site, suggesting that they are more reliant on maintaining access to deeper, more stable water resources throughout their geographic range compared to blue oaks. However, this xeric site also had the highest mortality rates for blue oak individuals that were not able to recover their seasonal water status (Chapter 1), suggesting that their degree of shallow water restriction may make them more vulnerable to drought induced mortality if they are incapable of physiologically acclimating to more prolonged drought conditions in the future. Contrary to my expectations, however, drought exposure did not scale with access to deeper soil water resources in either species, because both oaks at the intermediately drought exposed site (BORR) had the most seasonally-stable xylem water isotope signatures through the drought, despite undergoing substantial degrees of drought exposure with respect to precipitation reductions (Figure 2). Moreover, unlike at PW and CR, BORR LMWL departures were reduced in the spring 2015 campaign and thus did not continue to increase through the drought period as they did at PW and CR. This suggests that even under drought, subsurface groundwater recharge after the fall 2014 growing season was more sufficient to rehydrate trees than at PW and CR, further reiterating how trees growing in more historically xeric sites are not necessarily more likely to be vulnerable to drought stress than more historically mesic sites if the groundwater dynamics override climatic metrics of drought severity. Together, these were surprising and important results, because most vegetation modelling efforts geared towards predicting vulnerability to drought induced mortality simply do not account for this level of environmental heterogeneity, but rather rely on more top-down climatic estimates of potential drought stress. In addition, the average annual precipitation at this site was measured to be about half of that at the most mesic site (PW) (Chapter 1), yet the water resources both species maintained access to were more stable and seasonally permanent through the drought period compared to both the most mesic site (PW) and the most xeric site (CR). This result is consistent with recent work demonstrating how root access to hydrologic refugia may ameliorate the negative effects of extreme drought events, even in more drought exposed regions (McLaughlin et al. 2017), and underscores the

potential for resilience to extreme drought that would otherwise have gone unnoticed or unaccounted for.

Perhaps the most important result from this work was that seasonal increases in the magnitude of LMWL departure (i.e. the greater use of shallow, evaporatively enriched soil water) were sequentially associated with seasonal declines in predawn water status of both species (Figure 3), which were then associated with declines in midday-predawn water potential differentials (i.e. the gradient driving daily transpiration, Figure 4), which were then associated with declines in midday transpiration (Figure 5) that were responsible for reductions in foliar c_i concentrations (Figure 6). This mechanistic physiological link provides a new level of support for the power of stable isotopes in understanding important nuances of plant drought responses. With respect to xylem water isotopes, the literature is rich with important studies that have demonstrated their utility in characterizing variation in the sources or temporal dynamics of soil water resources that different coexisting species have access to (e.g. Dawson and Ehleringer 1991, Ehleringer and Dawson 1992, West et al. 2008, Oshun et al. 2016). However, I am not aware of any studies that have directly or mechanistically linked seasonal changes in xylem water isotopes to changes in physiological metrics of water status or photosynthetic performance. And although research on foliar carbon isotopes has an equally rich history in studying plant drought responses (e.g. Ehleringer 1993, Picon et al. 1996, McDowell et al. 2010), I am equally unaware of any studies that have combined measurements of seasonally- and daily-integrated c_i concentrations from them alongside seasonal changes xylem water isotopes to understand differences in the physiological performance, let alone under extreme drought conditions. Although I was unable to find comparable studies of the stable isotope composition of bulk leaf matter and leaf sugars within *Q. douglasii* (the most negatively impacted study species with respect to bulk leaf and leaf sugar c_i in response to drought), the results provide a stark contrast to previous studies that focused on bulk leaf c_i concentrations in this species (Matzner et al. 2001, 2003). Under the experimental drought treatments of reported by Matzner, bulk leaf c_i concentrations never dropped below ca. 200 μmol mol^{-1}, even at comparable rates of stomatal conductance experience in the field in the present study. With respect to the effects of seasonal trajectories of plant water status and stomatal conductance on carbon assimilation in response to drought, only in a study by Osuna et al. (2015) and another by Xu and Baldocchi (2003) was I able to find comparable extents of water status and transpiration reductions in response to seasonal water deficits to those observed in the blue oaks in this study, where net assimilation was also found to be significantly associated with seasonal water status and transpiration efficiency. Nonetheless, across all available related studies of carbon isotope discrimination and degrees of evaporative enrichment in xylem water that I could find throughout the literature, not only were the measurements of the $\Delta^{13}C$ and the foliar c_i concentrations of bulk leaf material and extracted leaf sugars reported here consistently far beyond in scale to previously reported values, but the magnitude of enrichment of xylem water δ^2H and $\delta^{18}O$ was likewise beyond any published value I could find. For scale, blue oaks reached seasonally-integrated c_i values as low as 148.9 μmol mol^{-1} and daily-integrated c_i values as low as 136.7 μmol mol^{-1}, while valley oaks reached levels as low as 177.7 μmol mol^{-1} and 145.2 μmol mol^{-1}, respectively. These values are within the physiological range generally only observed in nature in CAM plant species, and therefore may be some of the poorest photosynthetic performances ever recorded in C_3 species under natural field conditions. Still, it is worth acknowledging that previously stored carbon has been found to contribute to isotope values when they start to become this enriched (e.g. Smedley et al. 1991), and may have been a

factor in contributing to the values reported here. In addition to these carbon isotope signatures, xylem water isotopes at the driest site (CR) also reached enrichment levels outside of any range I could find in the literature, getting as enriched as -23.8 δ^2H as a function of 3.1 $\delta^{18}O$ (‰ VSMOW, Figure 1). Perhaps what is most remarkable about all of this is that although these are extremely low, if not unprecedented, values reminiscent of extremely poor physiological performance in response to extreme water deficits, it is important to note that the vast majority of the trees in this study still managed to survive through this historic drought event, underscoring their capacity for resilience to the extreme water deficits that were responsible for causing massive widespread instances of forest mortality in other tree species in other parts of the state (USFS 2015).

Despite the myriad studies incorporating stable isotope analyses of all levels of the physiological function of trees - from leaves and the photosynthates and starches they assimilate, to the phloem and xylem sap that is transported throughout plant organs, to stored carbon pools via non-structural carbohydrates, and finally down to the isotopic signatures imprinted in tree rings - there is still a lot to be understood about the physiological nature of storage of assimilated carbon and its overall importance, capacity, and lability (Gessler and Treydte 2016). With respect to this study, I acknowledge that the observed values of bulk leaf and leaf sugar stable carbon isotope ratios are potentially susceptible to diurnal and seasonal isotopic fluctuations in response to potential fluctuations in ambient environmental conditions such as vapor pressure deficits and the temperatures of leaves and of the air surrounding them (reviewed in Gessler et al. 2014). Though such considerations are important for more intensive experimental studies on shorter time scales and under more controlled environmental conditions, accounting for such potential fluctuations is out of the scope of this study as it aims to understand larger spatial and temporal scale effects of historic drought conditions on carbon assimilation. As such, this work adds to our understanding of important nuances behind *in-situ* tree responses to extreme drought by integrating novel stable isotope approaches under historic drought conditions. Together, these results provide strong support for the hypothesis that differential root access to stable groundwater between these species translates into reduced efficiency of carbon assimilation that is directly mediated directly through reductions in seasonal water status and their effects on inhibiting transpiration.

In Chapter 3, I further explore the potential consequences of poor photosynthetic performance in response to these severe water deficits with a focus on seasonal changes in functional leaf allocation in order to gain further insight into the drought responses of these oaks covered thus far in Chapters 1 and 2.

REFERENCES

Barbeta, A., Mejía-Chang, M., Ogaya, R., Voltas, J., Dawson, T.E. and Peñuelas, J., 2015. The combined effects of a long-term experimental drought and an extreme drought on the use of plant-water sources in a Mediterranean forest. *Global Change Biology*, 21(3), pp.1213-1225.

Bates, D., Maechler, M., Bolker, B., and Walker, S., 2015. Fitting Linear Mixed-Effects Models Using lme4. *Journal of Statistical Software*, 67(1), 1-48.

Benettin, P., Volkmann, T.H., Freyberg, J.V., Frentress, J., Penna, D., Dawson, T.E. and Kirchner, J.W., 2018. Effects of climatic seasonality on the isotopic composition of evaporating soil waters. *Hydrology and Earth System Sciences*, 22(5), pp.2881-2890.

Brandes, E., Kodama, N., Whittaker, K., Weston, C., Rennenberg, H., Keitel, C., Adams, M.A. and Gessler, A., 2006. Short-term variation in the isotopic composition of organic matter allocated from the leaves to the stem of *Pinus sylvestris*: effects of photosynthetic and postphotosynthetic carbon isotope fractionation. *Global Change Biology*, 12(10), pp.1922-1939.

Brugnoli, E., Hubick, K.T., von Caemmerer, S., Wong, S.C. and Farquhar, G.D., 1988. Correlation between the carbon isotope discrimination in leaf starch and sugars of C3 plants and the ratio of intercellular and atmospheric partial pressures of carbon dioxide. *Plant Physiology*, 88(4), pp.1418-1424.

Cernusak, L.A., Arthur, D.J., Pate, J.S. and Farquhar, G.D., 2003. Water relations link carbon and oxygen isotope discrimination to phloem sap sugar concentration in Eucalyptus globulus. *Plant Physiology*, 131(4), pp.1544-1554.

Coplen, T.B., 1995. Discontinuance of SMOW and PDB. *Nature*, 375(6529), p.285.

Craig, H., 1961. Isotopic variations in meteoric waters. *Science*, 133(3465), pp.1702-1703.

Dansgaard, W., 1964. Stable isotopes in precipitation. *Tellus*, 16(4), pp.436-468.

Dawson, T.E. and Ehleringer, J.R., 1991. Streamside trees that do not use stream water. *Nature*, 350(6316), p.335.

Dawson, T.E. and Ehleringer, J.R., 1993. Isotopic enrichment of water in the "woody" tissues of plants: Implications for plant water source, water uptake, and other studies which use stable isotopic composition of cellulose. *Geochimica et Cosmochimica Acta*, 57, pp.3487-3487.

Dawson, T.E., Mambelli, S., Plamboeck, A.H., Templer, P.H. and Tu, K.P., 2002. Stable isotopes in plant ecology. *Annual Review of Ecology and Systematics*, 33(1), pp.507-559.

Ehleringer, J.R. and Dawson, T.E., 1992. Water uptake by plants: perspectives from stable isotope composition. *Plant, Cell & Environment*, 15(9), pp.1073-1082.

Ehleringer, J.R., 1993. Variation in leaf carbon isotope discrimination in Encelia farinosa: implications for growth, competition, and drought survival. *Oecologia*, 95(3), pp.340-346.

Farquhar, G.D., O'Leary, M.H. and Berry, J.A., 1982. On the relationship between carbon isotope discrimination and the intercellular carbon dioxide concentration in leaves. *Functional Plant Biology*, 9(2), pp.121-137.

Farquhar, G.D., Ehleringer, J.R. and Hubick, K.T., 1989. Carbon isotope discrimination and photosynthesis. *Annual Review of Plant Biology*, 40(1), pp.503-537.

Feng, X., Dawson, T.E., Ackerly, D.D., Santiago, L.S. and Thompson, S.E., 2017. Reconciling seasonal hydraulic risk and plant water use through probabilistic soil–plant dynamics. *Global Change Biology*, 23(9), pp.3758-3769.

Feng, X., Ackerly, D.D., Dawson, T.E., Manzoni, S., Skelton, R.P., Vico, G. and Thompson, S.E., 2018. The ecohydrological context of drought and classification of plant responses. *Ecology Letters*, 21(11), pp.1723-1736.

Feng, X., Ackerly, D.D., Dawson, T.E., Manzoni, S., McLaughlin, B.C., Skelton, R.P., Vico, G., Weitz, A.P., Thompson, S.E., 2018. Beyond isohydricity: the role of environmental variability in determining plant drought responses. *Plant, Cell & Environment*, *in press*.

Fox, J. and Weisberg, S., 2011. An R Companion to Applied Regression, Second Edition. Thousand Oaks, CA. http://socserv.socsci.mcmaster.ca/jfox/Books/Companion

Gaudillère, J.P., Van Leeuwen, C. and Ollat, N., 2002. Carbon isotope composition of sugars in grapevine, an integrated indicator of vineyard water status. *Journal of Experimental Botany*, 53(369), pp.757-763.

Gessler, A., Rennenberg, H. and Keitel, C., 2004. Stable Isotope Composition of Organic Compounds Transported in the Phloem of European Beech-Evaluation of Different Methods of Phloem Sap Collection and Assessment of Gradients in Carbon Isotope Composition during Leaf-to-Stem Transport. *Plant Biology*, 6(6), pp.721-729.

Gessler, A., Tcherkez, G., Peuke, A.D., Ghashghaie, J. and Farquhar, G.D., 2008. Experimental evidence for diel variations of the carbon isotope composition in leaf, stem and phloem sap organic matter in *Ricinus communis*. *Plant, Cell & Environment*, 31(7), pp.941-953.

Gessler, A., Brandes, E., Buchmann, N., Helle, G., Rennenberg, H. and Barnard, R.L., 2009. Tracing carbon and oxygen isotope signals from newly assimilated sugars in the leaves to the tree-ring archive. *Plant, Cell & Environment*, 32(7), pp.780-795.

Gessler, A., Ferrio, J.P., Hommel, R., Treydte, K., Werner, R.A. and Monson, R.K., 2014. Stable isotopes in tree rings: towards a mechanistic understanding of isotope fractionation and mixing processes from the leaves to the wood. *Tree Physiology*, 34(8), pp.796-818.

Gessler, A. and Treydte, K., 2016. The fate and age of carbon–insights into the storage and remobilization dynamics in trees. *New Phytologist*, 209(4), pp.1338-1340.

Griffin, J.R., 1971. Oak regeneration in the upper Carmel Valley, California. *Ecology*, 52(5), pp.862-868.

Griffin, J.R., 1973. Xylem sap tension in three woodland oaks of central California. *Ecology*, 54(1), pp.152-159.

Griffin, J.R., 1976. Regeneration in *Quercus lobata* savannas, Santa Lucia Mountains, California. *American Midland Naturalist*, pp.422-435.

Grossiord, C., Sevanto, S., Dawson, T.E., Adams, H.D., Collins, A.D., Dickman, L.T., Newman, B.D., Stockton, E.A. and McDowell, N.G., 2017a. Warming combined with more extreme precipitation regimes modifies the water sources used by trees. *New Phytologist*, 213(2), pp.584-596.

Grossiord, C., Sevanto, S., Adams, H.D., Collins, A.D., Dickman, L.T., McBranch, N., Michaletz, S.T., Stockton, E.A., Vigil, M. and McDowell, N.G., 2017b. Precipitation, not air temperature, drives functional responses of trees in semi-arid ecosystems. *Journal of Ecology*, 105(1), pp.163-175.

Herrero, A., Castro, J., Zamora, R., Delgado-Huertas, A. and Querejeta, J.I., 2013. Growth and stable isotope signals associated with drought-related mortality in saplings of two coexisting pine species. *Oecologia*, 173(4), pp.1613-1624.

IPCC, 2014: Climate Change 2014: Synthesis Report. Contribution of Working Groups I, II and III to the Fifth Assessment Report of the Intergovernmental Panel on Climate Change [Core Writing Team, R.K. Pachauri and L.A. Meyer (eds.)]. IPCC, Geneva, Switzerland, 151 pp.

Lenth, R.V., 2016. Least-Squares Means: The R Package lsmeans. *Journal of Statistical Software*, 69(1), 1-33.

Matzner, S.L., Rice, K.J. and Richards, J.H., 2001. Factors affecting the relationship between carbon isotope discrimination and transpiration efficiency in blue oak (*Quercus douglasii*). *Functional Plant Biology*, 28(1), pp.49-56.

Matzner, S.L., Rice, K.J. and Richards, J.H., 2003. Patterns of stomatal conductance among blue oak (*Quercus douglasii*) size classes and populations: implications for seedling establishment. *Tree Physiology*, 23(11), pp.777-784.

Maunoury, F., Berveiller, D., Lelarge, C., Pontailler, J.Y., Vanbostal, L. and Damesin, C., 2007. Seasonal, daily and diurnal variations in the stable carbon isotope composition of carbon dioxide respired by tree trunks in a deciduous oak forest. *Oecologia*, 151(2), p.268.

McBranch, N.A., Grossiord, C., Adams, H., Borrego, I., Collins, A.D., Dickman, T., Ryan, M., Sevanto, S., McDowell, N.G. and Maurizio, M., 2018. Lack of acclimation of leaf area: sapwood area ratios in piñon pine and juniper in response to precipitation reduction and warming. *Tree Physiology*, *in press*.

McCarroll, D. and Loader, N.J., 2004. Stable isotopes in tree rings. *Quaternary Science Reviews*, 23(7-8), pp.771-801.

McDowell, N.G., Allen, C.D. and Marshall, L., 2010. Growth, carbon-isotope discrimination, and drought-associated mortality across a Pinus ponderosa elevational transect. *Global Change Biology*, 16(1), pp.399-415.

McLaughlin, B.C. and Zavaleta, E.S., 2012. Predicting species responses to climate change: demography and climate microrefugia in California valley oak (Quercus lobata). *Global Change Biology*, 18(7), pp.2301-2312.

McLaughlin, B.C., Ackerly, D.D., Klos, P.Z., Natali, J., Dawson, T.E. and Thompson, S.E., 2017. Hydrologic refugia, plants, and climate change. *Global Change Biology*, 23(8), pp.2941-2961.

Oshun, J., Dietrich, W.E., Dawson, T.E. and Fung, I., 2016. Dynamic, structured heterogeneity of water isotopes inside hillslopes. *Water Resources Research*, 52(1), pp.164-189.

Osuna, J.L., Baldocchi, D.D., Kobayashi, H. and Dawson, T.E., 2015. Seasonal trends in photosynthesis and electron transport during the Mediterranean summer drought in leaves of deciduous oaks. *Tree Physiology*, 35(5), pp.485-500.

Picon, C., Guehl, J.M. and Ferhi, A., 1996. Leaf gas exchange and carbon isotope composition responses to drought in a drought-avoiding (Pinus pinaster) and a drought-tolerant (Quercus petraea) species under present and elevated atmospheric CO2 concentrations. *Plant, Cell & Environment*, 19(2), pp.182-190.

R Core Team, 2017. R: A language and environment for statistical computing. R Foundation for Statistical Computing, Vienna, Austria.

Scartazza, A., Lauteri, M., Guido, M.C. and Brugnoli, E., 1998. Carbon isotope discrimination in leaf and stem sugars, water-use efficiency and mesophyll conductance during different developmental stages in rice subjected to drought. *Functional Plant Biology*, 25(4), pp.489-498.

Scartazza, A., Moscatello, S., Matteucci, G., Battistelli, A. and Brugnoli, E., 2015. Combining stable isotope and carbohydrate analyses in phloem sap and fine roots to study seasonal changes of source–sink relationships in a Mediterranean beech forest. Tree Physiology, 35(8), pp.829-839.

Simonin, K.A., Link, P., Rempe, D., Miller, S., Oshun, J., Bode, C., Dietrich, W.E., Fung, I. and Dawson, T.E., 2014. Vegetation induced changes in the stable isotope composition of near surface humidity. *Ecohydrology*, 7(3), pp.936-949.

Smedley, M.P., Dawson, T.E., Comstock, J.P., Donovan, L.A., Sherrill, D.E., Cook, C.S. and Ehleringer, J.R., 1991. Seasonal carbon isotope discrimination in a grassland community. *Oecologia*, 85(3), pp.314-320.

Stahle, D.W., Griffin, R.D., Meko, D.M., Therrell, M.D., Edmondson, J.R., Cleaveland, M.K., Stahle, L.N., Burnette, D.J., Abatzoglou, J.T., Redmond, K.T. and Dettinger, M.D., 2013. The ancient blue oak woodlands of California: Longevity and hydroclimatic history. *Earth Interactions*, 17(12), pp.1-23.

USFS, 2015. 2015 Forest Health and Protection Aerial Detection Survey. USDA Forest Service.

West, A.G., Hultine, K.R., Sperry, J.S., Bush, S.E. and Ehleringer, J.R., 2008. Transpiration and hydraulic strategies in a piñon–juniper woodland. *Ecological Applications*, 18(4), pp.911-927.

Wickham, H., 2009. ggplot2: Elegant Graphics for Data Analysis. Springer-Verlag New York.

Wickham, H., Francois, R., Henry, L. and Müller, K., 2017. dplyr: A Grammar of Data Manipulation. R package version 0.7.4. https://CRAN.R-project.org/package=dplyr.

Xu, L. and Baldocchi, D.D., 2003. Seasonal trends in photosynthetic parameters and stomatal conductance of blue oak (*Quercus douglasii*) under prolonged summer drought and high temperature. *Tree Physiology*, 23(13), pp.865-877.

Figure 1. Dual-isotope bivariate plots of xylem water δ^2H and $\delta^{18}O$ extracted from *Q. douglasii* and *Q. lobata* stems across each field site during all measurement campaigns. Points represent the values of stable isotope ratios from individual study trees during each field campaign and are plotted as a function of the local meteoric water line (LMWL) of each site. LWML regression equations for each site are $\delta^2H = 7.82\ \delta^{18}O + 9.42$ ‰ for PW, $\delta^2H = 7.93\ \delta^{18}O + 9.21$ ‰ for BORR, and $\delta^2H = 7.45\ \delta^{18}O - 0.95$ ‰ for CR.

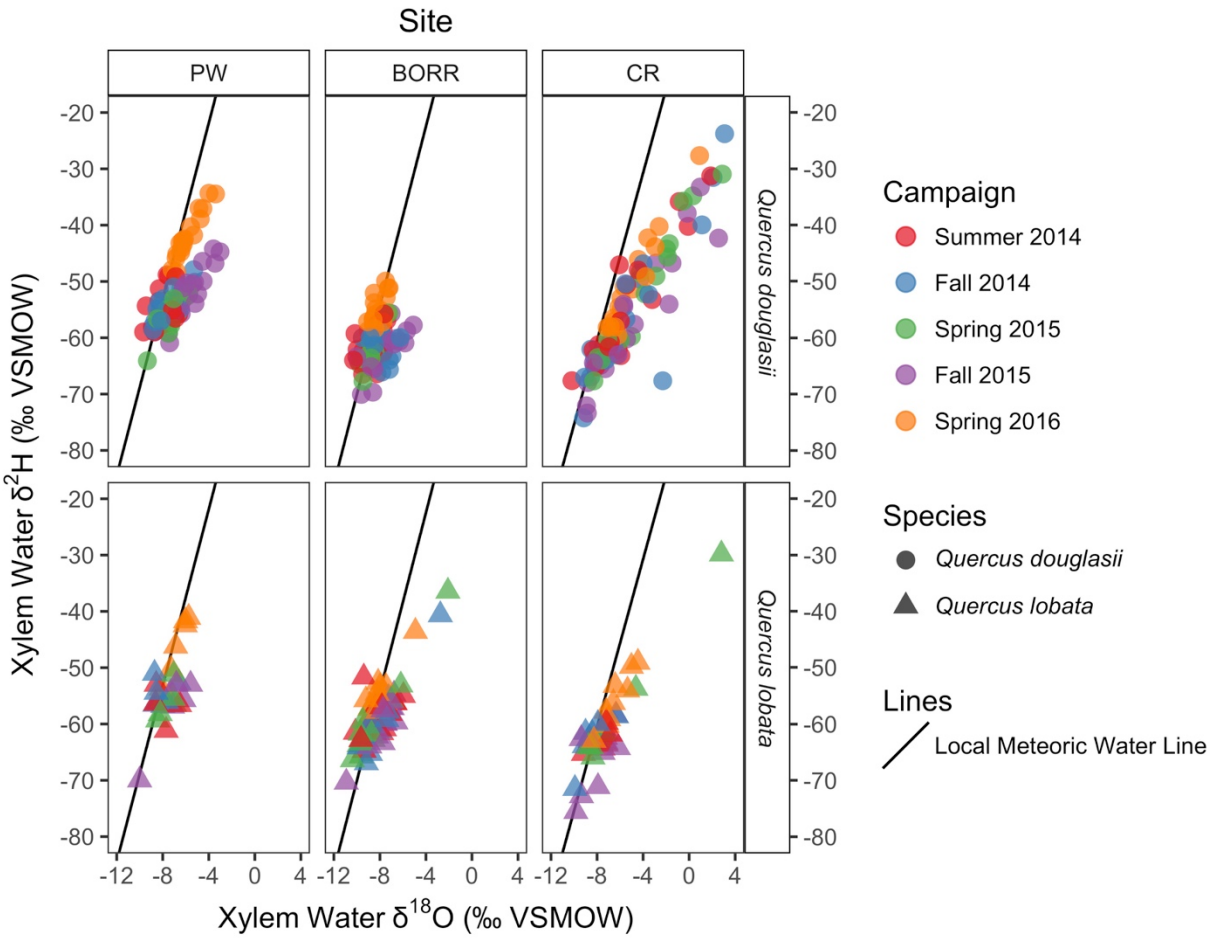

Figure 2. Seasonal changes in LMWL departure across study sites and species (**H1**). See Table 1 for analysis of deviance table for significant coefficients and their interactions.

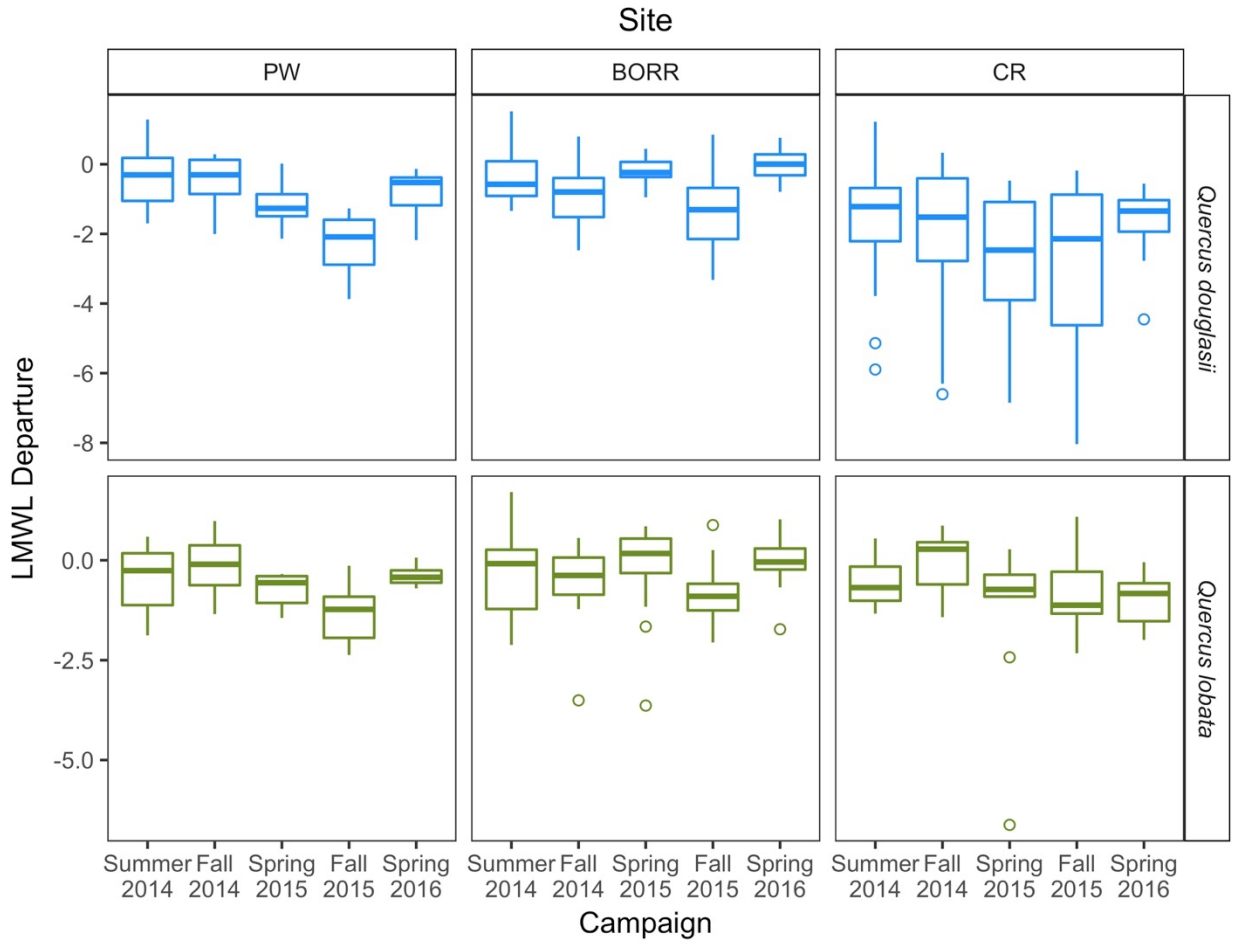

Figure 3. Model fits from Type III ANOVA testing **H2**: the effect of LMWL departure on predawn water of study trees across all sites, species, and campaigns. Fitted slopes represent significant coefficients and their interactions. See Table 2 for analysis of deviance table.

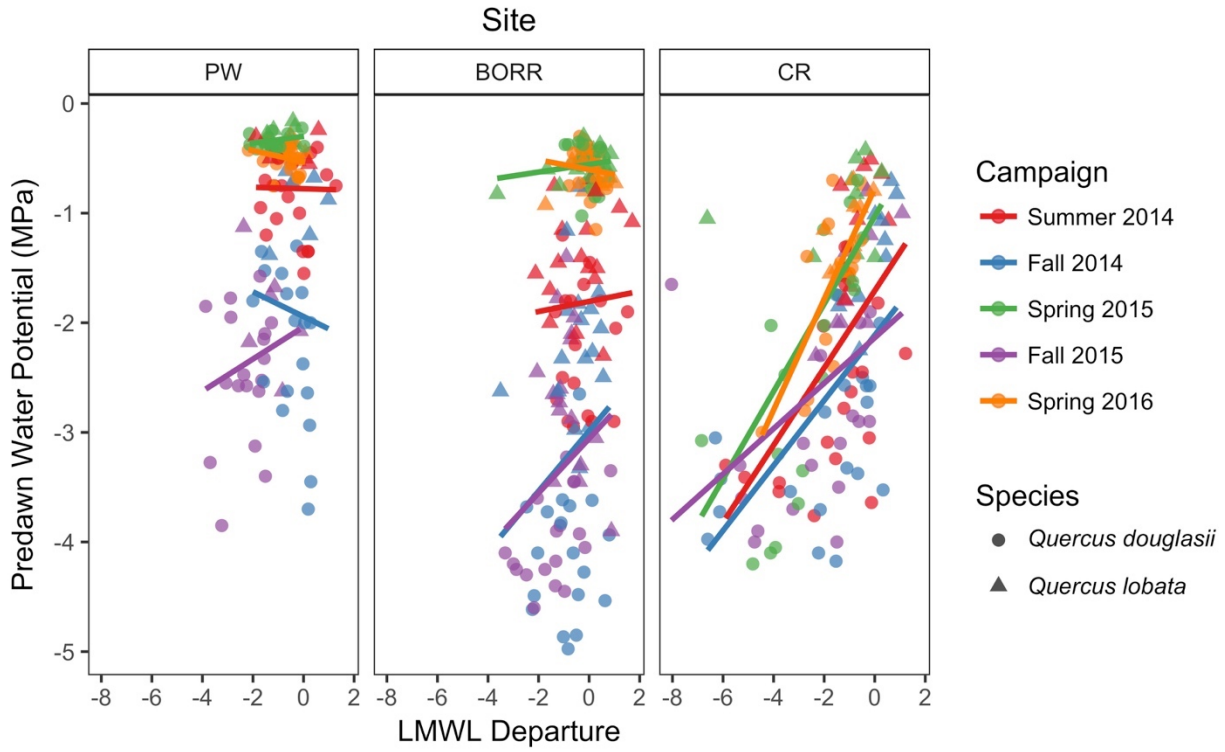

Figure 4. Model fits from Type III ANOVA testing **H2**: the effect of predawn water potential on the midday-predawn water potential differential of study trees across all sites, species, and campaigns. Fitted slopes represent significant coefficients and their interactions. See Table 3 for analysis of deviance table.

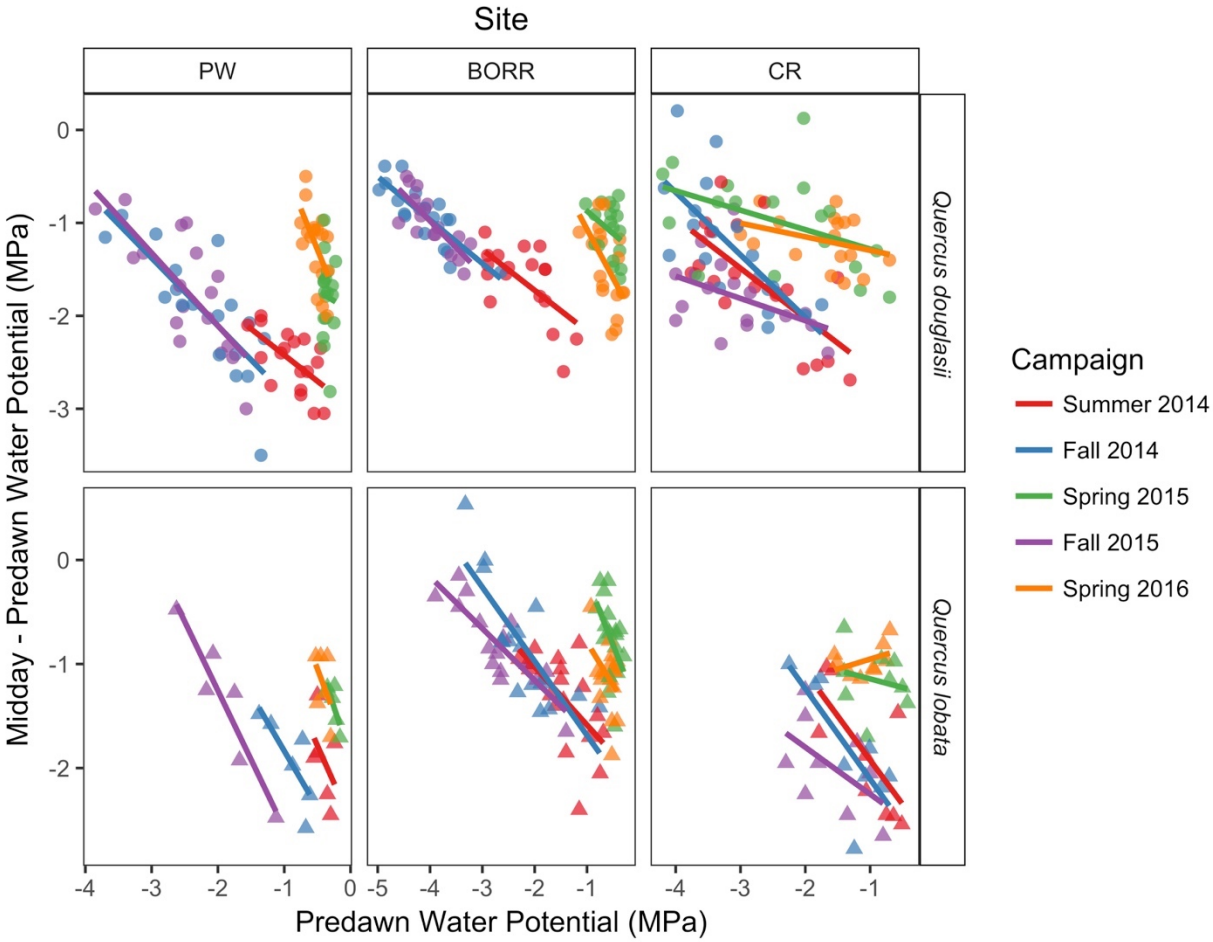

Figure 5. Model fits from Type III ANOVA testing **H3**: the effect of predawn water potential on midday stomatal conductance of study trees across all sites, species, and post-spring measurement campaigns. Fitted slopes represent significant coefficients and their interactions. See Table 4 for analysis of deviance table.

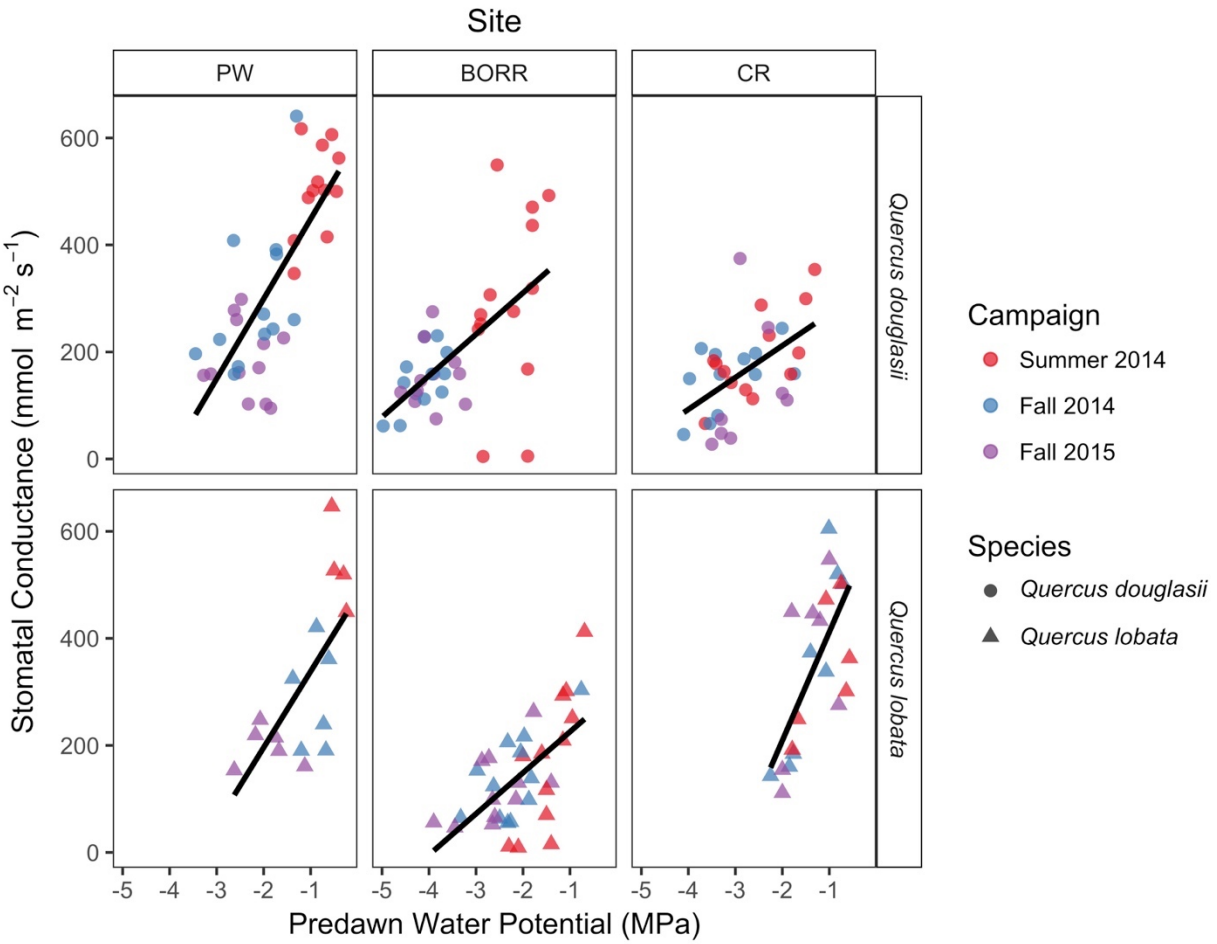

Figure 6. Model fits from Type III ANOVA testing **H3**: the effect of midday stomatal conductance on daily-integrated c_i of study trees across all sites, species, and post-spring measurement campaigns. Fitted slopes represent significant coefficients and their interactions. See Table 5 for analysis of deviance table.

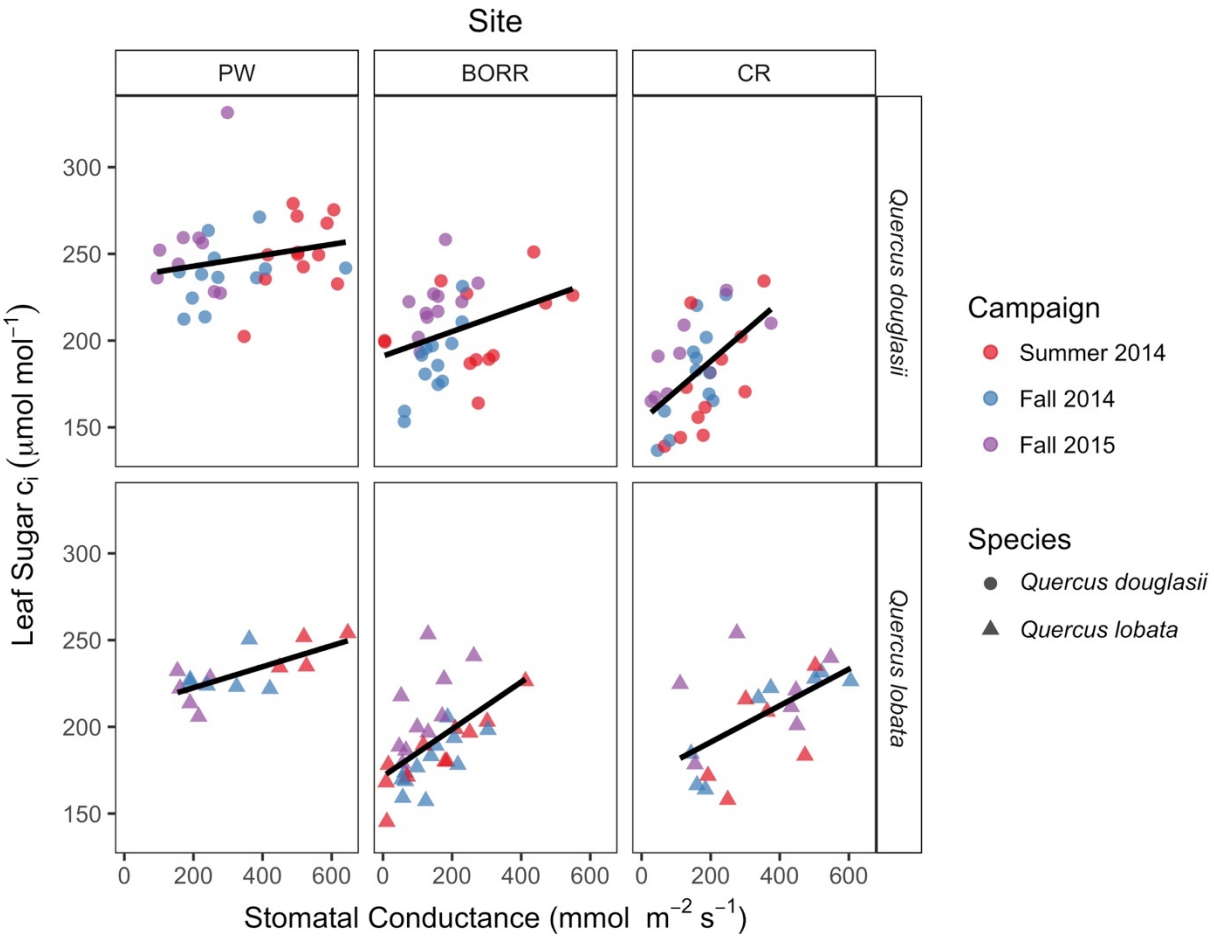

Figure 7. Model fits from Type III ANOVA testing **H3**: the effect of LMWL departure on daily-integrated c_i of study trees across all sites, species, and post-spring measurement campaigns. Fitted slopes represent significant coefficients and their interactions. See Table 5 for analysis of deviance table.

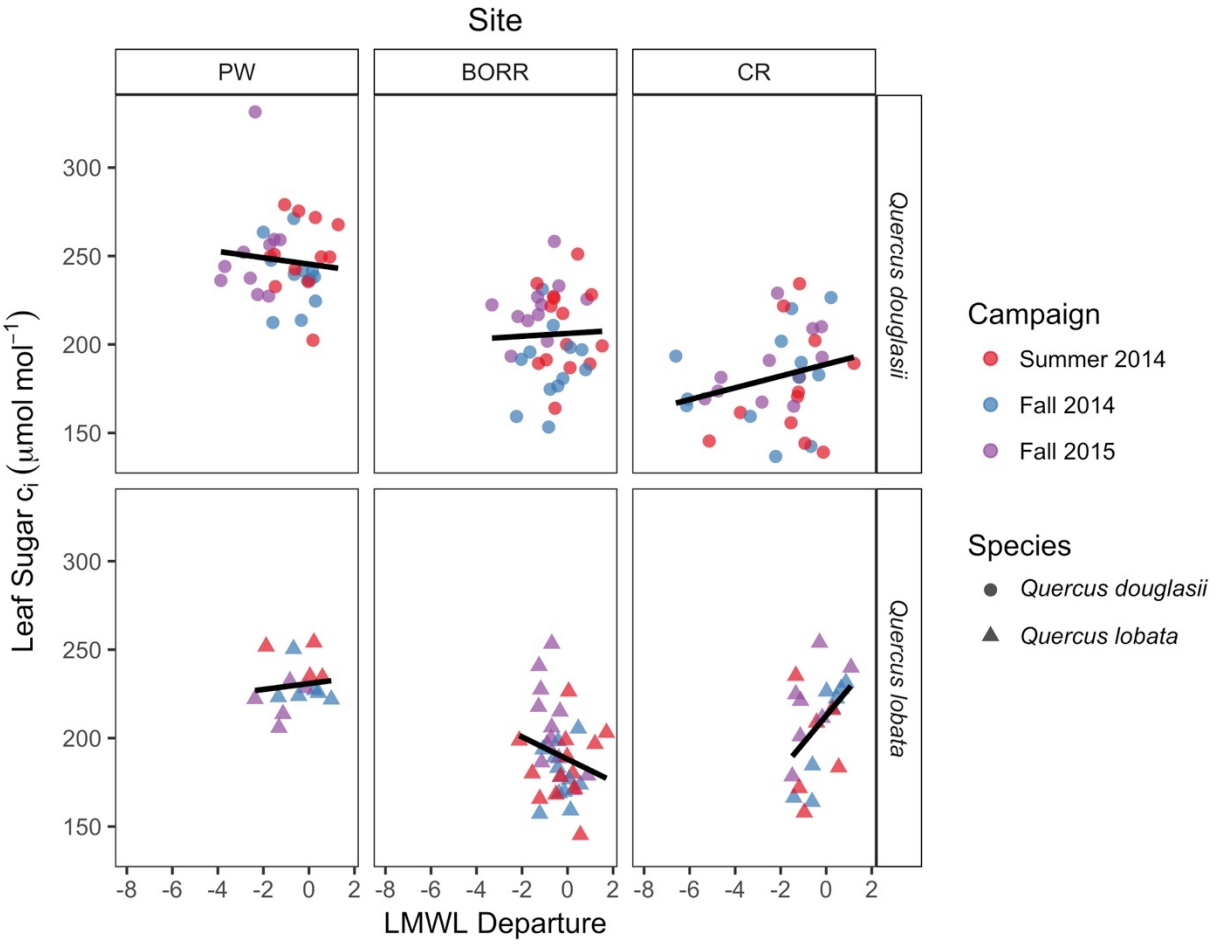

Figure 8. Seasonal changes in seasonally-integrated c_i across study sites and species (**H4**). See Table 6 for analysis of deviance table for significant coefficients and their interactions.

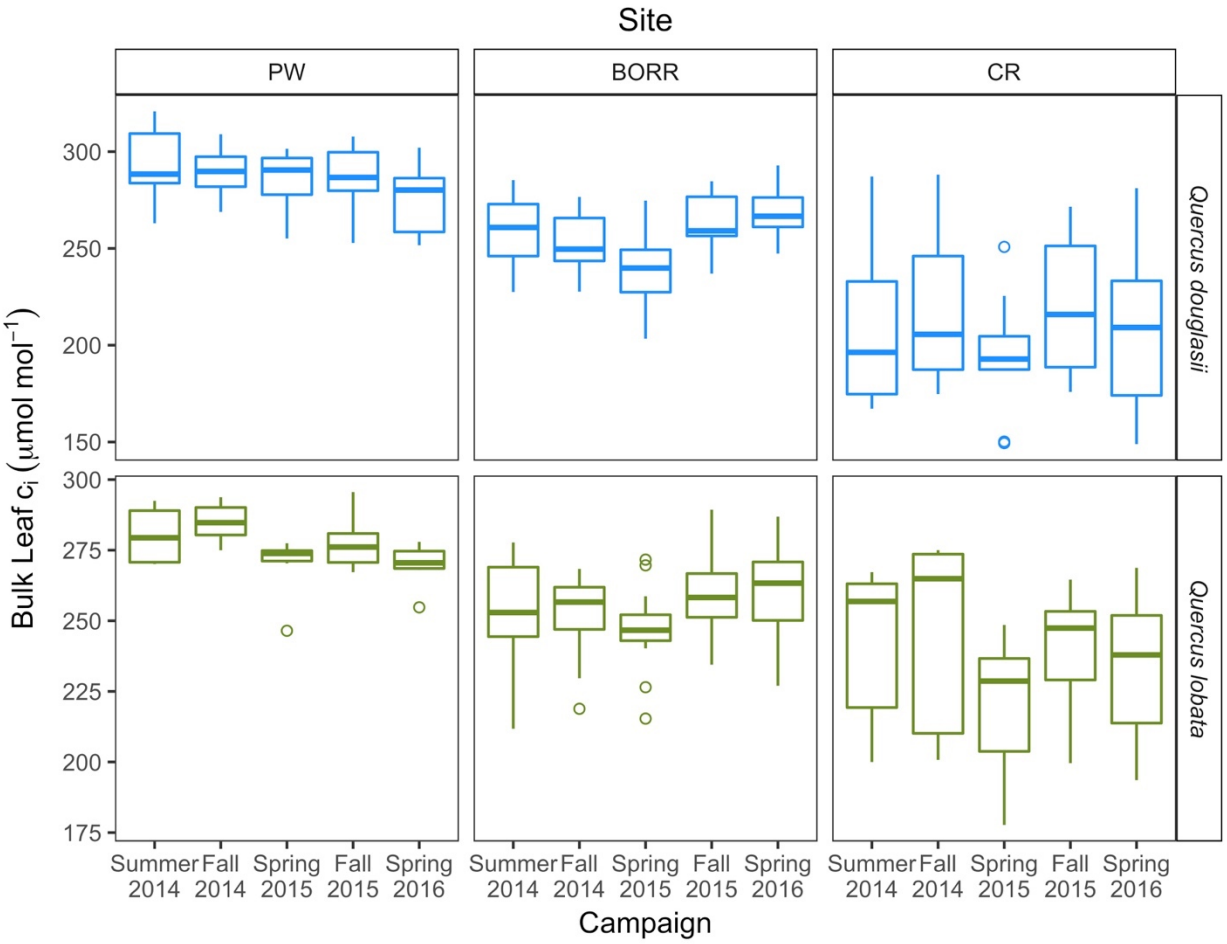

Table 1. Analysis of deviance table from Type III ANOVA testing **H1:** the response of LMWL departure through the drought across sites, species, and campaigns.

Analysis of Deviance Table (Type III Tests):
LMWL Departure

LMER 1 (**H1**): LMWL Departure ~ Site * Species * Campaign + (1 | Tree Individual)

Effect:	Chisq	Df	Pr(>Chisq)
Site	**17.3829**	**2**	**0.0002**
Species	**6.0051**	**1**	**0.0143**
Campaign	**24.7438**	**4**	**< 0.0001**
Site : Species	4.5873	2	0.1009
Site : Campaign	**25.1260**	**8**	**0.0015**
Species : Campaign	**9.6925**	**4**	**0.0459**
Site : Species : Campaign	3.5326	8	0.8966

Table 2. Analysis of deviance table from Type III ANOVA testing **H2**: the effect of LMWL departure on predawn water potential across all sites, species, and campaigns.

Analysis of Deviance Table (Type III Tests):
LMWL Departure

LMER 2 (**H2**): Predawn Water Potential ~ LMWL Departure * Site * Species * Campaign + (1 | Tree Individual)

Effect:	Chisq	Df	Pr(>Chisq)
LMWL Departure	**8.8681**	**1**	**0.0029**
Site	**84.7412**	**2**	**< 0.0001**
Species	**33.7212**	**1**	**< 0.0001**
Campaign	**111.6996**	**4**	**< 0.0001**
LMWL Departure : Site	2.3211	2	0.3133
LMWL Departure : Species	0.0968	1	0.7557
Site : Species	**7.6115**	**2**	**0.0222**
LMWL Departure: Campaign	**39.9375**	**4**	**< 0.0001**
Site : Campaign	**109.3567**	**8**	**< 0.0001**
Species : Campaign	**27.3136**	**4**	**< 0.0001**
LMWL Departure : Site : Species	0.0321	2	0.9841
LMWL Departure : Site : Campaign	**23.7929**	**8**	**0.0024**
LMWL Departure : Species : Campaign	**20.5684**	**4**	**0.0004**
Site : Species : Campaign	**18.9417**	**8**	**0.0152**
LMWL Departure : Site : Species : Campaign	**21.1631**	**8**	**0.0067**

Table 3. Analysis of deviance table from Type III ANOVA testing **H2**: the effect of predawn water potential on the midday-predawn water potential differentials across all sites, species, and campaigns.

Analysis of Deviance Table (Type III Tests):
Predawn Water Potential

LMER 3 (**H2**): Midday-Predawn Water Potential Differential ~ Predawn Water Potential * Site * Species * Campaign + (1 | Tree Individual)

Effect:	Chisq	Df	Pr(>Chisq)
Predawn Water Potential	**32.9802**	**1**	**< 0.0001**
Site	2.3558	2	0.3079
Species	0.8948	1	0.3441
Campaign	**51.5556**	**4**	**< 0.0001**
Predawn Water Potential: Site	0.9387	2	0.6254
Predawn Water Potential : Species	1.7340	1	0.1879
Site : Species	0.0193	2	0.9904
Predawn Water Potential: Campaign	**21.2181**	**4**	**0.0003**
Site : Campaign	12.5783	8	0.1272
Species : Campaign	1.3599	4	0.8511
Predawn Water Potential : Site : Species	0.8188	2	0.6641
Predawn Water Potential : Site : Campaign	**20.2078**	**8**	**0.0096**
Predawn Water Potential : Species : Campaign	1.1882	4	0.8800
Site : Species : Campaign	2.9123	8	0.9397
Predawn Water Potential : Site : Species : Campaign	2.9491	8	0.9375

Table 4. Analysis of deviance table from Type III ANOVA testing **H3**: the effect of late season predawn water potential on stomatal conductance across sites, species, and campaigns.

Analysis of Deviance Table (Type III Tests):
Predawn Water Potential

LMER 4 (**H3**): Stomatal Conductance ~ Predawn Water Potential * Site * Species * Campaign + (1 | Tree Individual)

Effect:	Chisq	Df	Pr(>Chisq)
Predawn Water Potential	**4.3877**	**1**	**0.0362**
Site	4.8576	2	0.0881
Species	0.7962	1	0.3722
Campaign	1.1255	2	0.5696
Predawn Water Potential: Site	0.6211	2	0.7331
Predawn Water Potential : Species	0.5349	1	0.4645
Site : Species	5.2579	2	0.0722
Predawn Water Potential: Campaign	0.8902	2	0.6408
Site : Campaign	4.1000	4	0.3926
Species : Campaign	5.3407	2	0.0692
Predawn Water Potential : Site : Species	**6.5579**	**2**	**0.0377**
Predawn Water Potential : Site : Campaign	2.7271	4	0.6045
Predawn Water Potential : Species : Campaign	4.1689	2	0.1244
Site : Species : Campaign	4.1672	4	0.3839
Predawn Water Potential : Site : Species : Campaign	**10.8748**	**4**	**0.0280**

Table 5. Analysis of deviance table from Type III ANOVA testing **H3**: the effect of predawn water potential on the bulk leaf c_i concentrations of leaves across all sites, species, and campaigns.

Analysis of Deviance Table (Type III Tests):
Stomatal Conductance and LMWL Departure

LMER 5 (**H3**): Leaf Sugar c_i ~ Stomatal Conductance * LMWL Departure * Site * Species * Campaign + (1 | Tree Individual)

Effect:	Chisq	Df	Pr(>Chisq)
Stomatal Conductance	**6.6849**	**1**	**0.0097**
LMWL Departure	0.6506	2	0.4199
Site	**7.8230**	**1**	**0.0200**
Species	**5.2823**	**2**	**0.0215**
Campaign	**8.3606**	**2**	**0.0153**
Stomatal Conductance : LMWL Departure	1.0204	1	0.3124
Stomatal Conductance : Site	5.3060	2	0.0704
LMWL Departure : Site	0.9681	2	0.6163
Stomatal Conductance : Species	**6.0052**	**1**	**0.0143**
LMWL Departure : Species	**6.1012**	**1**	**0.0135**
Site : Species	**8.2168**	**2**	**0.0164**
Stomatal Conductance : Campaign	**7.1883**	**2**	**0.0275**
LMWL Departure : Campaign	4.3635	2	0.1128
Site : Campaign	4.0181	4	0.4036
Species : Campaign	0.9145	2	0.6330
Stomatal Conductance : LMWL Departure : Site	0.9835	2	0.6115
Stomatal Conductance : LMWL Departure : Species	**5.9736**	**1**	**0.0145**
Stomatal Conductance : Site : Species	**8.0546**	**2**	**0.0178**
LMWL Departure : Site : Species	**6.4766**	**2**	**0.0392**
Stomatal Conductance : LMWL Departure : Campaign	4.9990	2	0.0821
Stomatal Conductance : Site : Campaign	6.3303	4	0.1758
LMWL Departure : Site : Campaign	1.8293	4	0.7671
Stomatal Conductance : Species : Campaign	0.9365	2	0.6261
LMWL Departure : Species : Campaign	2.2025	2	0.3325
Site : Species : Campaign	2.6703	4	0.6144
Stomatal Conductance : LMWL Departure : Site : Species	**6.1763**	**2**	**0.0456**
Stomatal Conductance : LMWL Departure : Site : Campaign	3.2987	4	0.5091
Stomatal Conductance : LMWL Departure : Species : Campaign	3.8477	2	0.1460
Stomatal Conductance : Site : Species : Campaign	0.5363	4	0.9699
LMWL Departure : Site : Species : Campaign	3.4334	4	0.4881
Stomatal Conductance : LMWL Departure : Site : Species : Campaign	2.5746	4	0.6313

Table 6. Analysis of deviance table from Type III ANOVA testing **H4**: the response of bulk leaf c_i through the drought across sites, species, and campaigns.

Analysis of Deviance Table (Type III Tests):
Bulk Leaf c_i

LMER 6 (**H4**): Bulk Leaf c_i ~ Site * Species * Campaign + (1 | Tree Individual)

Effect:	Chisq	Df	Pr(>Chisq)
Site	**89.4553**	**2**	**< 0.0001**
Species	**9.9604**	**1**	**0.0016**
Campaign	**52.9511**	**4**	**< 0.0001**
Site : Species	**11.7209**	**2**	**0.0029**
Site : Campaign	**70.6149**	**8**	**< 0.0001**
Species : Campaign	1.2650	4	0.8673
Site : Species : Campaign	10.5354	8	0.2294

CHAPTER 3

Seasonal modifications of leaf area:sapwood area ratios and leaf mass per area through years of extreme drought in Californian blue oak and valley oak

Seasonal changes in individual plant leaf area (ILA), leaf mass per area (LMA), and the leaf area-to-sapwood area ratios (A_l:A_s) can alter plant carbon and water balance, and may represent adaptive responses to progressive drought in summer-dry, semi-arid systems. I used the 2012 - 2016 historic drought in California as a natural experiment to test the effects of extreme changes in plant available moisture on the expression of these traits in two coexisting, drought-adapted oak species that differ in their water acquisition strategies: blue oak (*Quercus douglasii*) and valley oak (*Q. lobata*). I measured seasonal changes in these traits from summer 2014 - spring 2016 across three sites that spanned a gradient of drought exposure and historical climate, and tested them as a function of spatial and temporal patterns of drought exposure. ILA was overall the smallest at the most xeric site among blue oaks, by upwards of 197 % compared to the most mesic site. Among valley oaks, ILA was greatest at the intermediately xeric site by upwards of 170 % compared to the most xeric site. Blue oaks had 13 % higher LMA than valley oaks, but counter to expectation LMA was not higher in either species at the drier sites. While A_l:A_s was lowest at the driest site in both species by upwards of 196 % compared to the most mesic site, sites differed in how A_l:A_s responded through the drought. Reductions in A_l:A_s towards the end of the growing season were observed for both species at the more mesic sites, while A_l:A_s remained consistently low at the driest site. These seasonal reductions in A_l:A_s were associated with reductions in shoot leaf count rather than reductions in individual leaf size. In contrast, the most xeric site maintained consistently low A_l:A_s via more numerous and much smaller individual leaves. The smallest leaves were observed in trees with xylem water isotope signatures that reflect utilization of shallow, evaporatively enriched soil water zones. Together, these results suggest that reductions in leaf size along with seasonal reductions in leaf area per unit of sapwood area are important responses in blue oak and valley oak for maintaining water-carbon balance under extreme drought conditions, especially compared to changes in LMA. Such responses may be important in reducing the vulnerability of these species to hydraulic failure and drought-induced mortality due to their combined effects on reducing canopy-wide evaporative demands.

INTRODUCTION

Increased global climatic variability in response to anthropogenic climate change has been associated with increased rates of warming and extreme drought events around the world (Dai 2013, Cook et al. 2014, IPCC 2014). For plant communities facing increased likelihoods of exposure to such conditions, their acclimation and survival will require rapid morphological and physiological modifications (Nicotra et al. 2010). However, vegetation models tend to fail to incorporate seasonal changes in plant traits under projected warming and drought scenarios, despite the fact that plant physiologists have long demonstrated the ability of plants to seasonally modify their traits in response to rapid changes in water availability. It has therefore become increasingly important to quantify the *in-situ* physiological and morphological responses of different plant species to extreme drought events in order to more accurately assess their vulnerability to drought-induced mortality in the future.

Seasonal measurements of plant traits that reflect different capacities for plasticity in investment, allocation, and acclimation in response to changes in water availability allow for powerful insights into how different plant species maintain homeostatic water-carbon balance (Grossiord et al. 2017). Research on such traits has historically been accomplished in the field of functional ecology with analyses of trade-offs in plant functional traits within the leaf economics spectrum (LES), where leaf physiological traits that directly impact a given species' performance, reproduction, and lifetime fitness reflect their overall life history strategy (Violle et al. 2007, Wright et al. 2004). However, this body of literature has been limited to comparisons across large taxonomic, climatic, and geographic scales rather than seasonal comparisons within or between species. As a result, few studies exist that focus on how these traits vary intra- or inter-seasonally, particularly through long term drought events that are characterized by higher temperatures combined with extensive precipitation reductions. More recently, these LES trade-off analyses have been extended upon to place such functional traits into more of an ecophysiological context by investigating how they change in response to changes in water availability rather than just overall carbon and nutrient availability (Reich et al. 2014). In this 'fast-slow' trait space, species generally tend to fall along a spectrum of fast-to-slow response rates of allocation towards growth, survival, and reproduction in response to changes in water availability and acquisition capacity. For example, a tree species at the 'fast' end of this spectrum inhabiting a summer-dry, semi-arid environment would typically embody a suite of traits integrated across its roots, stems, and leaves that collectively confer rapid water uptake and movement (e.g. high leaf and stem hydraulic conductivity), greater photosynthetic investment per unit of leaf area (e.g. higher leaf mass per unit leaf area and/or reduced leaf area), and shorter leaf lifespans (e.g. a deciduous life history). Conversely, the opposite would be exhibited for each of these traits in a species at the slow end of this spectrum. Consequently, there exists an extensive amount of variation in how plant leaves can be constructed and maintained in response rapid changes in water availability. For example, variation in structural investments per unit leaf area that either help **(a)** deter herbivores or pathogens from inflicting damage, **(b)** inhibit turgor loss and facilitate rehydration under seasonal drought, or **(c)** maximize water transport to photosynthetic tissues under peak growing season conditions (Westoby et al. 2002, Wright et al. 2004, Poorter et al. 2009). Additionally, leaf size varies over 100,000 fold globally in response to variation in the effects of temperature and precipitation gradients on leaf energy balance (Wright et al. 2017). As a result, both individual leaf area (ILA) and leaf mass per area (LMA) are

powerfully informative traits that have great potential to indicate a plant's overall carbon acquisition strategy in response to drought. With respect to seasonal acclimation in response to extreme drought conditions, ILA can be expected to decrease while LMA can be expected to increase due to the negative effects of water deficits on turgor pressure and foliar expansion rates, thus reducing the amount of water required to support carbon assimilation per unit of transpiring photosynthetic area (Quero et al. 2006, Lopez-Iglesias et al. 2014, Enrique et al. 2016). By extension, trees acclimating to multiple growing seasons under extreme water deficits can generally be expected to exhibit decreased canopy-level ILA and increased LMA over time as a function of the degree of water stress they are experiencing.

Explorations of seasonal changes in the leaf area to sapwood area ratios (A_l:A_s; also referred to as the Huber Value, Huber 1928) of trees undergoing drought help place drought-induced changes in ILA and LMA into a more ecophysiological context, because the A_l:A_s of trees can be rapidly modified over time to maintain their overall canopy water-carbon balance (Mencuccini and Grace 1995, Mencuccini 2002, Bhaskar et al. 2007). For example, the A_l:A_s of trees can decline in response to declines in subsurface water availability across multiple growing seasons, vary within growing seasons to maximize transpiration when water is not limiting, or minimize evaporative demands in response to seasonal drought by reducing canopy-level leaf area through leaf senescence and shedding (Carter and White 2009, McBranch et al 2018). Moreover, recent investigations of the relationships between A_l and A_s in both broadleaf and conifer tree species across broad geographic and climatic scales have found further support that trees adjust their functional water-carbon balance by adjusting both investment in leaf area as well as in growing xylem tissue to maximize hydraulic conductance and foliar water availability (Petit et al. 2018). Despite the importance of ILA, LMA, and tree A_l:A_s in maintaining water-carbon balance, very few studies exist that have tested the combined effects of multiple years of extreme precipitation reductions and temperature increases on their expression under natural field conditions (Grossiord et al. 2017). Investigating the *in-situ* seasonal responses of the ILA, LMA, and A_l:A_s of trees when historic, multi-year drought conditions arise is thus important for progressing our understanding of their future vulnerability to drought-induced mortality.

With this motivation, I expand on my research framework in Chapters 1 and 2 to test the effects of California's historic 2012 - 2016 drought on seasonal changes in ILA, LMA, and A_l:A_s in blue oak (*Quercus douglasii*) and valley oak (*Q. lobata*). As I outlined in these previous chapters, these oaks are iconic California endemic tree species that coexist in woodlands, which form among the most diverse and geographically extensive ecosystems within the entire state (Stahle et al. 2013). Both oaks are drought-adapted (Griffin 1971, 1973), and can live from 200 to more than 500 years old (Griffin 1976, Stahle et al. 2013). They are also both winter-deciduous, with leaves flushing once in the spring following precipitation inputs over the winter, and senescing at the end of the growing season in the fall. More importantly, I have demonstrated that my study design captured a range of climate and drought severity conditions, and covered a substantial extent of both oak species' geographic ranges. Moreover, I have demonstrated that these species differed significantly in their ability to recover their seasonal water status and their ability to efficiently assimilate carbon as a function of overall drought exposure, the degree to which xylem may have undergone embolism formation, and differences in the zones of water extraction that their roots have access to. For example, blue oaks at the most xeric site were significantly less able to recover their seasonal water potentials through the drought compared to valley oaks,

and exhibited the highest levels of canopy damage and mortality (Chapter 1). The lack of water status recovery at this site was most strongly associated with the degree to which roots lost access to stable soil water resources through the growing season, suggesting that these species can differ substantially in their water acquisition strategies with respect to the zones of water extraction that they exploit along the landscape. These shallower rooted trees also had the most significantly reduced rates of stomatal conductance through the growing season, and as a result, exhibited the most reduced levels of foliar c_i (Chapter 2). Lastly, previous studies have documented significant inter-annual variability in blue oak LMA in response to seasonal drought under natural field conditions (Xu and Baldocchi 2003, Osuna et al. 2015), suggesting that LMA modifications could be important drought acclimation responses within California Oak Woodlands. Taken together, these results suggest that these oaks may also differ in how they morphologically and physiologically acclimate to extreme drought with respect to modifications in their foliar- and canopy-level architecture that aid in the maintenance of homeostatic water-carbon balance and the resistance to mortality. Thus, these oaks are excellent candidates in which to investigate morphological and physiological changes in their foliar and water transporting tissues in response to this unique drought event.

The objective of this chapter is to extend this research framework to test the effects of this drought on seasonal changes in the functional and structural responses of the leaves and sapwood area (a proxy for water delivery to leaves) of these species. To accomplish this, I measured seasonal changes in ILA, LMA, and shoot-level A_l:A_s from summer 2014 - fall 2015 and tested them as a function of the changes in drought exposure that the study sites capture. This chapter focuses on the following three hypotheses:

H1: Leaf size (ILA) will be smaller in drier sites, with the smallest sizes observed in blue oaks compared to valley oaks.
H2: Leaf mass per area (LMA) will be highest in drier sites, with the highest values observed in blue oaks compared to valley oaks.
H3: Leaf area:sapwood area ratios (A_l:A_s, or Huber Values) will be smallest in drier sites, with seasonal reductions towards the end of the growing season observed in both species.

MATERIALS AND METHODS

Study species, site selection, climate, and study design

In this chapter, I extend upon the same experimental system and study design that is described in detail in Chapters 1 and 2. Therefore, all details about the selection of study species and sites, the overall climatic severity and degrees of spatial water deficit that these sites capture, and the overall study design are not repeated here. However, I focus here on only four of the five original measurement campaigns (Summer 2014, Fall 2014, Spring 2015, Fall 2015), as collecting and analyzing leaf and stem samples during the final Spring 2016 campaign was not feasible. The methodology behind all additional measurements that were made involving leaf area, leaf mass, and sapwood area within this same experimental framework is described below.

Individual leaf area (ILA) and leaf mass per area (LMA)

To quantify seasonal changes in leaf size (or ILA) of study trees, the same two individual shoot samples that were collected for the water potential measurements used in Chapters 1 and 2 were defoliated after being measured, and each sample's set of leaves were mounted to digital image scanners. Leaves were then scanned fresh in the field at 1200 dpi resolution, and afterwards placed together into paper envelopes along with the stems they came from. The area of each leaf (cm^2) was then measured digitally via the ASSESS 2.0 software package released by the American Phytopathological Society, ensuring each digital scan was accurately calibrated to $\pm$ 0.01 cm^2 pixel area across all image files. The overall length and size of shoots sampled was standardized across sites and measurement campaigns for comparisons for seasonal comparisons of ILA, sapwood area, and total leaf count per shoot. To quantify the LMA of the same shoot sample leaves used for these leaf area measurements, each sample's set of leaves was dried at 60 ºC for at least three days. These leaves were then weighed to the nearest 0.0001 g, and their subsequent dry mass was matched to the sample's cumulative leaf area to calculate LMA (g m^{-2}).

Sapwood area and A_l:A_s (Huber Value) calculations

To quantify the sapwood area of each branch sample used for ILA and LMA calculations, approximately 5 cm of stem material was excised as a lateral cross section of the base of each stem using razor blades. These stem cross sections were then imaged with a Canon EOS DSLR camera mounted to a Zeiss dissecting microscope (Carl Zeiss AG, Oberkochen, Germany). All subsequent image files were then loaded into the APS ASSESS software and digitally calibrated down to $\pm$ 0.1 mm^2 pixel area across all image files. The pith area within each cross section was digitally removed from all xylem tissue prior to sapwood area calculations. The resulting sapwood areas were then matched to their total leaf areas to calculate leaf area:sapwood area ratios (cm^2 mm^{-2}).

Statistical analyses

To test my hypotheses involving seasonal changes in leaf size (**H1**), leaf mass per area (**H2**), and leaf area:sapwood area ratios (**H3**) in response to the drought, I ran multiple linear mixed effects models for each of these predictor variables. Because this study made repeated measures on the same individual trees among sites through time, each study tree individual is statistically treated as a random effect in each linear mixed effects model to account for non-independence of measurements. Within each model, sites, species, and measurement campaigns are therefore treated as interacting fixed effects. ILA, LMA, and A_l:A_s were treated as response variables to test each hypothesis using the following model structures:

Model 1 (**H1**): LA ~ Site * Species * Campaign + (1 | Tree Individual)
Model 2 (**H2**): LMA ~ Site * Species * Campaign + (1 | Tree Individual)
Model 3 (**H3**): A_l:A_s ~ Site * Species * Campaign + (1 | Tree Individual)

Because changes in A_l:A_s ratios are mathematically sensitive to changes in both the total number of leaves per shoot as well as the overall sizes of shoot leaves, I performed one additional linear mixed effects model on leaf count to account for this. In doing so, I am able to disentangle the relative contributions of leaf shedding in addition to changes in leaf size across sites and

measurement campaigns. This model accounts for the same fixed and random effects as the first three, and takes the following structure:

Model 4: Shoot Leaf Count ~ Site * Species * Campaign + (1 | Tree Individual)

Significance tests for each coefficient factor in each model were performed using Type III ANOVA via Wald chi-square tests to account for all model coefficient interactions. All statistical pairwise contrasts between each interacting set of site, species, and campaign factors in each model were performed via least-squares means comparisons. All statistical analyses and figures were produced using the R statistical platform (R Core Team 2017) and the following packages: *lme4* (Bates et al. 2015), *car* (Fox and Weisberg 2011), *lsmeans* (Lenth 2016), *dplyr* (Wickham et al. 2017), and *ggplot2* (Wickham 2009).

RESULTS

Individual leaf area (H1)

ILA was significantly different between species and sites, with a significant site by species interaction (Table 1, *Site : Species* χ^2 17.8605, P = 0.0001). For blue oak, ILA scaled with drought exposure and historical climate in that the smallest leaves were observed at the driest site and most drought exposed site (CR), with intermediate ILA values observed at the intermediately xeric and drought exposed site (BORR) and the largest values at the most mesic and least drought exposed site (PW). Though these results for blue oak are in support of **H1**, the ILA of valley oaks did not decrease with drought exposure, but rather were largest at the intermediately dry site (BORR) (Figure 1). The most striking example of this result is the massive range of variation in the average ILA of blue oaks across sites, with values as low as 0.14 cm^2 at CR compared to ILA values of as high as 17.8 cm^2 at both PW and BORR. Conversely, the valley oaks at BORR that had the largest ILA values reached as high as 36.9 cm^2, and remained larger over time through each growing season compared to values reached at PW and CR. The only seasonal reductions in ILA were observed at PW, where blue oaks had lower ILA in fall 2014 compared to summer 2014 and valley oaks had lower ILA in both fall campaigns. Taken together, these results partially support **H1** in that the blue oaks at the most drought exposed site (CR) consistently exhibited the most reduced ILA through the drought.

Leaf mass per area (H2)

Differences in LMA were significant between species and campaigns, with a significant interaction between sites and campaigns (Table 2, *Site : Campaign* χ^2 25.2741, P = 0.0003). Contrary to **H1**, LMA did not scale with drought exposure for either species across sites in that drier sites did not have lower LMA through the drought compared to mesic sites. However, LMA was consistently lower during the spring 2015 measurement campaign across sites, followed by increases in the following fall season (Figure 2). This suggests that biomass investment per unit leaf area increases in time after the onset of spring leaf flush for these species, up to 138.3 g m^{-2} across all summer and fall campaigns for blue oaks and 122.0 g m^{-2} for valley oaks. However, this pattern of increasing LMA through the growing season is slightly less

consistent in the blue oaks and valley oaks at the most mesic site (PW), where LMA during the summer 2014 campaign was lower than the values realized in the following fall 2014 campaign. Overall, although these results are not in entirely in support of **H2** in that CR trees did not have significantly higher LMA compared to PW and BORR, LMA was still found to be higher overall in blue oaks than valley oaks.

Leaf area:sapwood area (Huber Values) and leaf senescence (H3)

Seasonal differences in A_l:A_s through the drought were significant across sites (Table 3, *Site : Campaign* χ^2 19.9345, P = 0.0029), with the lowest A_l:A_s observed at the driest site (CR) in both species (Figure 3). While reductions in A_l:A_s from summer 2014 to fall 2014 as well as spring 2015 to fall 2015 occurred in both species at PW and BORR, A_l:A_s remained consistently low at CR between these time points. Meanwhile, seasonal differences in shoot leaf count through the drought were also significant across sites (Table 4 *Site : Campaign* χ^2 18.3827, P = 0.0053), with leaf count reductions occurring simultaneously with A_l:A_s reductions in summer 2014 to fall 2014 and spring 2015 to fall 2015 (Figure 4). Because leaf size between growing season comparisons remained quite consistent through the drought (Figure 1), this strongly suggests that leaf shedding and/or senescence was responsible for the seasonal reductions in A_l:A_s at PW and BORR. Conversely, leaf size was much smaller at CR, with no substantial changes in leaf count across growing seasons. Overall, these results support **H3** in that these leaf area:sapwood area ratios were found to be the smallest in the drier site in both species, with seasonal reductions towards the end of each growing season in response to progressive leaf loss.

DISCUSSION

This study further expanded upon a natural experiment that used a historic drought event to test the *in-situ* effects of extreme reductions in water availability on the seasonal expression of different traits that affect canopy water-carbon balance in two coexisting, drought-adapted oak species. By integrating multiple years of measurements of leaf size, leaf mass per area, and leaf area:sapwood area ratios (Huber Values), this work provides support for the hypotheses that under extreme drought conditions, both oak species can express vastly different leaf sizes and effective leaf area per unit of hydraulic conductive area, and that these responses are more prevalent than changes in leaf mass per area. Because these responses reduce canopy-level evaporative demands, I infer that this is an important acclimation response to extreme drought conditions. Such a response will reduce overall vulnerability to hydraulic failure and drought-induced mortality (McDowell et al. 2008, McBranch et al. 2018). In this study, these responses were most pronounced in the blue oaks at the most drought exposed site, as they exhibited almost 200 % reductions in average leaf size compared to less drought-exposed and historically mesic sites (Figure 5). LMA, however, stayed relatively constant through the drought across sites and species, and thus seasonal modifications may not be an important part of these species' acclimation responses to summer drought.

With respect to ILA, because these two oak species flush their canopy leaves discretely rather than continuously through the growing season (as observed in many evergreen oaks), the seasonal differences in ILA observed at PW were not expected. However, leaf loss could

influence this pattern if larger sized leaves had higher likelihoods of senescence compared to smaller leaves. Because the overall magnitude of seasonal leaf loss was greatest at PW, these fluctuations may thus be attributed to large leaf senescence. Additionally, that the valley oaks at BORR had the highest leaf sizes through the drought was a surprising result considering that, counter to my expectations, they does not scale with the precipitation gradient captured across sites (Chapter 1). This could potentially be due to the results I outlined in Chapters 1 and 2 involving how the water acquisition strategies differ between these two species. In these chapters, I demonstrated that these species differ in their functional root architectures, such that the zones of water extraction that valley oaks draw upon are deeper and less evaporatively enriched than the soil zones that blue oaks draw upon. Moreover, the degree of evaporative enrichment of soil water that valley oaks at BORR were using was less than that observed at PW and CR (reflected by more positive LMWL departure values). Therefore, it is reasonable to assert that the valley oaks at BORR had access to deeper and more stable water resources throughout the drought, and that this allowed them to support larger ILA values compared to PW and CR. As an initial test of this hypothesis, an additional relationship of all ILA values measured in this study as a function of seasonal LMWL departure suggests that the most shallow-rooted trees also had the smallest ILA, whereas trees with comparatively deeper roots had larger ILA (Figure 6). This result is consistent with several previous studies of drought-adapted Californian species that have also demonstrated linkage between functional rooting depth and leaf size (Ackerly 2004, Bhaskar et al. 2007). Thus it is plausible that shallow versus deep functional root architectures could explain the deviations in valley oak ILA observed in this study.

With respect to LMA, the result that no differences in maximum seasonal LMA were found across sites was somewhat surprising given how higher LMA values have widely been associated with drought-adapted species (Wright et al. 2004, Poorter et al. 2009). Additionally, these results are inconsistent with previous studies that have documented significant inter-annual variability in blue oak LMA in response to seasonal drought under natural field conditions (Xu and Baldocchi 2003, Osuna et al. 2015), suggesting that LMA modifications could still occur in this species under certain environmental conditions. Nonetheless, investigations of deciduous versus evergreen species suggest that even across broad taxonomic scales, deciduous species can be less sensitive than evergreen species to variation in mean annual precipitation in terms of maximum seasonal LMA (Wright et al. 2005), consistent with the lack an increase in LMA in either species at the driest site in this study. Moreover, meta-analysis of the environmental conditions associated with seasonal changes in LMA suggest that this trait is greatly, if not predominantly, influenced by light and nutrient availability (e.g. LMA differences between sun and shade leaves) despite being associated with seasonality in water availability (Poorter et al. 2009). Nonetheless, LMA was still found to be higher in blue oaks than valley oaks, which is consistent with the results reported in Chapters 1 and 2 that they experienced more peak water stress (interpreted via minimum seasonal water potentials). Additionally, that the only seasonal differences in LMA observed in this study occurred during spring after leaves had flushed is not surprising, because foliar biomass investment increases over time with leaf maturation after leaf flush. However, this pattern was most reduced in the blue oaks at the most xeric site (CR), suggesting that leaves reached maturity after spring flush at a faster rate than at PW and BORR.

Sites differed in how A_l:A_s responded through the drought in surprisingly contrasting ways. Due to the fact that both leaf size as well as leaf number per shoot both contribute to the effective A_l:A_s of trees, disentangling the relative importance of each of these facets of A_l:A_s is essential to understand drought responses. However, it is important to note that although the sizes of all shoot samples were controlled for across sites and measurement campaigns, it is still possible that seasonal leaf count values may have been sensitive to inconsistencies in sampling. Here, oaks growing under the driest conditions through this drought maintained lower seasonal A_l:A_s than at other study sites, and they did so by flushing out numerically greater smaller leaves that are more seasonally permanent. That is, leaf size remained comparatively much smaller at CR, with no substantial changes in leaf count across growing seasons. This suggests that these sites captured fundamental differences in how A_l:A_s responded through the drought that were driven by site differences in the overall sizes and senescence rates of leaves. These results are quite novel because although various different A_l:A_s reduction mechanisms have been documented individually in response to drought (e.g. Mencuccini and Grace 1995, Mencuccini 2002, Carter and White 2009, McBranch et al. 2018), I am not aware of any studies that have detected them operating simultaneously across the large geographic and climatic scales that my study sites capture. Moreover, observations on or even near the scale of the massive differences in leaf size observed in this study are not well represented in the literature, especially in the context of drought responses across large climatic and geographic scales. All together, these results suggest that substantial differences in leaf size expression along with seasonal reductions in leaf area per unit of sapwood area are important acclimation responses in blue oak and valley oak for maintaining water-carbon balance under extreme drought conditions, especially compared to changes in LMA. I infer that such acclimation responses may be important in reducing the vulnerability of these species to hydraulic failure and drought-induced mortality due to their combined effects on reducing canopy-wide evaporative demands. Moreover, these measurements provide important physiological metrics of the functional responses of these oak species under historic drought stress conditions within natural field conditions, and will allow for more informed model predictions of both tree- and community-level responses to future drought events.

Placing these results in context with the drought responses demonstrated in Chapters 1 and 2, it is clear that although both species exhibited extensive degrees of morphological and physiological acclimation and were incredibly resilient in the face of extreme drought conditions, both species were still prone to damage and mortality under certain circumstances. Identifying the ecophysiological context underlying these circumstances has been the focus of this dissertation, and it has succeeded in providing multiple physiological mechanisms and environmental conditions that are directly associated with reduced plant performance, canopy damage, and mortality. First, in Chapter 1 I demonstrated the importance of water status recovery for each species from the end of each growing season through to the following spring for avoiding canopy damage and mortality. Seasonal water status recovery was driven by the extent of water stress experienced during the previous growing season, likely due to promotion of xylem embolism. This lack of recovery was most pronounced in the blue oaks at the most xeric and drought exposed study site, where the greatest extent of canopy damage and mortality was also documented. Next, in Chapter 2 I placed these responses into more of an ecophysiological context by drawing on the power of stable isotopes to better understand the effects of the drought on variation in subsurface water availability both within and across sites,

variation within and between each species in their functional root access to these water resources, and how this variation in water acquisition translated into different degrees of photosynthetic performance through the drought. Seasonal changes in the isotopic signatures of xylem water revealed that these species had different water acquisition strategies within and across study sites, likely reflecting differences in root architecture in relation to soil water profiles throughout the landscape. Consequently, seasonal gas exchange was most inhibited in the blue oaks at the most xeric and drought exposed site that had roots restricted to shallow rooting zones. Seasonal reductions in transpiration and water potential across sites were directly associated with a lack of root access to stable groundwater resources in deeper soils in both species. Here in Chapter 3, I have demonstrated how morphological changes in leaf and canopy architecture were also driven by subsurface water access through the drought. Extensive reductions in leaf size, leaf number, and leaf area-to-sapwood area ratios were exhibited by blue oaks at the most xeric and drought exposed site that had roots which were restricted to shallow rooting zones. These modifications act to reduce vulnerability to hydraulic failure and drought-induced mortality due to their effects on reducing canopy-level evaporative demands. Valley oaks, which maintained more stable access to deeper groundwater through the drought, exhibited larger leaves and larger leaf area-to-sapwood are ratios. In contrast to these responses, changes in leaf mass per area were not observed in either species.

Taken together, these results reiterate the importance of accounting for spatial and temporal variability in drought exposure and subsurface water availability across species' geographic ranges in the pursuit of more accurately understanding how trees respond to extreme drought. Having such an understanding will allow for more accurate modeling efforts geared toward predicting vulnerability to drought in the future across wider ranges of climatic, topographic, and environmental conditions. These results also indicate that physiological water-carbon balance for these species in response to extreme drought is driven by the nature of their seasonal water acquisition capacities, which directly affects their seasonal trajectories of water status, water status recovery, and the efficiency of gas exchange through growing seasons. Despite the resilience of these oak species to such extreme drought conditions demonstrated in this work under natural, *in-situ* field conditions, their inability to sufficiently acclimate and maintain water-carbon balance can still lead to significant degrees of canopy damage and mortality. With the greatest drought impacts observed in individuals of both species that had more restricted capacities for water acquisition through this historic drought event, this work demonstrates the ecophysiological conditions under which these species are most vulnerable to damage and mortality.

REFERENCES

Ackerly, D.D., 2004. Functional strategies of chaparral shrubs in relation to seasonal water deficit and disturbance. *Ecological Monographs*, 74(1), pp.25-44.

Bates, D., Maechler, M., Bolker, B., and Walker, S., 2015. Fitting Linear Mixed-Effects Models Using lme4. *Journal of Statistical Software*, 67(1), 1-48.

Bhaskar, R., Valiente-Banuet, A. and Ackerly, D.D., 2007. Evolution of hydraulic traits in closely related species pairs from mediterranean and nonmediterranean environments of North America. *New Phytologist*, 176(3), pp.718-726.

Carter, J.L. and White, D.A., 2009. Plasticity in the Huber value contributes to homeostasis in leaf water relations of a mallee Eucalypt with variation to groundwater depth. *Tree Physiology*, 29(11), pp.1407-1418.

Cook, B.I., Smerdon, J.E., Seager, R. and Coats, S., 2014. Global warming and 21st century drying. *Climate Dynamics*, 43(9-10), pp.2607-2627.

Dai, A., 2013. Increasing drought under global warming in observations and models. *Nature Climate Change*, 3(1), p.52.

Enrique, G., Olmo, M., Poorter, H., Ubera, J.L. and Villar, R., 2016. Leaf mass per area (LMA) and its relationship with leaf structure and anatomy in 34 Mediterranean woody species along a water availability gradient. *PloS one*, 11(2), p.e0148788.

Fox, J. and Weisberg, S., 2011. An R Companion to Applied Regression, Second Edition. Thousand Oaks, CA. http://socserv.socsci.mcmaster.ca/jfox/Books/Companion

Griffin, J.R., 1971. Oak regeneration in the upper Carmel Valley, California. *Ecology*, 52(5), pp.862-868.

Griffin, J.R., 1973. Xylem sap tension in three woodland oaks of central California. *Ecology*, 54(1), pp.152-159.

Griffin, J.R., 1976. Regeneration in *Quercus lobata* savannas, Santa Lucia Mountains, California. *American Midland Naturalist*, pp.422-435.

Grossiord, C., Sevanto, S., Adams, H.D., Collins, A.D., Dickman, L.T., McBranch, N., Michaletz, S.T., Stockton, E.A., Vigil, M. and McDowell, N.G., 2017. Precipitation, not air temperature, drives functional responses of trees in semi-arid ecosystems. *Journal of Ecology*, 105(1), pp.163-175.

Huber, B., 1928. Weitere quantitative Untersuchungen über das Wasserleitungssystem der Pflanzen. *Jahrbücher für Wissenschaftliche Botanik*, 67, pp.877–959.

IPCC, 2014: Climate Change 2014: Synthesis Report. Contribution of Working Groups I, II and III to the Fifth Assessment Report of the Intergovernmental Panel on Climate Change [Core Writing Team, R.K. Pachauri and L.A. Meyer (eds.)]. IPCC, Geneva, Switzerland, 151 pp.

Lenth, R.V., 2016. Least-Squares Means: The R Package lsmeans. *Journal of Statistical Software*, 69(1), 1-33.

Lopez-Iglesias, B., Villar, R. and Poorter, L., 2014. Functional traits predict drought performance and distribution of Mediterranean woody species. *Acta Oecologica*, 56, pp.10-18.

McBranch, N.A., Grossiord, C., Adams, H., Borrego, I., Collins, A.D., Dickman, T., Ryan, M., Sevanto, S., McDowell, N.G. and Maurizio, M., 2018. Lack of acclimation of leaf area: sapwood area ratios in piñon pine and juniper in response to precipitation reduction and warming. *Tree Physiology*, *in press*.

McDowell, N., Pockman, W.T., Allen, C.D., Breshears, D.D., Cobb, N., Kolb, T., Plaut, J., Sperry, J., West, A., Williams, D.G. and Yepez, E.A., 2008. Mechanisms of plant survival and mortality during drought: why do some plants survive while others succumb to drought? *New Phytologist*, 178(4), pp.719-739.

Mencuccini, M. and Grace, J., 1995. Climate influences the leaf area/sapwood area ratio in Scots pine. *Tree Physiology*, 15(1), pp.1-10.

Mencuccini, M., 2002. Hydraulic constraints in the functional scaling of trees. *Tree Physiology*, 22(8), pp.553-565.

Nicotra, A.B., Atkin, O.K., Bonser, S.P., Davidson, A.M., Finnegan, E.J., Mathesius, U., Poot, P., Purugganan, M.D., Richards, C.L., Valladares, F. and van Kleunen, M., 2010. Plant phenotypic plasticity in a changing climate. *Trends in Plant Science*, 15(12), pp.684-692.

Osuna, J.L., Baldocchi, D.D., Kobayashi, H. and Dawson, T.E., 2015. Seasonal trends in photosynthesis and electron transport during the Mediterranean summer drought in leaves of deciduous oaks. *Tree Physiology*, 35(5), pp.485-500.

Petit, G., von Arx, G., Kiorapostolou, N., Lechthaler, S., Prendin, A.L., Anfodillo, T., Caldeira, M.C., Cochard, H., Copini, P., Crivellaro, A. and Delzon, S., 2018. Tree differences in primary and secondary growth drive convergent scaling in leaf area to sapwood area across Europe. *New Phytologist*, 218(4), pp.1383-1392.

Poorter, H., Niinemets, Ü., Poorter, L., Wright, I.J. and Villar, R., 2009. Causes and consequences of variation in leaf mass per area (LMA): a meta-analysis. *New Phytologist*, 182(3), pp.565-588.

Quero, J.L., Villar, R., Marañón, T. and Zamora, R., 2006. Interactions of drought and shade effects on seedlings of four Quercus species: physiological and structural leaf responses. *New Phytologist*, 170(4), pp.819-834.

R Core Team, 2017. R: A language and environment for statistical computing. R Foundation for Statistical Computing, Vienna, Austria.

Stahle, D.W., Griffin, R.D., Meko, D.M., Therrell, M.D., Edmondson, J.R., Cleaveland, M.K., Stahle, L.N., Burnette, D.J., Abatzoglou, J.T., Redmond, K.T. and Dettinger, M.D., 2013. The ancient blue oak woodlands of California: Longevity and hydroclimatic history. *Earth Interactions*, 17(12), pp.1-23.

Violle, C., Navas, M.L., Vile, D., Kazakou, E., Fortunel, C., Hummel, I. and Garnier, E., 2007. Let the concept of trait be functional! *Oikos*, *116*(5), pp.882-892.

Westoby, M., Falster, D.S., Moles, A.T., Vesk, P.A. and Wright, I.J., 2002. Plant ecological strategies: some leading dimensions of variation between species. *Annual Review of Ecology and Systematics*, 33(1), pp.125-159.

Wickham, H., 2009. ggplot2: Elegant Graphics for Data Analysis. Springer-Verlag New York.

Wickham, H., Francois, R., Henry, L. and Müller, K., 2017. dplyr: A Grammar of Data Manipulation. R package version 0.7.4. https://CRAN.R-project.org/package=dplyr.

Wright, I.J., Reich, P.B., Westoby, M., Ackerly, D.D., Baruch, Z., Bongers, F., Cavender-Bares, J., Chapin, T., Cornelissen, J.H., Diemer, M. and Flexas, J., 2004. The worldwide leaf economics spectrum. *Nature*, 428(6985), p.821.

Wright, I.J., Reich, P.B., Cornelissen, J.H., Falster, D.S., Groom, P.K., Hikosaka, K., Lee, W., Lusk, C.H., Niinemets, Ü., Oleksyn, J. and Osada, N., 2005. Modulation of leaf economic traits and trait relationships by climate. *Global Ecology and Biogeography*, 14(5), pp.411-421.

Wright, I.J., Dong, N., Maire, V., Prentice, I.C., Westoby, M., Díaz, S., Gallagher, R.V., Jacobs, B.F., Kooyman, R., Law, E.A. and Leishman, M.R., 2017. Global climatic drivers of leaf size. *Science*, 357(6354), pp.917-921.

Xu, L. and Baldocchi, D.D., 2003. Seasonal trends in photosynthetic parameters and stomatal conductance of blue oak (Quercus douglasii) under prolonged summer drought and high temperature. *Tree Physiology*, 23(13), pp.865-877.

Figure 1. Seasonal changes in individual leaf area (ILA) across study sites and species (**H1**). See Table 1 for analysis of deviance table for significant coefficients and their interactions.

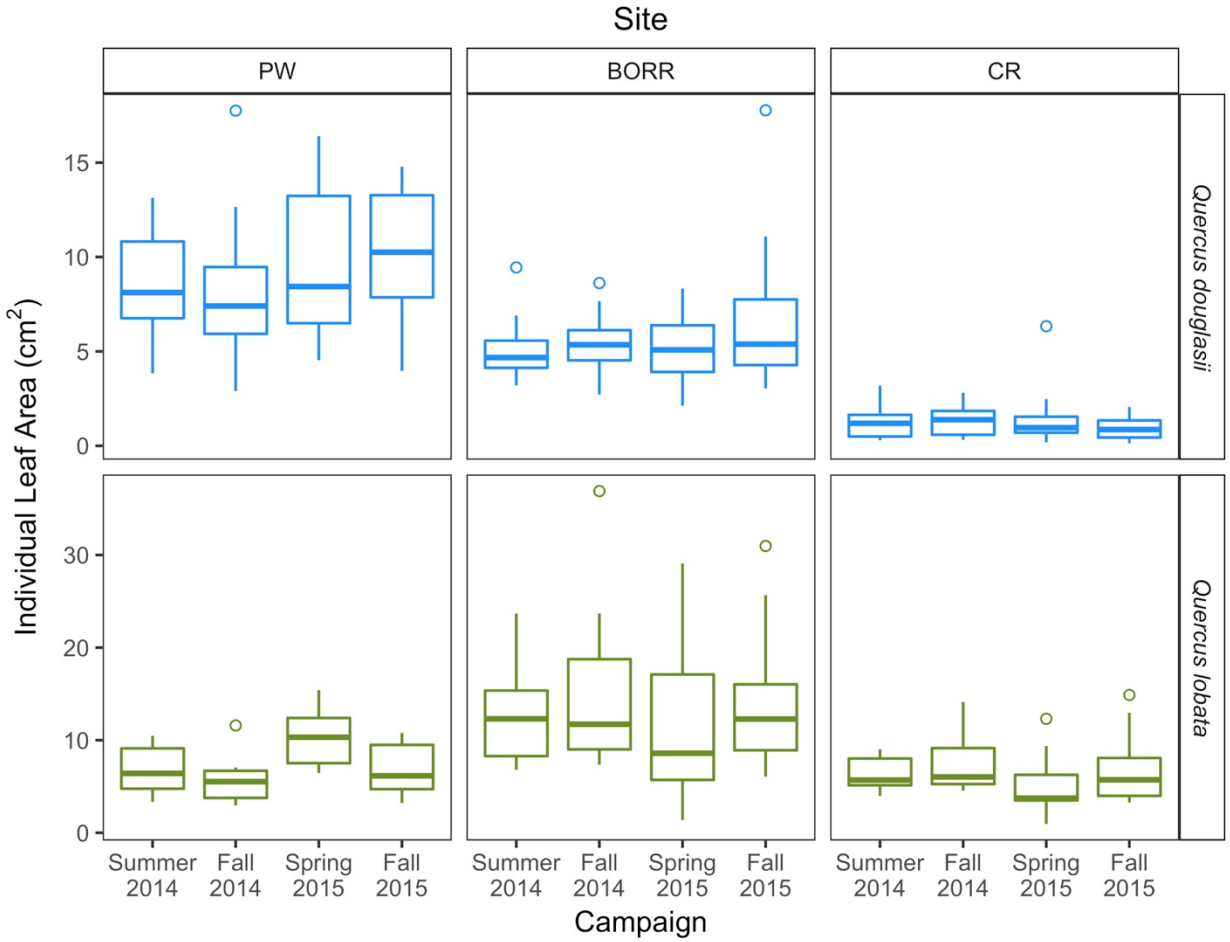

Figure 2. Seasonal changes in leaf mass per area (LMA) across study sites and species (**H2**). See Table 2 for analysis of deviance table for significant coefficients and their interactions.

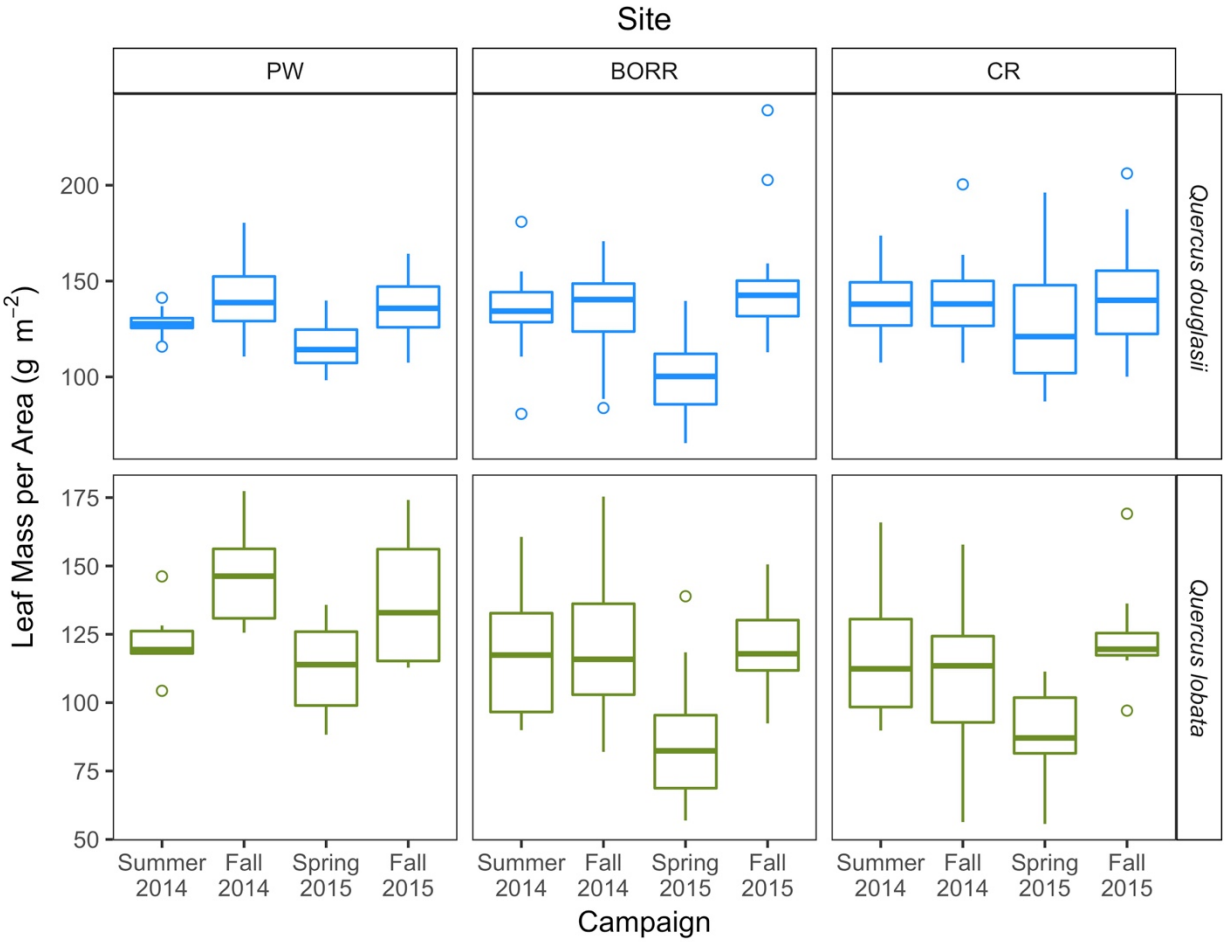

Figure 3. Seasonal changes in leaf area:sapwood area ratios (A_l:A_s) across study sites and species (**H3**). See Table 3 for analysis of deviance table for significant coefficients and their interactions.

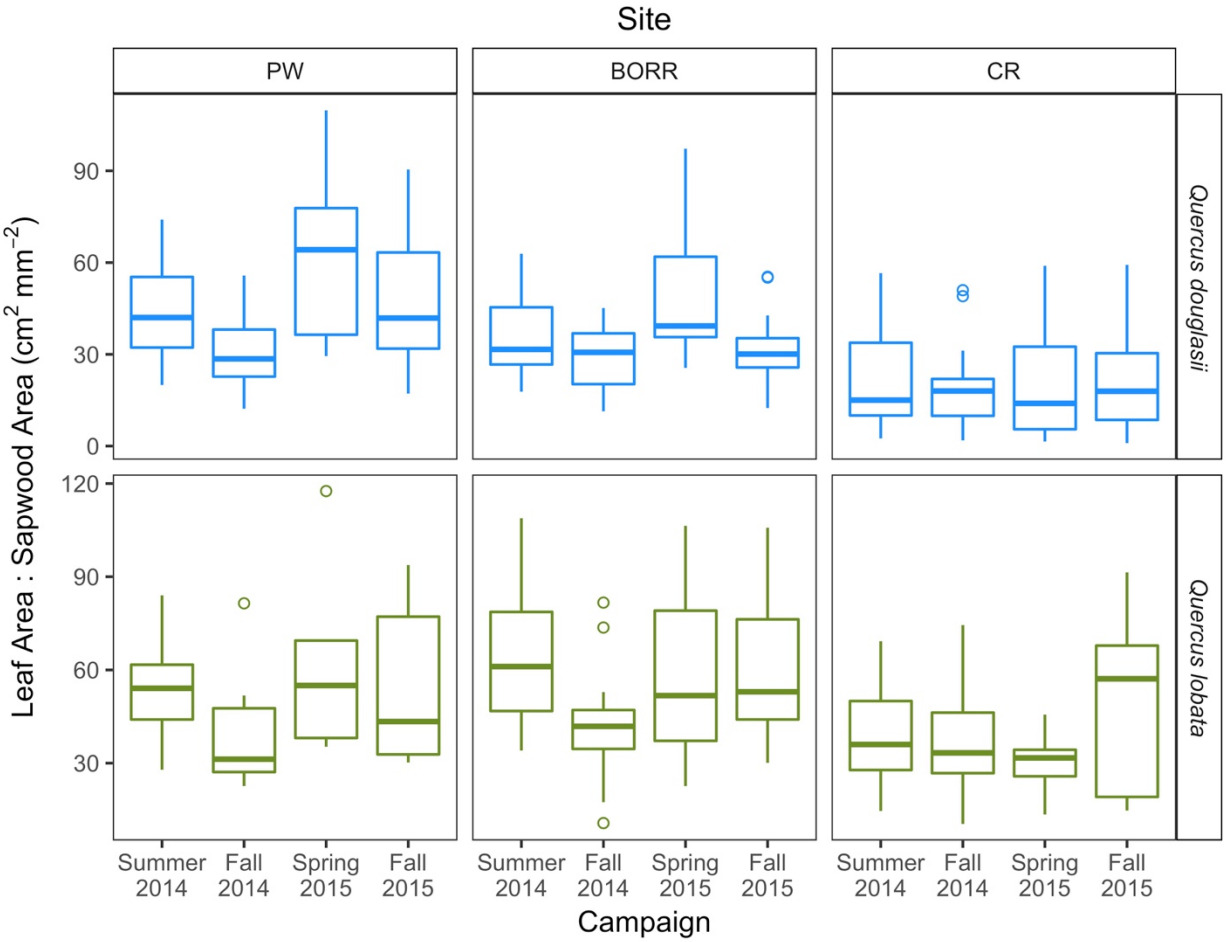

Figure 4. Seasonal changes in leaf senescence across study sites and species. See Table 4 for analysis of deviance table for significant coefficients and their interactions.

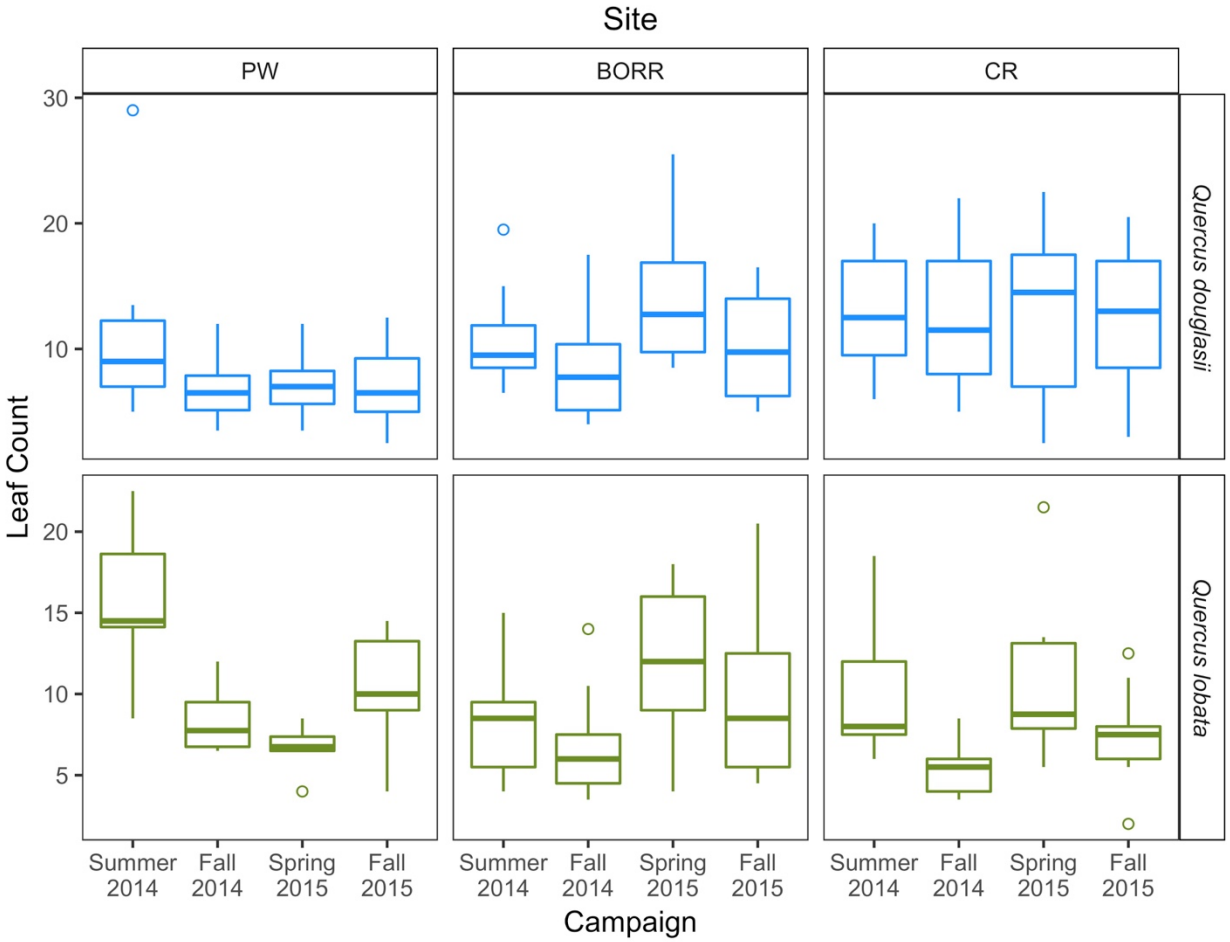

Figure 5. Scale differences in the leaf size of blue oaks between the most xeric site (CR, top) and the most mesic site (PW, bottom). Leaves were sampled in the first study campaign, summer 2014.

Figure 6. Relationship between leaf size (ILA) and LMWL departure for both species across all sites and campaigns.

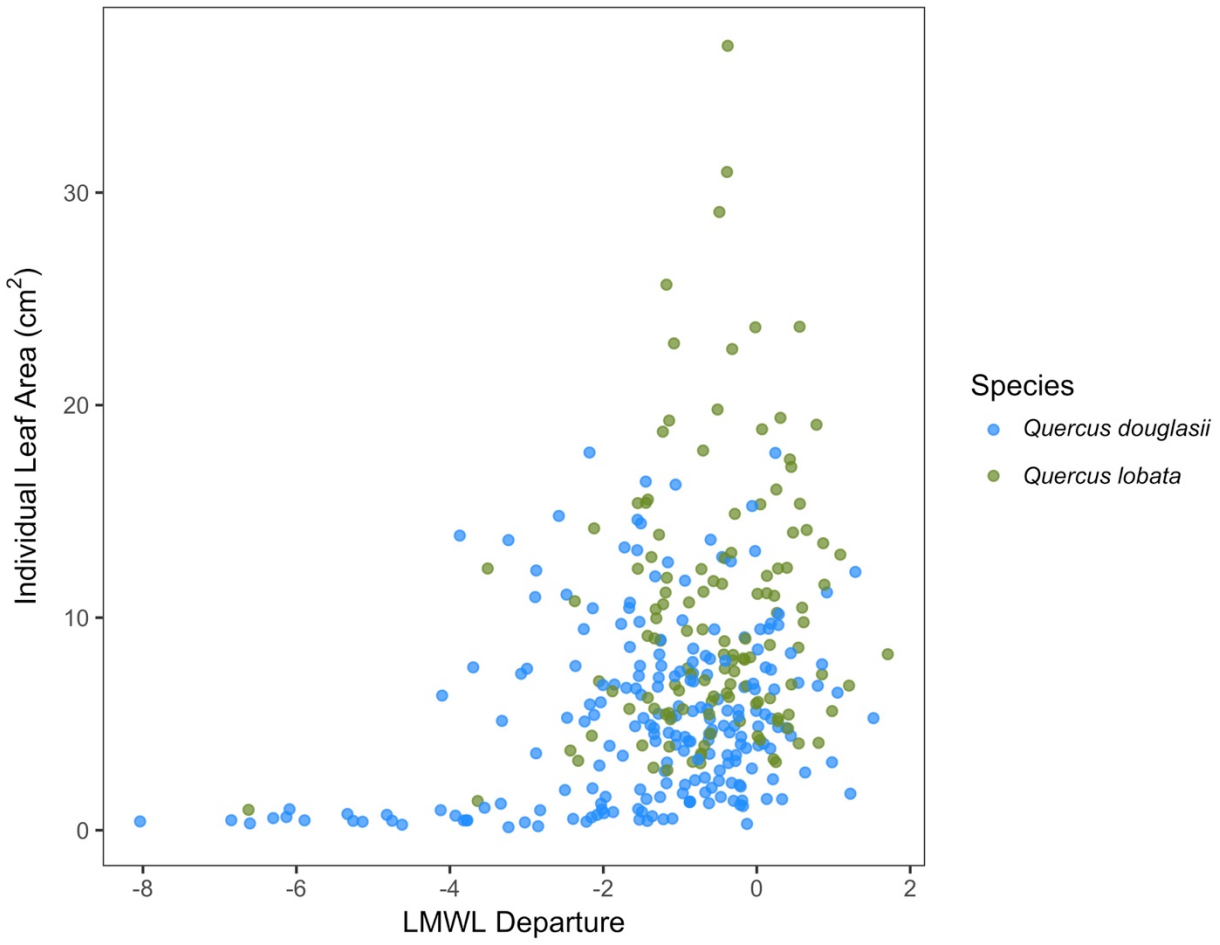

Table 1. Analysis of deviance table from Type III ANOVA testing **H1:** the response of tree leaf size (ILA) through the drought across sites, species, and campaigns.

Analysis of Deviance Table (Type III Tests):
Leaf Size (ILA)

LMER 1 (**H1**): ILA ~ Site * Species * Campaign + (1 | Tree Individual)

Effect:	Chisq	Df	Pr(>Chisq)
Site	**32.9555**	**2**	**< 0.0001**
Species	**10.5517**	**1**	**0.0012**
Campaign	0.2598	3	0.9674
Site : Species	**17.8605**	**2**	**0.0001**
Site : Campaign	7.7711	6	0.2553
Species : Campaign	3.6523	3	0.3015
Site : Species : Campaign	**12.9100**	**6**	**0.0445**

Table 2. Analysis of deviance table from Type III ANOVA testing **H2:** the response of tree leaf mass per area (LMA) through the drought across sites, species, and campaigns.

Analysis of Deviance Table (Type III Tests):
Leaf Mass per Area (LMA)

LMER 2 (**H2**): LMA ~ Site * Species * Campaign + (1 | Tree Individual)

Effect:	Chisq	Df	Pr(>Chisq)
Site	1.3813	2	0.5012
Species	**4.7237**	**1**	**0.0297**
Campaign	**9.0974**	**3**	**0.0280**
Site : Species	0.9980	2	0.6071
Site : Campaign	**25.2741**	**6**	**0.0003**
Species : Campaign	4.6989	3	0.1952
Site : Species : Campaign	8.8097	6	0.1846

Table 3. Analysis of deviance table from Type III ANOVA testing **H3:** the response of shoot leaf area:sapwood area ratios through the drought across sites, species, and campaigns.

Analysis of Deviance Table (Type III Tests):
Leaf Area : Sapwood Area Ratio (A_l:A_s)

LMER 3 (**H3**): A_l:A_s ~ Site * Species * Campaign + (1 | Tree Individual)

Effect:	Chisq	Df	Pr(>Chisq)
Site	**12.1961**	**2**	**0.0022**
Species	**5.0862**	**1**	**0.0241**
Campaign	0.7049	3	0.8720
Site : Species	3.1346	2	0.2086
Site : Campaign	**19.9345**	**6**	**0.0029**
Species : Campaign	2.4761	3	0.4796
Site : Species : Campaign	4.3936	6	0.6236

Table 4. Analysis of deviance table from Type III ANOVA testing the response of shoot leaf senescence through the drought across sites, species, and campaigns.

Analysis of Deviance Table (Type III Tests):
Leaf Senescence (Shoot Leaf Count)

LMER 4: Shoot Leaf Count ~ Site * Species * Campaign + (1 | Tree Individual)

Effect:	Chisq	Df	Pr(>Chisq)
Site	**6.1495**	**2**	**0.0462**
Species	3.7544	1	0.0527
Campaign	0.9817	3	0.8057
Site : Species	**13.1205**	**2**	**0.0014**
Site : Campaign	**18.3827**	**6**	**0.0053**
Species : Campaign	4.7522	3	0.1909
Site : Species : Campaign	8.2253	6	0.2221